INFORMATION TO USERS

.

NUMERICAL MODELLING OF UNDERGROUND OPENINGS IN BEDDED ROCK

By

Ivan Flaviano Vicenzi

Department of Mining and Metallurgical Engineering

McGill University,

Montreal, Quebec, Canada

May 2000

A thesis submitted to the Faculty of Graduate Studies and Research
in partial fulfillment of the requirements of the degree of Master of Engineering

ABSTRACT

Finite element analysis of tunnel excavations has been widely used by geotechnical engineers for assessing the deformations and stress conditions. Discontinuities in the rock mass play a major role when simulating the behaviour of the rock mass around an opening. A crucial point in such analyses is the choice of the constitutive model. Although numerical modelling of jointed rock mass has been suggested by several authors in the last three decades and different modelling codes have been developed, the simulation of discontinuities is still a complex task. After reviewing the various constitutive models, the author of this thesis presents the simulation of bedded rock mass based on the concept of an equivalent media proposed by Amadei and Goodman. The model has been implemented in a two-dimensional finite element code. In addition to the properties of the bedding planes, the spacing between them is considered. The performance of the model is shown by a parametric study focusing on the influence brought by the scale effect. For the latter control, a comparison with the results from the design of the Piora exploratory tunnel in the Swiss Alps has been carried out.

RÉSUMÉ

L'analyse de stabilité des tunnels par la méthode des éléments finis est largement utilisée par les ingénieurs géotechniques pour la prédiction des déformations et contraintes autour le tunnel. Il est aussi bien connu que, dans le cadre de telles analyses, les fractures contenues dans le massif rocheux jouent un rôle important dans la définition du comportement du massif même. C'est ainsi que l'aspect le plus important de l'analyse concerne le choix de la loi constitutive du model. Nombreux modèles numériques simulant un massif rocheux fracturé ont étés proposés par différents auteurs dans les trois dernières décades sur la base des quelles plusieurs logiciels ont été conçus. Néanmoins, la simulation des joints demeure un problème complexe. Après une revue des modèles majeurs proposés, l'auteur de cette thèse présent la simulation d'un massif rocheux stratifié en se basant sur la théorie du média équivalent, décrite par Amadei et Goodman (1981). Par la suite, le modèle à été implémenté dans un logiciel d'éléments finis bi-dimensionnel avec lequel les propriétés des joints ainsi que la distance entre eux sont considérées. La performance du modèle est démontrée par une étude paramétrique donnant l'accent sur l'influence apportée par les fractures relativement à l'échelle du creusement (scale effect). La validation finale à été conduite par la comparaison des résultats du modèle numérique avec ceux sortant du projet du tunnel de sondage de la Piora dans les Alpes suisses.

ACKNOWLEDGEMENTS

The author wishes to acknowledge the warmth and friendship of both the staff and students of the Department of Mining and Metallurgical Engineering at McGill University.

Furthermore, it is a great pleasure to express my sincere gratitude to my supervisor, Professor Hani S. Mitri for his guidance, patience and steady encouragement throughout my entire M.Eng. Program. Besides the technical advices, his friendship made a great difference in my work giving me full support at any time and without whose this thesis would not be completed.

Acknowledgements are also due to my colleagues from the Numerical Modelling Laboratory of the same Department, in particular to Joseph Marwan, Research Associate, for their helpful discussions and suggestions and their assistance regarding the modification on e-z tools software.

I wish to give my warm thanks and to acknowledge co-operation and assistance of the following persons:

- The management of Impregilo S.P.A., General Contractor, Milan (Italy), in particular Mr. Riccardo Corti, Area Manager for Europe, for the financial aid and the trust granted to me during my studies.
- The Government of Canton Ticino (Southern-Switzerland) as the only founding institution for his conclusive financial support.
- Mr. Renzo Tarchini, Chief engineer, Lombardi Consulting Engineers S.A., Locarno-Minusio (Switzerland) for his assistance and time. Data supplied from the Piora exploratory tunnel was crucial in my thesis for program validation.
- The Swiss National Railways (SBB) for the permission to access documents regarding the design of the Piora exploratory tunnel.

I am also deeply indebted to my beloved wife Katia and sons Rocco and Vania, for their understanding, support and encouragement, for all the evenings, weekends and vacations which I spent in front of a computer, when many other things could have been done together. Finally I am grateful to my mother and father for having supported me in all my endeavours.

TABLE OF CONTENTS

List of figures

List of tables

Chapter 1

INTRODUCTION

1.1 General

The engineering mechanics problem posed in all structural designs is the prediction of the performance of the structure under the loads imposed on it during its prescribed functional operation. Likewise the rock engineer is concerned with the application of the principles of engineering mechanics to the design of the rock structures created by underground excavation such as mines or tunnels, while maintaining their integrity and safety.

These ideas may seem rather elementary. However, even limited application of the concepts of mechanics in underground structural design is a relatively recent innovation.

The ultimate objective in the structural design of an underground opening is to control rock displacements around the excavation. Analytical techniques are required to evaluate each of the possible modes or response of the rock mass, for the given excavation conditions and proposed geometry. However, as the problems take on greater reality and the complexity of the design condition increases, the use of analytical methods becomes limited to the point where other, more realistic methods must be sought.

The complexity of many practical engineering problems makes it necessary to use numerical methods. A number of factors have contributed to the relatively recent emergence of numerical methods in rock engineering. One major cause is the increased performance of computer hardware technology over the last two decades. As a result, it is nowadays possible to run sophisticated numerical modelling software to solve large-scale problems with hundreds, even thousands of unknown variables, using affordable computers.

1.2 Problem definition

The large capital investment of tunnelling projects requires greater assurance of their satisfactory performance in the long term. Therefore more rigorous techniques are required in the design process. The increasing physical scale of underground tunnelling operations has also had a direct effect on the need for safe and efficient underground geotechnical design. The need to rationalise the planning of underground traffic ways has pushed engineers to deal with unfavourable geological environments. In particular, the increased depth of excavation in the Alps requires thorough knowledge and application of rock mechanics sciences.

Research efforts have been successfully made over the last three decades to apply numerical methods of analysis like finite elements and distinct elements to mining and civil rock mechanics problems. As a result, a variety of numerical modelling tools have been developed and have become available to meet the needs of the underground construction industry.

Rock mechanics science together with numerical modelling attempt to better understand and predict phenomena that occur in rock masses. In mining and tunnelling problems, joints and other geological fractures play a major role in evaluating stability. In particular, engineering design of drifts and tunnels in jointed rock masses must take into consideration the scale effect; see Figure 1.1.
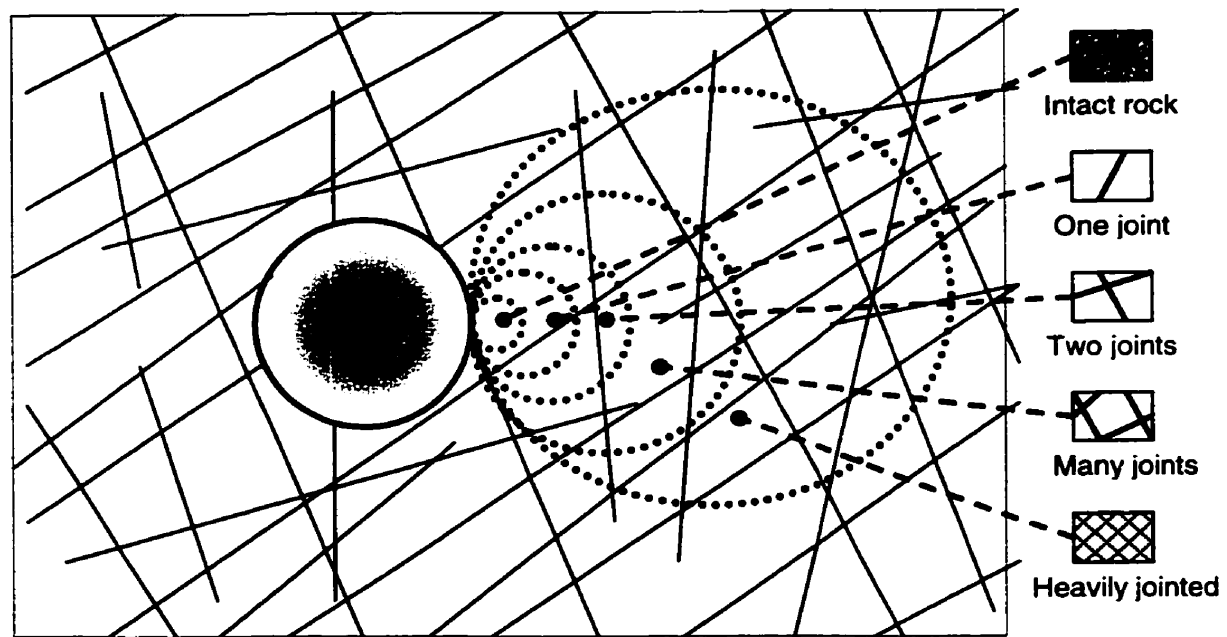
Figure 1.1 The scale effect

When the spacing between joint sets is relatively small compared to the size of the excavation, the strength and deformation properties of the rock mass are influenced by both the properties of the rock material and those of the joints, while on a large scale, the jointed rock mass may demonstrate the properties of a pseudo-continuum.

These considerations suggest that both the intact rock and the joints should define the specification of the rock mass in a numerical model. This may not be an easy task, particularly when the mass has more than one family of joints. Distinct element codes are best suited for this type of problems. The problem, however, becomes merely an academic exercise in the absence of adequate information about the rock block sizes and the geomechanical behaviour of each joint set.

When the rock mass contains parallel bedding planes, it may be characterised as layers of intact rock separated by a single set of discontinuities; see Figure 1.2. This situation is commonly encountered in sedimentary rock formations, e.g. limestone and sandstone, in underground mines as well as in civil engineering tunnels.

1-3
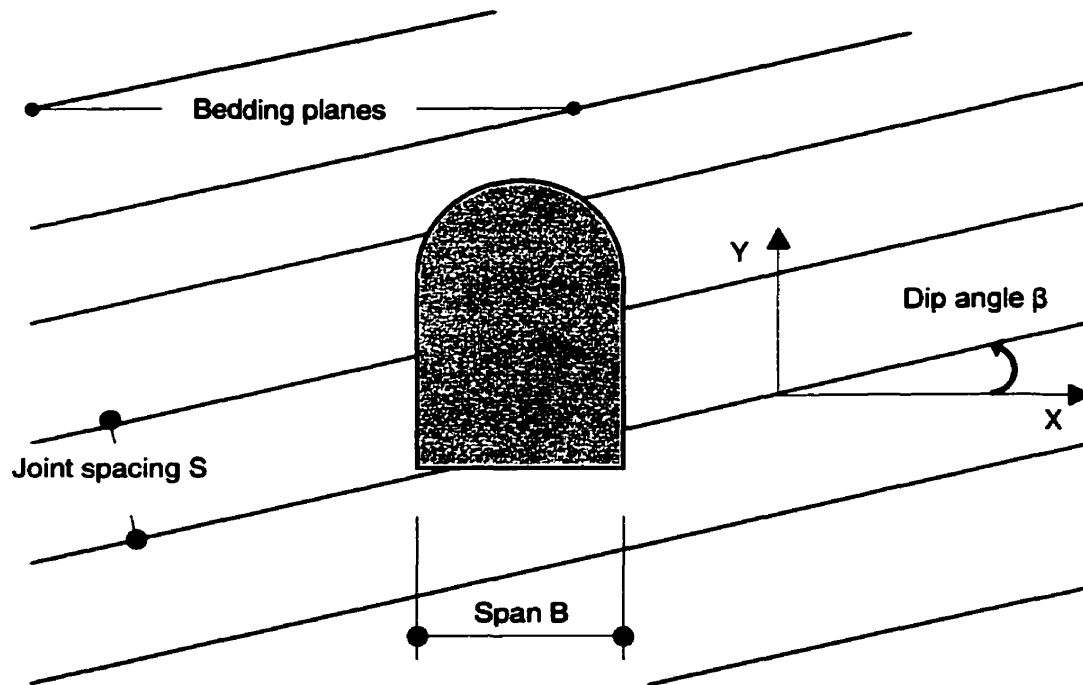
Figure 1.2 Excavation in bedded rock

The response of rock excavation in bedded rock will depend primarily on different major parameters. They are:

1. Excavation span, B
2. In situ stress (or depth below ground surface)
3. Spacing between bedding planes, S
4. Dip angle of bedding, β
5. Properties of the bedding planes (shear and normal stiffness)

The first two parameters can be easily treated by a wide variety of numerical modelling software. However, the treatment of the bedding planes as discrete layers or not will depend on the layer thickness.

1-4

The following three scenarios can be postulated:

1. Closely spaced discontinuities, Figure 1.3a. In this case, the excavation roof can be treated as a homogeneous, but transversely isotropic material where properties in the direction parallel to the joints are different from those perpendicular to them;

2. Moderately spaced discontinuities, Figure 1.3b. Here the effect of discontinuities between layers must be considered. Both the shear and normal stiffness characteristics of the bedding plane must be considered. The rock layer may be treated as isotropic or transversely isotropic as in the first case;

3. Widely spaced discontinuities. In this situation, the presence of discontinuities may have little or no influence on the deformation and strength behaviour in the excavation roof. The rock may be treated as homogeneous isotropic, see Figure 1.3c.
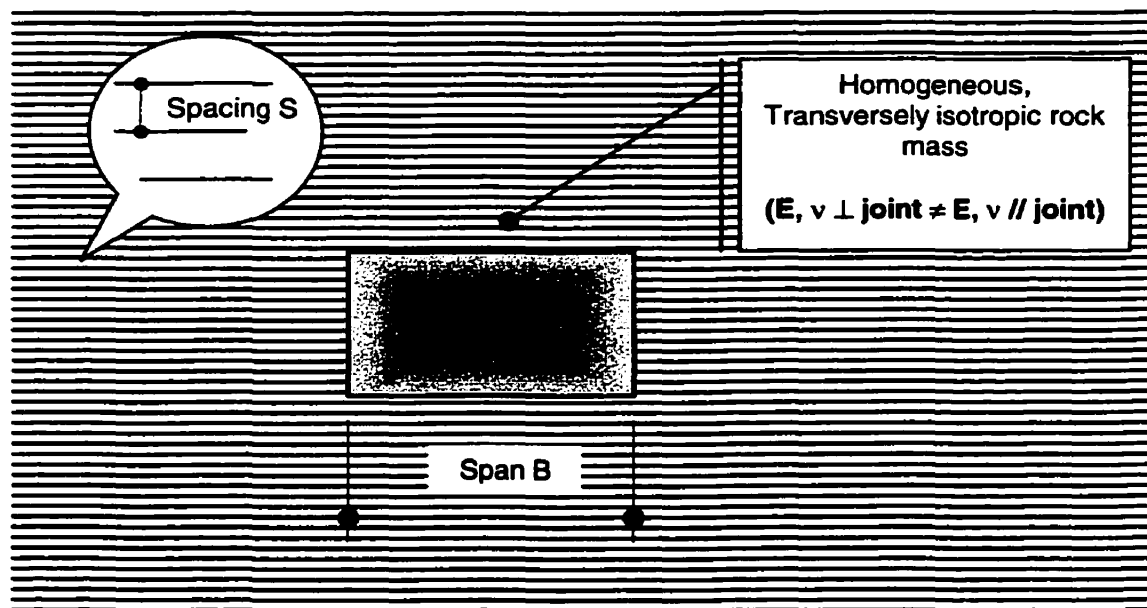
Figure 1.3 Problem definition:

a) Closely spaced discontinuities, B/S >>
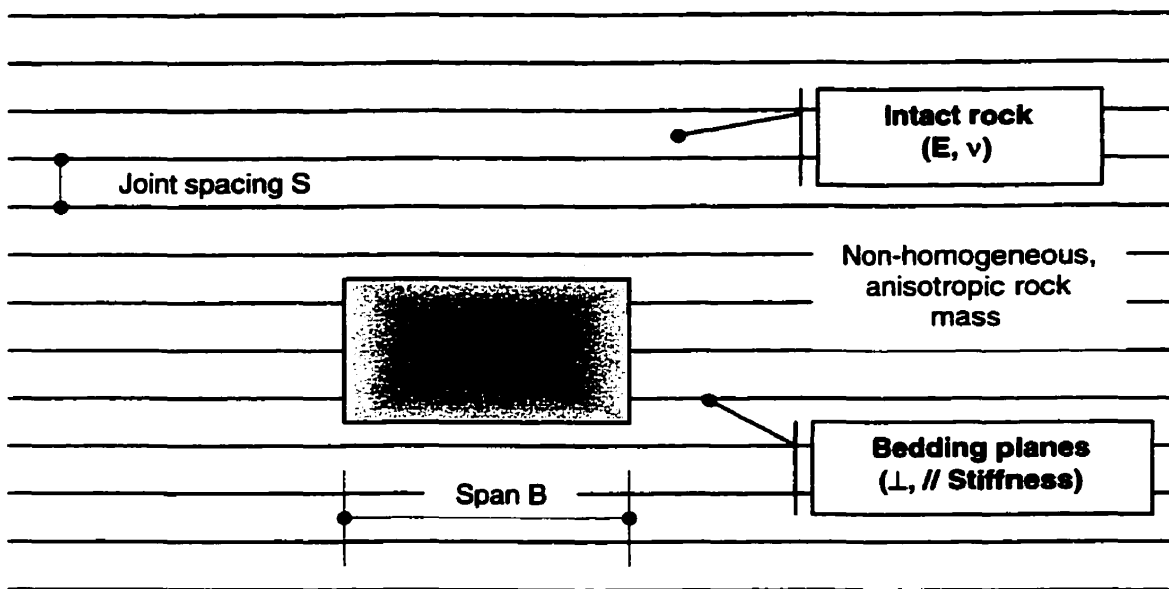
Figure 1.3 Problem definition:

b) Moderately spaced discontinuities, << B/S <<
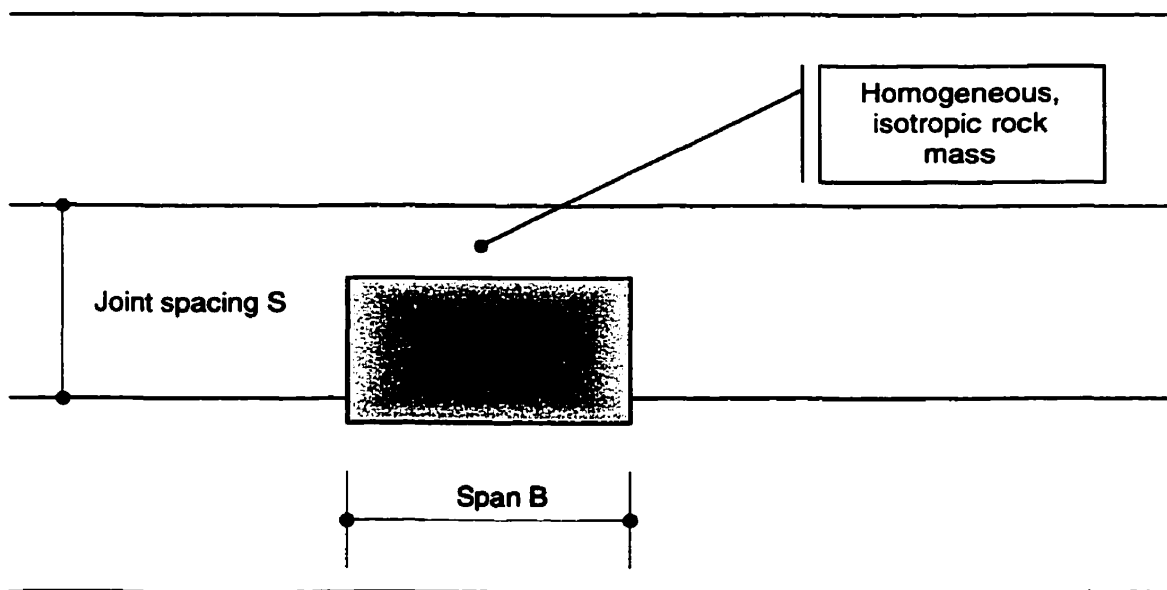
Figure 1.3 Problem definition:

c) Widely spaced discontinuities, << B/S

There are many geomechanical finite element codes that are available today on the market. Nevertheless, the majority of these software do not take special consideration of the modelling of bedded rock.

Nevertheless, a stratified rock mass in a mine or in a tunnel is not uncommon in the underground hard rock environment. The use of numerical modelling in combination with in situ monitoring can give good feedback in designing underground openings in bedded rock.

The objective of this research is to develop a simple numerical model, which will simulate the behaviour of a bedded rock mass in underground tunnels as demonstrated in Figure 1.3.

Such model should take into consideration the following:

- Arbitrary excavation geometry
- Presence of in situ stresses
- Mechanical properties of the rock (E, v)
- Bedding planes, in particular:
  - o Spacing between joints
  - o Inclination (dip) of bedding plane (angle β)
  - o Normal and shear stiffness characteristics of the bedding planes

The numerical model will be based on the Finite Element method. It will perform deformation and stress analyses.

Following a detailed model parametric study, the new model will be applied to a case study of the Piora Exploratory Tunnel in the Swiss Alps; see Figure 1.4.
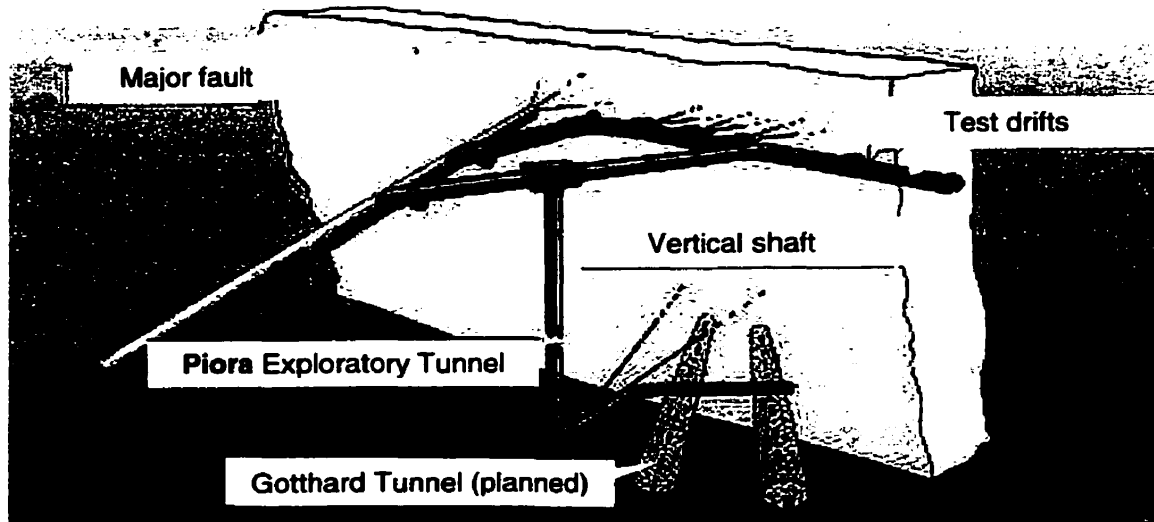
Figure 1.4 Case study: 3-D view of the Piora Exploratory Tunnel

1.4 Thesis outline

Chapter one presents an introduction. The importance of a correct design in underground structures as well as the role of modelling the rock media taking into account discontinuities are outlined. The last section of this chapter describes the thesis objectives and related methodologies.

Chapter two deals with the characterisation and modelling of rock masses. Continuum and discontinum models are briefly reviewed with particular emphasis on the different methods used in modelling continuum media.

Chapter three presents the proposed finite element model. The selected constitutive model for bedded rock mass is described first. The main characteristics of the code along with the governing equations are presented. The input parameters are identified and the methods of their determination are given.

In Chapter four, the model the model is verified. The case study is about the simulation of the rock mass behaviour for a critical section of the Exploratory Piora Tunnel in the Swiss Alps. A brief presentation of this project is given as well as an explanation of the design method.

Chapter five summarises the conclusions of the thesis. Recommendations for further developments of this work are given.

Chapter 2

LITERATURE REVIEW

2.1 Introduction

This section presents the engineering properties of rock masses, followed by a description of discontinuity characterisation. The second part of the Chapter introduces the concept of the equivalent elastic modulus for a fractured media along with an overview of approaches proposed by different authors to model the joints as well as the interaction with the rock matrix.

2.2 Rock mass classification methods

2.2.1 Objective of the classification

A general rock mass characterisation starts with a general rock mass classification dividing rocks into two major classes, intact rock and fractured respectively jointed rock. Intact rock is considered a continuous media while a discontinuous media describes jointed rock. The properties used to classify rocks will vary according to the purpose of the study and may include various criteria: shear strength, flexural strength, tensile strength, elasticity, creep rate, in situ stress, drillability, formations characteristics, density, thermal expansion, mineralogy and colour.

In essence, rock mass classifications are not to be taken as a substitute for engineering design. They should be applied and used in conjunction with observational methods as well as analytical and numerical studies to formulate an overall design compatible with the design objectives and site particularities. The objectives of rock mass characterisation are therefore:

- identify the most significant parameters influencing the behaviour of a rock mass,
- divide a particular rock mass formation into groups of similar behaviour, i.e. rock mass classes of various qualities,
- provide a basis for understanding the characteristics of each rock mass class,
- compare the experience of rock condition at one site to the conditions and experience encountered at other sites,
- derive quantitative data and guidelines for the engineering design,
- provide a common basis between engineers and geologists.

Basically, it can be nowadays stated that rock mass classifications are divided into families with regard to the use and the information the classification should provide. So stated,

- the geological family classifies the rock masses by the genesis, the geological history and by the composition of the media. The main „mechanical" purpose of such a classification is to better understand the in situ state of stress;
- the geotechnical family of classifications systems should provide the engineers with classes of the rock mass helping for designing underground works with an empirical tool. This goal is achieved by classifying the media disregarding the geology but dividing it in classes of same mechanical properties.
- the numerical modelling family, which is a personally extension of the geotechnical one with particular regard, in the intention of the author of this thesis, to the simulation of the media by a computer code. The principal question is here how to model the fractured media. The rock mass is simply divided in homogenous (continuous) or fractured (discontinuous) media.

At the beginning of this century, when the study of rock masses was starting, scientists tried to establish procedures and guidelines in this new science. During the last decades, rock engineering developed many tools to create a new image of rock and rock masses. Their effort is now used in rock mass classification and characterisation. Many classification systems have been developed. Most of them have become popular in tunnelling and mining and despite their explicit empirical approach still

in use: "Rock Load" (Terzaghi, 1946), RQD (Deere et al., 1967) RMR (Bieniawski, 1973 and 1979), Q-System (Burton, 1974).

When studying the behaviour of a regularly jointed rock mass for mining purposes, the characterisation of the medium is influenced by the discontinuities. Depending on the spacing within the bedding planes related to the largest dimension of the opening, the discontinuities characterisation and their oncoming parameters are very important.

An important issue in rock classifications is the selection of the parameters of greatest significance. There appears to be no single parameter or index that can fully and quantitatively describe a jointed rock mass for engineering purposes. Various parameters have different significance, and only if taken together can they describe a rock mass satisfactorily. Those parameters play a major role in choosing a model for the numerical simulation of the jointed rock mass.

According to the International Society of Engineering Geology, different guidelines are based on the following features, which affect the physical and mechanical properties of the rock:

1. the mineral composition
2. the structure and the texture
3. the degree of weathering.

In the categories above, it is assumed that the physical and mechanical properties of a rock, in its present state, result form different processes, such as: genesis, metamorphism, tectonics and surface weathering. Thanks to these processes, one can explain not only the lithological and physical features of the rock, but also their locations on Earth. A proposed classification distinguishes the following rock mass units according to the degree of homogeneity:

- geotechnical unit
- lithological unit
- lithological complex.

In 1981, the International Society of Rock Mechanics proposed that a basic geotechnical description of the rock masses should include the following characteristics:

1. rock name with simplified geological description
2. the layer thickness and fractures that intercept the rock mass
3. the unconfined compressive strength of the rock material and the angle of friction of the fractures.

2.2.2 Intact rock properties

The design engineer is confronted with rock as an assemblage of blocks of rock material separated by various types of discontinuities, faults, bedding planes, etc. This assemblage constitutes a rock mass. Therefore, the properties of both intact rock and the rock mass must be considered. Figure 2.1 shows different classes of rock mass.

| Intact | Faulted | Blocky | Bedded | Jointed | Heavily Jointed |
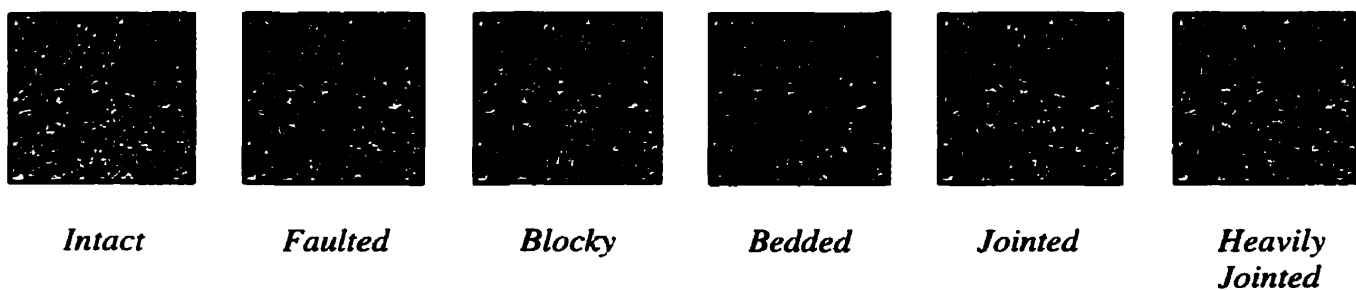
Figure 2.1 Rock mass classes

The most commonly required properties of the intact rock mechanics studies include:

- unit weight
- deformation properties (e.g. modulus of elasticity)
- strength properties (e.g. uniaxial compressive strength).

It is then possible to estimate the rock mass properties using the intact rock properties and the rock mass classification system. This is described below.

2.2.3 Rock Quality Designation (RQD)

The first rational method of rock mass classification was introduced by Terzaghi in 1946 and was formulated for the evaluation of rock loads for the design of appropriate steel sets. This was an important development as steel sets have been the most common support type in tunnels excavated in rock. In this classification, the rock is divided into nine classes ranging from intact hard rock (class 1), to swelling rock (class 9). Terzaghi's classification was later found to be too general and overestimate rock load. It was later modified by Deere et al. in 1970, by Rose in 1982 and by Deere and Deere in 1988.

The modified rock load classification included a new index known as the RQD or the Rock Quality Designation. The Rock Quality Designation index, which is a practical parameter, is defined as a core recovery percentage of sound pieces of rock that are 100 mm or greater in length, see Figure 2.2. The following are the relationships between the engineering quality fo the rock mass and RQD proposed by Deere (1968).

< 25	Very poor
25 to 50	Poor
50 to 75	Fair
75 to 90	Good
90 to 100	Excellent

Table 2.1 Relationship between RQD and rock mass quality

Although the RQD is a simple and inexpensive index, alone it is not sufficient to provide an adequate description of a rock mass because it disregards joint orientation, tightness and filling material. Therefore, particular attention to the discontinuities characterisation is given by integrating the RQD

index by other parameters. In fact, the RQD supplied by six parameters forms a basic element of the most popular classifications that are the RMR or Rock Mass Rating system (Bieniawski, 1973, modified 1979) and the rock mass Quality, Q-system (Barton, 1974)
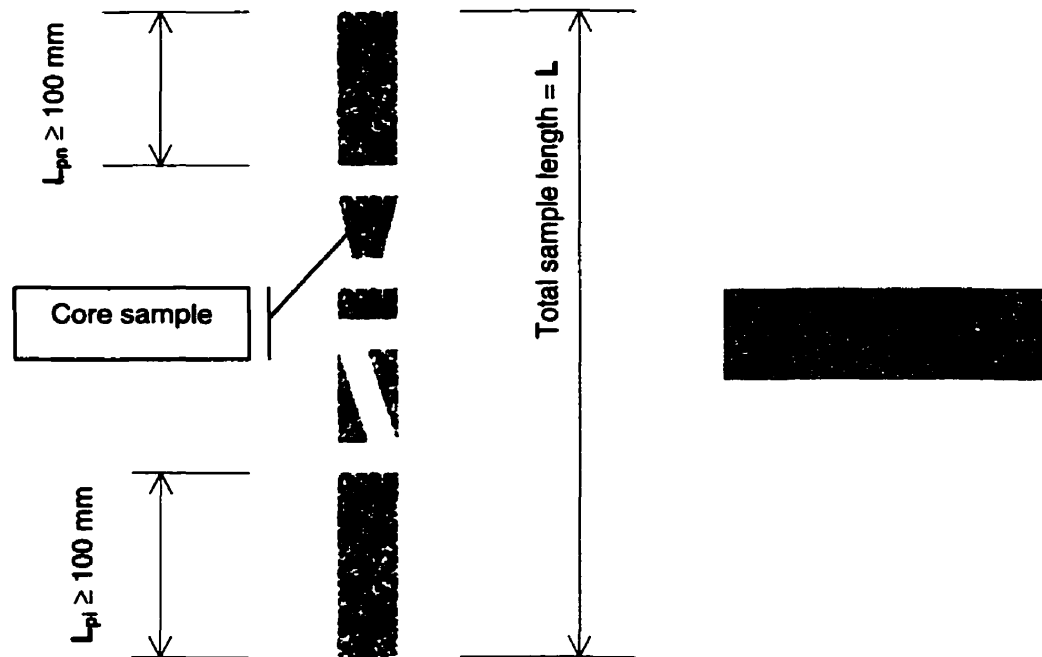
Figure 2.2 RQD index determination by core sample

2.2.4 Rock Mass Rating (RMR)

The Rock Mass Rating system was developed by Bieniawski in 1973. It was modified over the years as more case histories became available to conform with international standards and design procedures. The classification system depicts the rock mass quantitatively; in fact, the following six parameters are used to classify a rock mass using the RMR system:

1. uniaxial compressive strength of rock material

2. RQD

3. spacing of discontinuities

4. orientation of discontinuities

5. condition of discontinuities

6. groundwater conditions.

Each of the above parameters is assigned a certain number of rating points. The total number of such points is the RMR with higher rating indicating a better rock mass condition as shown in the next Table 2.2.

Parameter	Rating points	Comment
Uniaxial compressive strength	1 to 15	at 240 MPa = 15 points
RQD	3 to 20	at 100% = 20 points
Spacing of discontinuities	5 to 20	at 2'000 mm = 20 points
Condition of discontinuities	0 to 30	very rough, not continuous, no separation, unweathered = 30 points
Groundwater conditions	0 to 15	completely dry = 15 points
Orientation of discontinuities	0 to –12 (mines) 0 to –60 (slopes)	very favourable = 0 points very unfavourable = -60 points
Total (RMR)	0 to 100	

Table 2.2 RMR point ratings associated with each parameter

The rock mass quality can then be described according to its RMR value as follows:

< 20	V	Very poor
21 to 40	IV	Poor
41 to 60	III	Fair
61 to 80	II	Good
81 to 100	I	Very good

Table 2.3 Relationship between RMR, rock mass class and rock mass quality

2.2.5 Rock mass quality (Q-system)

The Q-system was proposed in 1974 in Norway by Barton et al. It's based on a numerical assessment of the properties of the rock mass making use of six parameters as listed below:

1. RQD
2. J_n Joint frequency number
3. J_r Joint roughness
4. J_a Joint weathering
5. J_w Groundwater reduction factor
6. SRF   In situ stress reduction factor.

The computation of the quality assessment of the rock mass follows then by the mean of the equation including al the six parameters:

$$Q = (RQD/J_n) (J_r/J_a) (J_w/SRF) \qquad (2.1)$$

Similar to the RMR classification each of the above parameters is assigned a rating as shown in the next Table 2.4 except the RQD parameter, which applies to the formula with its own value.

RQD	10 to 100	0% < RQD < 10%, rating = 10
J_n	0.5 to 20.0	highly fractured rock mass, cohesion less = 20
J_r	0.5 to 4.0	persistent joint, smooth surfaces = 0.5 non-persistent joint = 4
J_a	0.75 to 20.0	$\varphi_{filling}$ > 35 grad, rating = 0.75 $\varphi_{filling}$ < 6 grad, rating = 20.0
J_w	0.1 to 1.0	completely dry = 1.0
SRF	0.5 to 20.0	very favourable = 0.5 very unfavourable = 20.0
Total (Q-system)	0.001 to 1000	

Table 2.4 Q-system rating associated with each parameter

The rock mass quality can then be described in detail according to its Q value as follows:

Q-index	Rock mass quality
0.001 to 0.01	Exceptionally poor
0.01 to 0.1	Extremely poor
0.1 to 1	Very poor
1 to 4	Poor
4 to 10	Fair
10 to 40	Good
40 to 100	Very good
100 to 400	Extremely good
100 to 1000	Exceptionally good

Table 2.5 Relationship between Q-index and rock mass quality

2.2.6 Rock mass classification for modelling purposes

Essentially, the purpose of all the modern geotechnical classification systems is to gather a mostly wide range of indications on the rock mass in an index, which is strictly related to the rock support to put in place. While the early rock mass classifications were based on extremely general assumptions to provide quantitative information of the properties of rock masses, the latest geotechnical classifications are based on large site observations of the peculiarity of the rock mass. In particular, to the characterisation of discontinuities in the media is paid great attention.

Many other classifications, based on engineering criteria referring to specific works or to payment purposes, are well known and used in practice such as the New Austrian Tunnelling Method (NATM) developed between 1957 and 1964, and the ISRM classification (1981), which is more simplified then Q and RMR systems.

As already stated at the beginning of this Chapter, all geotechnical classification systems are the base for empirical methods in designing underground structures.

Non-empirical methods make use of constitutive modelling of jointed rock masses, which has long been a subject of interest and numerous models have been developed in attempts to simulate the mechanical responses of a rock mass. The mainly accepted classification divides the currently available models in two groups:

1. discontinum models
2. continuum models.

In discontinum models, the joints are explicitly modelled while in the continuum models the fractured rock mass is treated as a continuum with equivalent material properties, which reflect the effect of the joints.

Modelling of discontinuities found in rocks is a major issue when defining the approach developing a numerical method simulating a media. The principal approaches for continuum and discontinum models for rock masses will be discussed later in this chapter, after the discontinuities characterisation.

The following chart summarizes the classification of medium models along with the solving methods used in rock mechanics.

MODELING TECHNIQUES IN ROCK MECHANICS

Medium models ← → **Displacement equations solvers**

Continuous

Discontinuous
(Discontinuities and blocks treated separately)

Isotropic   **Anisotropic**

Blocks   **Discontinuities**

Homogeneous   **Non-Homogeneous**

Single stiffness   **Double stiffness**

Equivalent isotropic medium

Rigid   **Elastic**

Linear   **Non-linear**

Basic equations

Effects superposition

Analog   Analytical

Simple problems

F.D.M.
F.E.M.
B.E.M.
D.E.M.
or
combination

Figure 2.3 Definition of continuum and discontinum in rock mechanics

2-12

2.3 Characterisation of rock discontinuities

The presence of discontinuities in rock formations distinguishes rock from rock mass. Any type of rock formation contains discontinuities. The origin of discontinuities can be attributed to the orogenic and tectonic movements, weathering processes, etc. Discontinuities are considered as either faults or joints. An example of discontinuities classification based on descriptive-structural criteria was made by Thiel (1989), and is shown in Figure 2.4.
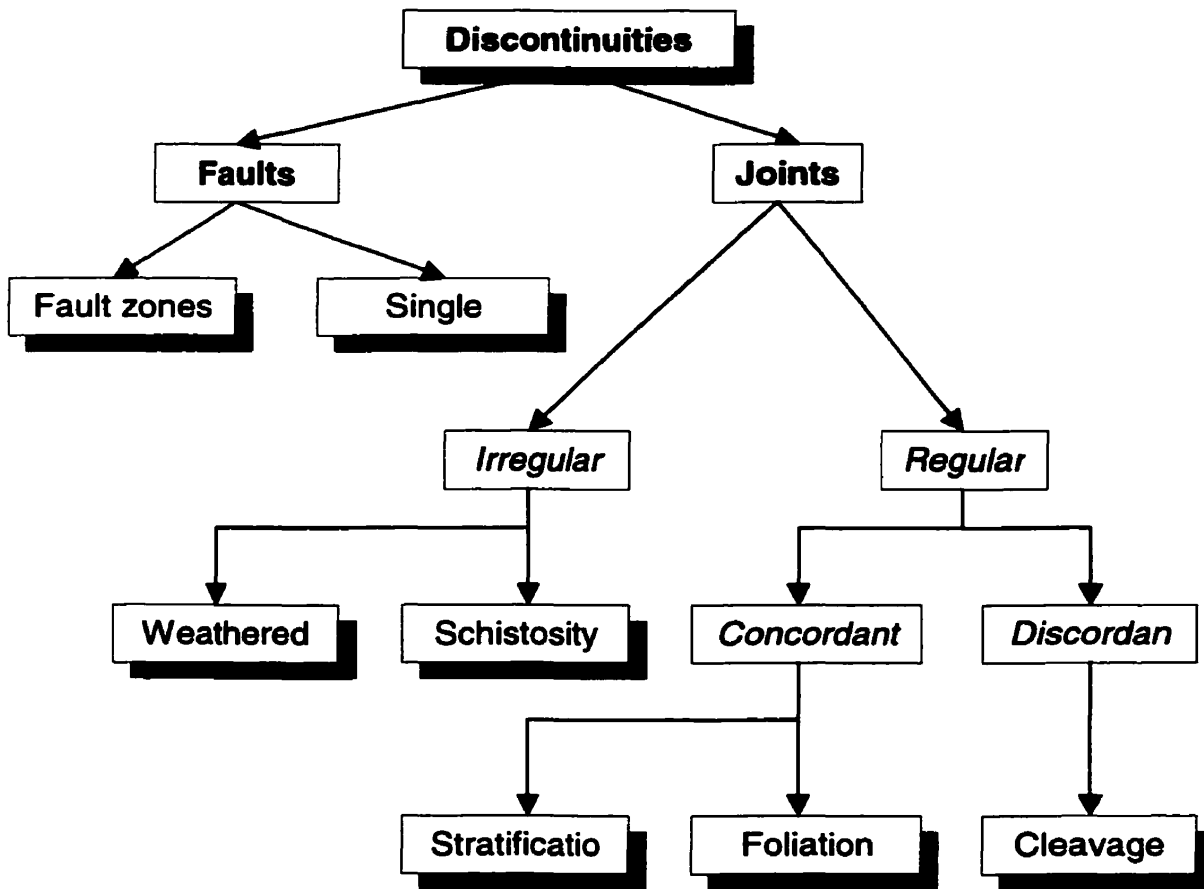
Figure 2.4 Classification of discontinuities (Thiel, 1989)

Discontinuities modify the qualitative aspect of the rock mass and affect its behaviour. Dealing separately with the discontinuity characterisation is the only way to reach a point where the interaction between rock mass and discontinuity can be analysed. Understanding the behaviour of the rock-joints ensemble is extremely important when studying stresses in this type of medium.

The properties of discontinuities that control the behaviour of the rock mass are orientation, spacing or frequency, intensity, shape, roughness and aperture. Each of these parameters can have a statistical interpretation because, in nature, their variation is widely spread. There are no particular rules when considering their influence on the rock behaviour. It's difficult to measure these parameters and to generalise them when dealing with large-scale studies.

Joint orientation can be measured from cores or exposures. It is quantified by the joint dip and dip direction. Methods for discontinuity orientation measurements, presentation and analysis have been described by many authors such as Priest (1985), Goodman (1976), Einstein and Baecher (1983). In 1981, the Association Francaise des Travaux Souterrains (AFTES) released a classification of the discontinuity pattern according to the joint spacing and RQD index designation. This classification is presented in Table 2.6 below.

		RQD
S1	>200	90
S2	60-200	75-90
S3	20-60	50-75
S4	6-20	25-50
S5	<6	<25

Table 2.6 Rock mass classification according to joint spacing and RQD (Thiel, 1989)

Discontinuity shape refers to the relation between the trace length and its orientation. Simplified discontinuity shapes are usually assumed to be circular, square, elliptical or rectangular. The number of joint sets and the inter-connection strongly influence the behaviour of the media.

Roughness and aperture of the discontinuity raise the question related to the actual mechanical properties of the joint. In the literature, Barton (1973) introduced the Joint Roughness Coefficient (JRC) as an empirical measure. The commission of International Society of Rock Mechanics published in 1978 a classification of discontinuity roughness based on description of rock joints and their aspect. There are some other studies, which simulate fracture roughness, e.g. Maini (1971), or fracture aperture, e.g. Amadei et al., (1995).

2.4 Numerical modelling techniques

In this section the different approaches used in modelling rock mass excavations are reviewed. As previously stated, basically any method to model a jointed rock mass will fall in one of two major classes. They are:

1. discontinuous models
2. continuous models.

The joint element method, the block theory and the distinct element method fall in the first class of models. Goodman and Ke (1995) propose to separate the joint element method and the block theory classifying them into the continuous models with interface element and the statics of rigid blocks model respectively. The block theory model is not considered a discontinuous mechanism by these authors because it does not consider the kinematics of moving blocks.

If the spacing of joints is relatively large compared with the problem domain, the effect of joints can no longer be simply represented by a continuum model, and the contribution of individual joints has to be

taken into account. Accordingly, based on the framework of the continuum approach, interface elements were introduced to simulate the distinct behaviour of joints, starting in the late 1960s.

Goodman (1968) first proposed joint elements to model discontinuities by handling a complex problem with hundreds of interfaces. This model incorporated the elastic stiffness and strength parameters of joints, and assumed a zero thickness for each joint element. Zienkiewicz et. al. (1973) introduced transversally isotropic paralinear elements, with an arbitrary small thickness while Ghaboussi (1973) developed an element for joints based on the relative displacement scheme and the concept of plasticity. Desai (1984) proposed a thin-layer element, which is a solid element with a constitutive law for contact, sliding, separation and rebounding of joints.

The joint element method provides a means to simulate individual joints, which would not otherwise be modelled realistically. However, this method has major limitations such the relatively small number of interface elements that can be handled and the small displacements or rotations that can be accommodated.

Block theory, developed by Goodman and Shi (1985) is an analytical method rather than a numerical modelling approach. In addition to the assumption of rigid block, it also assumes that all joint surfaces are perfectly planar and extend entirely through the volume of interest, and sliding is the only failure mode.

The distinct element method has become widely used in rock mechanics in the last decade because of its integration in many commercial applications. Since Cundall (1971) first introduced it to simulate progressive movements in blocky rock systems, it has been strenuously developed.

In 1980, the distinct element method code UDEC was established and marketed. It employs an explicit central difference time-marching scheme to integrate the equations of motion directly. At the start of every step, contacts are detected based on the current penetrations between blocks. Given the elastic contact stiffness, the amount of penetrations at each contact determines the contact forces between two

blocks, which are regarded as additional external forces of the system at the current step of the calculation.
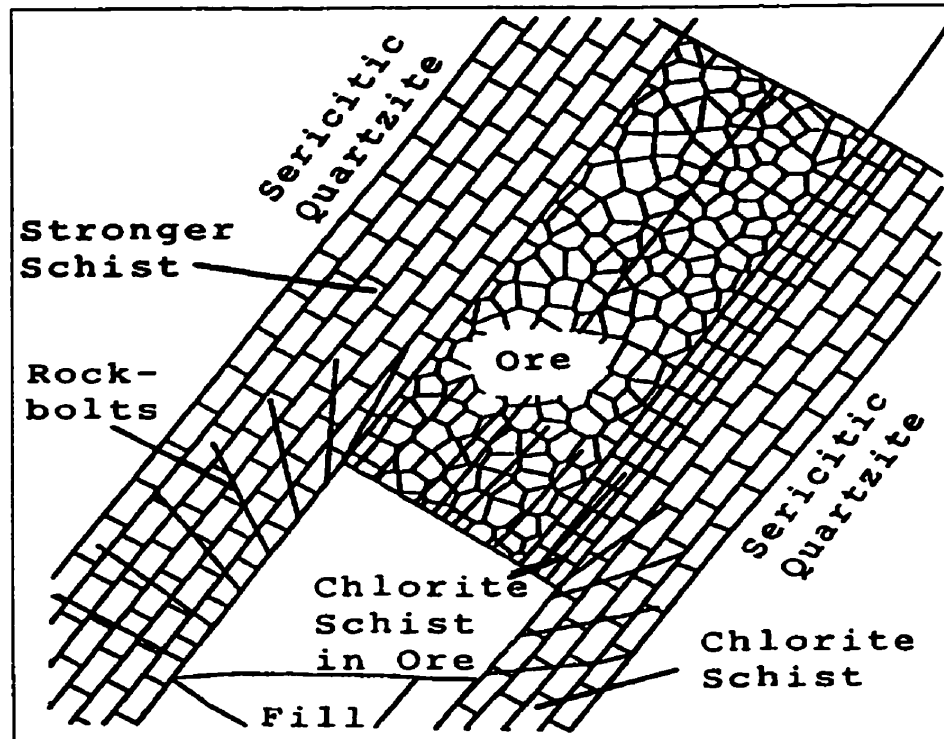
Figure 2.5 Distinct element model of the stope 804 at the Kristineberg Mine in Sweden (Board et al. 1992)

Two situations allow a rock mass to be treated as a continuum: the rock mass is relatively free of discontinuities on the scale of a given problem and discontinuities in the rock mass are so pervasive relative to the size of the problem domain as to create a statistical continuum with equivalent rock mass properties, like soils. Within the continuum models three different approaches are used in order to depict the rock mass behaviour, i.e. the empirical one, the analytical one and the numerical one.

As treated in a previous section, the most popular empirical approach is related to the RMR classification system. Bieniawski (1978), Serafim and Pereira (1983) and Mitri (1994) have proposed equations that empirically relate RMR values to mean values of deformation modulus determined from sets of data that show considerable scatter. Furthermore, Bieniawski (1980) found that measured static modulus of deformation could be empirically related to the shear wave frequency generated by a hammer blow and received on the rock surface by a linear equation.

Dealing with analytical methods, some authors have worked on the rock mass factor, which is the ratio between the Young's modulus of the rock mass and the Young's modulus of the intact rock, and reflects the decrease in the modulus due to the presence of joints in the rock mass, their characteristics and spacing. Those authors have investigated theoretical models that can be used to predict rock mass factor values. Walsh and Brace (1966) derived approximate mathematical expressions for apparent elastic modulus of a material, which has dilute concentration of spherical cavities and elliptical cracks and proposed an expression for the rock mass factor. Hobbs (1975) assumed that asperities in the rock joints could be regarded as miniature circular loaded areas through which stress is transmitted. Based on his theory, he also proposed an equation giving the rock mass factor.

Due to rapid advancements in computers and their universal availability to engineers, numerical approaches now make computational methods perhaps the most promising approach. As mentioned in the beginning of the section, when joints are too numerous to be modelled individually, one can attempt to establish a constitutive law to represent the combined behaviour of rock and the set of joints. A regularly jointed media would be idealised as linear elastic an isotropic material.

A few basic definitions regarding the mechanical behaviour of different materials – i.e. homogenous / heterogeneous, isotropic / anisotropic, continuous / discontinuous - are given in the next section related to a short introduction to the elasticity theory. The concept of linear elastic is shown in figure 2.6 here below:

2-18
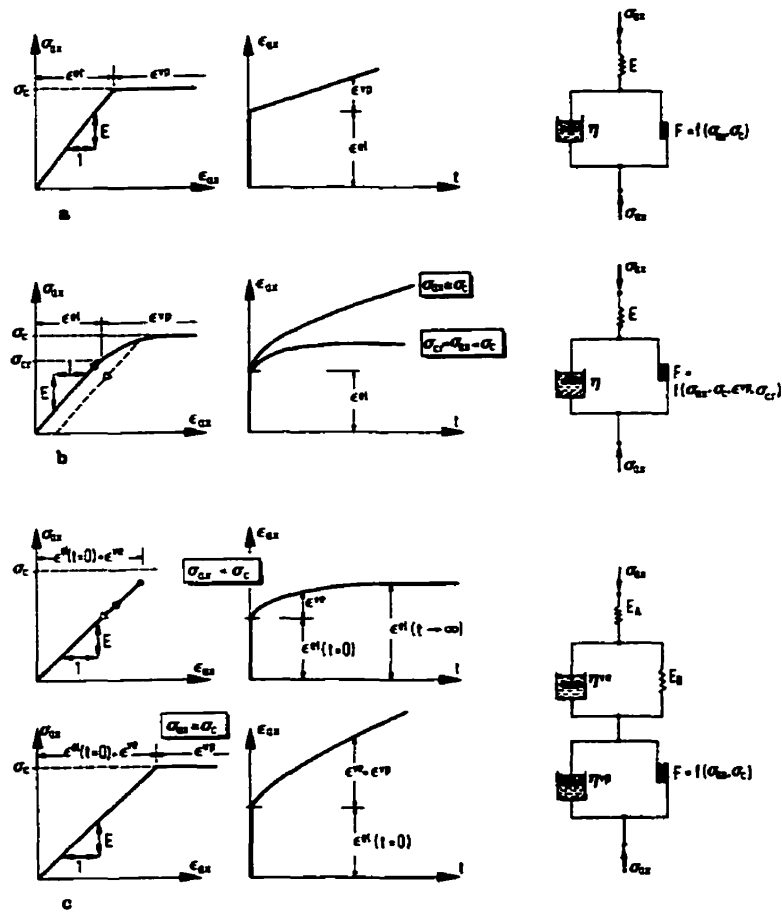
Figure 2.6 Constitutive laws of different materials (Wittke, 1990)

Linear elastic behaviour with:

a) ideally viscoplastic range b) viscoplastic range with hardening c) ideally viscoelastic range

Salomon (1968) regarded layered media as a continuous, transversely isotropic rock. Wittke (1977) applied an idealised three-dimensional constitutive model to static analyses of underground openings in jointed rock. Zienkiewicz et al. (1977) introduced the concept of representing a randomly jointed rock mass by a no-tension material and a multilaminate framework of models to study the time-dependant behaviour of a regularly jointed medium. Amadei and Goodman (1981) developed a three dimensional constitutive relation for jointed rock masses.

2.5 Equivalent elastic modulus in fractured rock

This section is devoted to the presentation of the equivalent elastic media theory. It implies also explanations about the background that led the author of this thesis to adopt a particular model simulating bedded rock masses to implement with the finite element method.

Equivalent continuum models for jointed rock masses are based on the assumptions that single or multiple sets of parallel joints exist in the rock mass, and that the precise location of the joints is unimportant.

The simplest of these models is linear, ascribing to the equivalent continuum elastic properties through superposition of the properties of the matrix and the joints – e.g. Morland (1976), Amadei and Goodman (1981), Gerrard (1982). These models usually represent specialisation of equivalent continuum for layered media – Salamon (1968), Gerrard (1982).

Of more relevance are the models in which the non-linear properties of the joints are considered, i.e. the ubiquitous models of Zienkiewicz and Pande (1977). In this models the joints "exist everywhere at the same time".

Before extending the concept of equivalent elastic media a concise review of the elasticity theory must be given.

A medium possesses the property of elasticity if the deformations associated with its loading are fully recovered upon unloading. In terms of a load deformation curve there is a one-to-one correspondence between load and deformation. If stress and strain are linearly related the material is said to be linear elastic.

A particularly attractive property of the linear elastic theory is the principle of superposition of effects. Furthermore, the applicability of the theory of elasticity is a function of the duration of loading. Elasticity assumes an immediate response upon the application or removal of load.

A common procedure for deriving the elastic properties of a rock mass is to assume that the rock mass is linearly elastic, isotropic, continuous and homogeneous, e.g. the empirical methods. However, any rock is to a certain extent anisotropic and/or heterogeneous and/or discontinuous and somewhat nonlinearly elastic.

In solid mechanics a medium is considered anisotropic if its properties vary with direction, it is heterogeneous if they vary from point to point and it is discontinuous if there are separations or gaps in the stress field. These three definitions are in general scale dependent. They depend upon the relative size of the smallest structural feature of the problem of interest with respect to the largest structural feature of the medium.

If we assume that the anisotropic rock material can be described as linear, elastic, homogeneous and continuous, its general constitutive relation relating stress and strain tensors can be written as follows:

$$\tau_{ij} = C_{ijkl} \in_{kl}$$ (2.2)

which is known as the Generalised Hooke's Law. In the most general 3D case, the tensor of elastic constants C_{ijkl} has 81 independent components, Lekhnitskii (1993).

However, by utilising the symmetry of τ_{ij} and $\in_{kl}$, and by assuming the existence of a strain-energy density function, the maximum number of independent elastic modulus reduces to 21, which represents the maximum possible degree of anisotropy and equation (2.1) can be rewritten as follows:

$$\{\in\} = [A] \{\sigma\}$$ (2.3)

2-21

in the arbitrary x, y, z coordinate system, or

$$\{\sigma\} = [D]\ \{\in\}$$

where:

$[A]^{-1} = [D]$ and $[D]$ is the elasticity matrix.
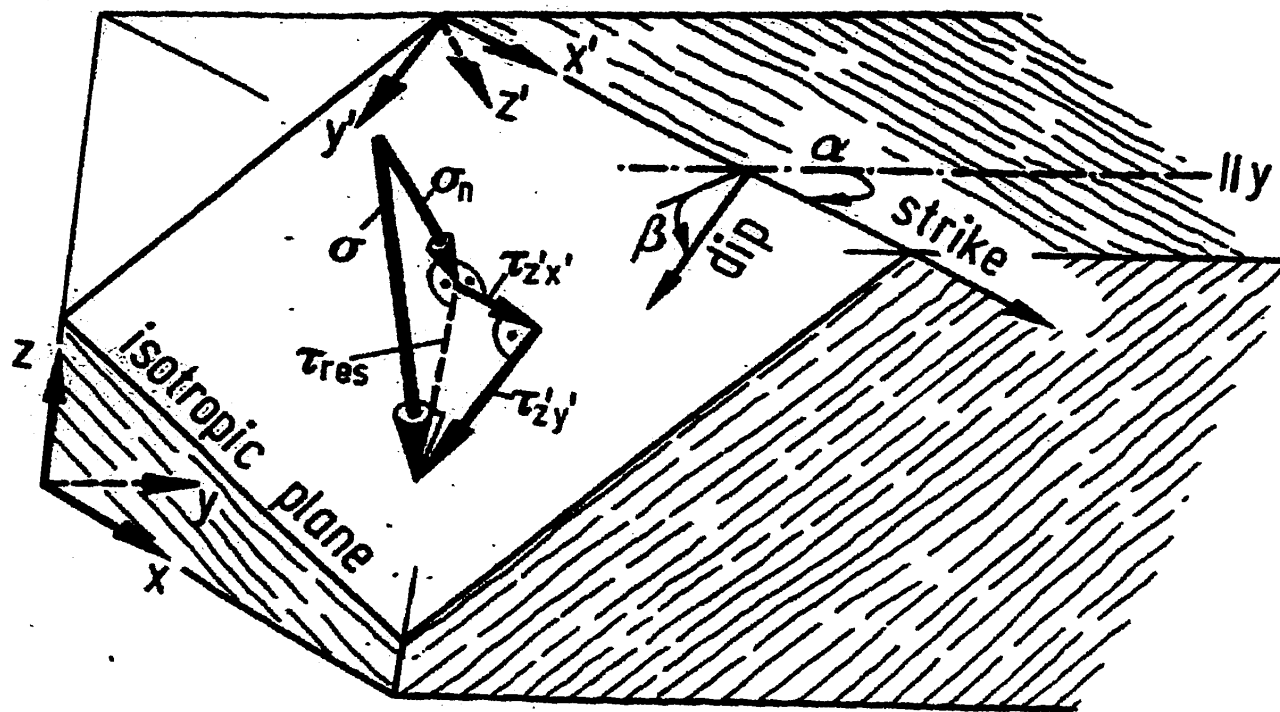
Figure 2.7 Geometry of the problem, definition of the coordinate systems (Wittke, 1990)

2-22

The matrix [A] with 21 independent elastic constants, describes the complete stress-strain relationship in three dimensions for a general anisotropic material. This number of constants is so large that it has been impossible to obtain them for any rock.

If the internal composition of the rock material possesses symmetry of any kind, then symmetry can be also observed in its elastic properties. So, the number of independent elastic constants is less than 21.

In the analysis of rock masses, four cases of elastic symmetry are of particular interest:

1. one plane of elastic symmetry
2. three orthogonal planes of elastic symmetry
3. one axis of elastic symmetry of rotation
4. complete symmetry.

A plane of elastic symmetry exists at a point if the elastic constants have the same value for every pair of coordinate systems that are the reflected image of one another with respect to the plane. The number of independent elastic constants is then reduced to 13.

If we assume that three orthogonal planes of elastic symmetry pass through each point of the rock, it can be shown that the number of independent elastic constants is reduced to 9, which are

- 3 Young's modulus E_x, E_y, E_z,
- 3 shear moduli G_{yz}, G_{xz}, G_{xy} and
- 3 Poisson's ratios υ_{yx}, υ_{xz} and υ_{zy}.

A rock mass that possesses this type of elastic symmetry is called <u>orthotropic</u>.

A rock mass that shows one axis of elastic symmetry of rotation is called transversely isotropic. Plane x0y of figure 2.7 and any plane perpendicular to it are planes of elastic symmetry. The number of independent elastic constants is reduced to 5. Accordingly, they are

- 2 Young's moduli $E = E_x = E_y$ and $E' = E_z$,

- 1 shear modulus $G' = G_{yz} = G_{xy}$, and

- 2 Poisson's ratios $\upsilon = \upsilon_{yx} = \upsilon_{xy}$ and $\upsilon' = \upsilon_{xz} = \upsilon_{zy}$.

Finally, if all planes and axes are one of elastic symmetry the rock mass is <u>isotropic</u>. The number of independent elastic constants is reduced to 2:

- 1 Young's modulus $E = E_x = E_y = E_z$ and

- 1 Poisson's ratio $\upsilon = \upsilon_{yx} = \upsilon_{zx} = \upsilon_{zy}$.

Many rock masses are stratified or bedded and are clearly non-homogeneous. They may be divided into several layers of randomly varying thickness and properties. Sometimes, only two types of rock are regularly interlayered. Since it does not seem feasible to take into account the individual properties and geometry of each stratum in any mechanical model of a stratified rock mass, it is more practical to replace the latter by an equivalent homogeneous continuum.

Salamon (1968), and Wardle and Gerrard (1972) have worked on this subject and their theories, which are reviewed in detail in the next section, have been used as a base for developing more complex constitutive laws by other authors.

In the case of anisotropy derived from regular discontinuities, the theory of linear elasticity is invalid. However, as mentioned in the previous section, numerical techniques such as the Finite Element Method or the Boundary Element Method can be used to incorporate the discontinuous character of rock masses, i.e. by joint elements, when modelling their deformability.

Another procedure is to replace the regularly jointed rock mass by a homogeneous, anisotropic and continuous medium, the behaviour of which is equivalent to the behaviour of the jointed rock mass. The work done by Singh (1973) on this subject is further discussed in detail. This procedure can be regarded as a special case of the one presented previously for stratified rock masses. It can also be used

when rock anisotropy is derived from regular discontinuities and the intrinsic character of the intact rock.

The concept of an "equivalent medium" can be also used to describe the non linear behaviour of a discontinuous, non-homogeneous and anisotropic body containing up to three orthogonal joint sets, as done by Amadei and Goodman (1981), and discussed later in this chapter as well. The intact rock between two joints is here assumed to behave in a linear elastic manner with up to three orthogonal planes of elastic symmetry, each on being parallel to one of the joint sets. The joints are modelled in a non-linear inelastic fashion in compression and decompression and in a linear or non-linear elastic fashion in shear.

The applicability of the concept of an equivalent medium for modelling the deformability of a stratified or a regularly jointed rock mass depends upon two conditions: a representative sample of the rock mass on the basis of which the equivalent homogeneous properties are calculated must contain a large number of layers of joints and, second, that representative sample must be sufficiently small to be exposed to a homogeneous stress distribution in the equivalent medium. Those two conditions can only be satisfied if the size of the problem to be dealt with is considerably larger than the average layer thickness or the joint set spacing.

2.5.1 Elastic moduli of a stratified rock mass – M.D.G. Salamon (1968)

Salamon's work was concerned with the rock mass surrounding coal seams. Such rock mass is usually strongly stratified and the elastic properties of the layers vary appreciably. While each stratum can be regarded as a homogeneous and transversely isotropic, the mass itself is clearly non-homogeneous. Salomon did not favour an approach to solve practical problems by taking into account the individual properties of all strata. Instead, he thought it would be more practical to introduce the concept of equivalent homogeneous continuum, which behaves in a manner similar to that of the stratified rock mass. He postulated that all layers are homogeneous, transversely isotropic and that their thickness and elastic properties vary randomly with the depth below surface.

Salmon's analysis is based on an examination of the behaviour of two cubes both having an edge dimension L. One of these cubes is cut from the rock mass and the other from the equivalent homogeneous medium. Assuming that the bedding planes are parallel, the rock cube is so cut that two of its sides are parallel with these planes. The cube must be sufficiently large to constitute a representative sample of the rock mass.

A cube so defined will possess certain elastic symmetry. Its behaviour will be invariant with respect to rotation around an axis perpendicular to the bedding planes and with respect to reflection in one of these planes. Salamon concluded, therefore, that the cube, and consequently the equivalent medium, would be transversely isotropic.

In order to establish relationship between the stresses and strains in the two cubes, the relations giving the average tensor stress and strain from the continuum mechanics theory are employed:

$$\sigma = 1/V \int \sigma dV \qquad (2.5)$$

$$\epsilon = 1/V \int \epsilon dV \qquad (2.6)$$

where V represents the volume of the cube, that is $V = L^3$.

The stress-strain relations of the equivalent medium are derived from the condition that the strain energies stored in the cubes cut from each of the materials should be equal. So:

$$U_r = U_e \qquad (2.7)$$

where U_r is the strain energy in the cube cut from the rock mass and U_e is the strain energy in the equivalent cube.

2-26

Based on this, Salamon shows that the five elastic constants of the equivalent transverse isotropic homogeneous continuum can be expressed in terms of the elastic properties and thickness of each layer:

$$\upsilon_1 = f(\upsilon_{1i}, E_{1i}, h_i)$$ (2.8)

$$\upsilon_2 = f(\upsilon_{1i}, \upsilon_{2i}, h_i)$$

$$E_1 = f(\upsilon_{1i}, E_{1i}, h_i)$$

$$E_2 = f(\upsilon_{1i}, \upsilon_1, \upsilon_{2i}, \upsilon_2, E_{1i}, E_1, E_{2i}, h_i)$$

$$G_1 = f(G_{1i}, h_i)$$

$$G_2 = f(G_{2i}, h_i)$$

where $i = i^{th}$ layer, h_i = thickness of the ith layer.

2.5.2 The equivalent anisotropic properties of layered rock and soil masses – L. J. Wardle and C. M. Gerrard (1972)

In their work, Wardle and Gerrard showed that there are restrictions on the ranges of permissible variation of some of the five characteristic elastic constants previously derived by Salamon for the general case.

Furthermore, they gave consideration to the special cases in which:

1. the Poisson's ratios are equal in all layers,
2. all layers are incompressible and
3. the shear moduli are equal in all layers.

As a result, Wardle and Gerrard developed charts that allow for rapid assessment of the properties of the equivalent medium for a range of two material systems, thus facilitating the application of the elastic solutions for homogeneous, transversely isotropic bodies to layered media.

2.5.3 Continuum characterisation of jointed rock mass – B. Singh (1972)

Singh (1972) developed an anisotropic continuum model in which the average influence of joints, bedding planes and similar planar features can be taken into account. Singh stated that the work done by Salamon who used anisotropic continuum theory to describe rock mass have brought a limited progress due to the imposed restrictions of the general solution.

Furthermore, he believes that the reason for the lack of a continuum model applicable for more general jointed rock mass systems is the increased mathematical complexity of such problem. So, he used a different approach by assuming a new model for the joints.

In this model, the joints are considered as a surface of discontinuity in the rock mass along which displacements are uniquely related to the corresponding stresses. In the continuum characterisation, the joints and the intact rock are considered the two component phases of an elastic system. Thus, Singh has used the elasticity theory of composite materials as a base upon which to develop the characterisation.

This theory differs somewhat from the corresponding problem of determining the elastic behaviour of a rock mass, in that that in the latter the actual behaviour of the joint phase is rather unknown. It states that the rock mass may be regarded as a composite material involving two main components, i.e. relatively intact blocks and joints or planes of discontinuity, and makes several assumptions concerning the interaction between the various phases of the material. The stress strain relations are derived from the energy equations.

It was shown that the energy equation

$$W = f([B_j])$$
(2.9)

where $[B_j]$ is a matrix that relates the average of the stresses in the jth phases to the overall average stress. It is termed as stress concentration factor. Singh showed that any problem in composite elasticity may then be completely and simply solved by determining the matrix $[B_j]$.

As a result Singh derived the constitutive equations to characterise an anisotropic rock containing two orthogonal sets of joints.

2.5.4 A 3D constitutive relation for fractured rock mass – B. Amadei and R. Goodman (1981)

The purpose of the Amadei and Goldman's work was to introduce a constitutive relation describing the non linear behaviour of a discontinuous, homogeneous and anisotropic body of rock containing up to three orthogonal joints sets. Together with 1982's Gerald's works, this work is a milestone in the study of jointed rock masses.

Here, the intact rock is assumed to behave in a linear elastic manner with up to three orthogonal planes of symmetry parallel to the joint sets. The joint sets are modelled to behave in a non-linear inelastic fashion in compression and decompression, and in a linear or non-linear elastic fashion in shear. For each joint set, the normal stiffness kn is expressed in terms of the normal stress acting on it and properties such as the seating pressure and maximum closure. The jointed rock mass is described as an equivalent anisotropic continuum.

For Amadei and Goodman (1981), the basic problem to be addressed in proposing constitutive relations for jointed rocks is the mechanical behaviour of a single discontinuity surface. This discontuinity can produce a jump in tangential stresses since it becomes an interface between bodies behaving dissimilarly.

So, their discussion centres on the stress–deformation relations for jointed rocks and makes use of an equivalent anisotropic medium concept. It begins with a description of the behaviour of a single joint, takes up the concept of equivalent anisotropic media, and considers the effect of water pressure on deformations.

In order to fully understand Amadei and Goldman's work, their theory on the behaviour of the joint under changing normal stress with constant shear stress is briefly reviewed.

There are a number of parameters that are fundamental for a proper model of joint behaviour; these include peak and residual shear strengths, maximum joint closure, tensile strength, shear and normal stiffness and dilatancy properties.

The experiments conducted by Goodman in 1976, led to establish a normal pressure-deformation curve describing the behaviour of joints under changing normal stress with constant shear stress. This curve is hyperbolic as shown in Figure 2.8
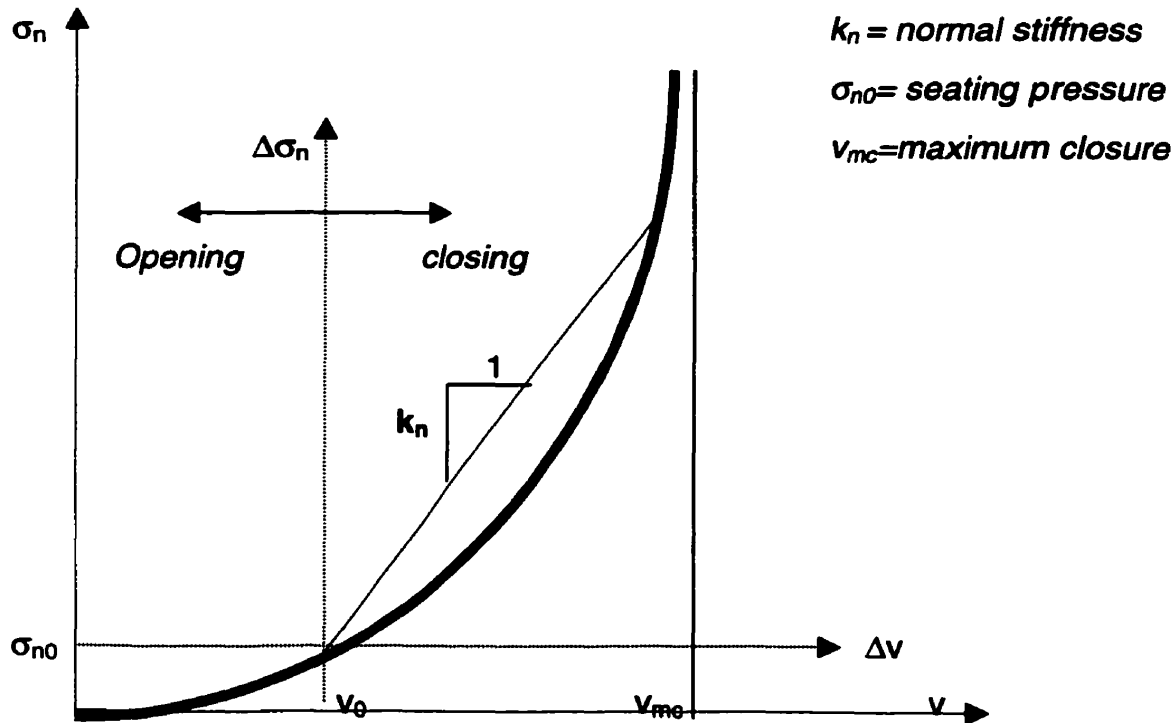
Figure 2.8 Idealised normal stress-deformation of a joint (Goodman, 1976)

and is expressed by:

$$\sigma_n = A[v \, / \, (v_{mc} - v)]^t \tag{2.10}$$

where v represents the difference in normal displacements across the joint and A, t are constants defined by curve fitting. The seating pressure σ_{n0} defines the initial conditions to measure the relative normal deformation Δv such that:

$$\Delta \sigma_n = \sigma_n - \sigma_{n0} \tag{2.11}$$

and

$$\Delta v = v - v_0 \tag{2.12}$$

Combining the three above-mentioned equations, Amadei and Goodman define the secant normal stiffness kn as follows:

$$\Delta v \, / \, \Delta \sigma_n = 1 \, / \, k_n = (v_{mc} \, / \, \Delta \sigma_n) \, f(A, t, \Delta \sigma_n, \sigma_{n0}) \tag{2.13}$$

or as the slope of the normal stress deformation curve, then:

$$k_n = \partial \sigma_n \, / \, \partial v \tag{2.14}$$

In both cases, k_n is a function of the normal stress applied across the joint.

Now let us consider the behaviour of a joint under changing shear stress with constant normal stress. Such a deformation curve can be characterised by elastic, peak and post-peak regions as depicted in Figure 2.9:
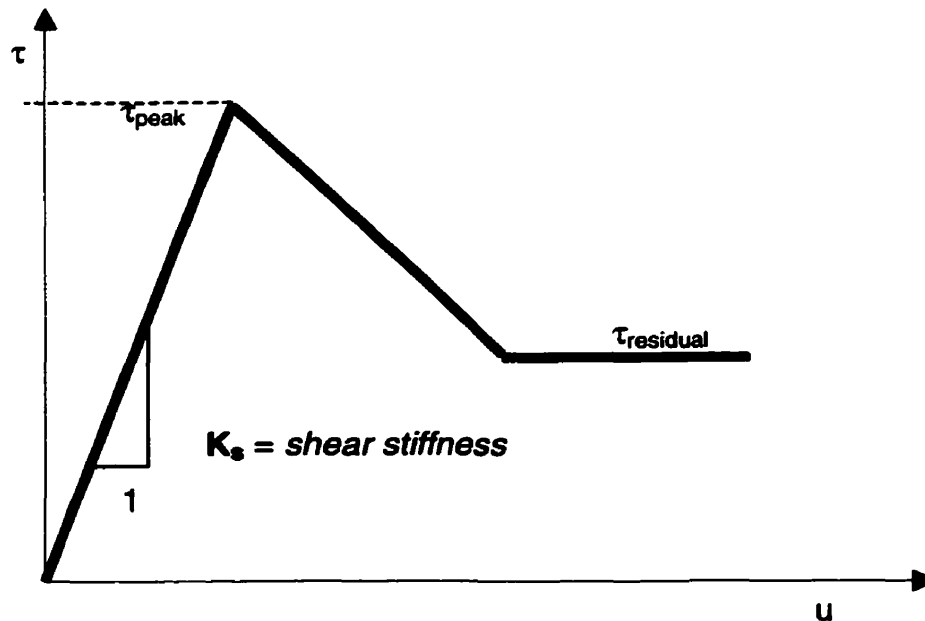
Figure 2.9 Idealised shear stress-deformation of a joint

Peak and residual shear strengths and their relative importance as well as the shear stiffness are greatly influenced by the joint type, joint properties, filling material, state of applied stress and testing procedures. Note that the slope characterising the elastic region is termed the unit shear stiffness k_s.

The definitions of the normal and shear stiffness in previous sections are precise when there is no dilatancy. As a brief recall, dilatancy means volumetric change accompanying deformation. It can also connote thickening or thinning of a discontinuity undergoing shear deformation at constant normal stress; so, the term dilation is used to connote an increase in the separation of the two joint blocks, as opposed to contraction which connotes a closing of a joint. As a result, Amadei and Goodman propose a more general constitutive relation for a joint taking into account its dilatancy. This relation is a function of four stiffness components that can be determined theoretically and/or experimentally.

Regarding the concept of an equivalent anisotropic continuum for an isotropic body with one joint set, Amadei and Goodman (1981) assume the intact rock is linearly elastic and isotropic with two

constants: Young's modulus E and Poisson's ratio v. The deformations within jointed rocks subjected to both normal and shear stresses result from compressive and shear strains within the rock between the joints and from interface normal and shear displacements on the joints. They considered a basic unit consisting of a single thickness of rock and a single joint as follows:

$\delta 1,4 = f(joint)$
$\delta 2,3 = f(intact$
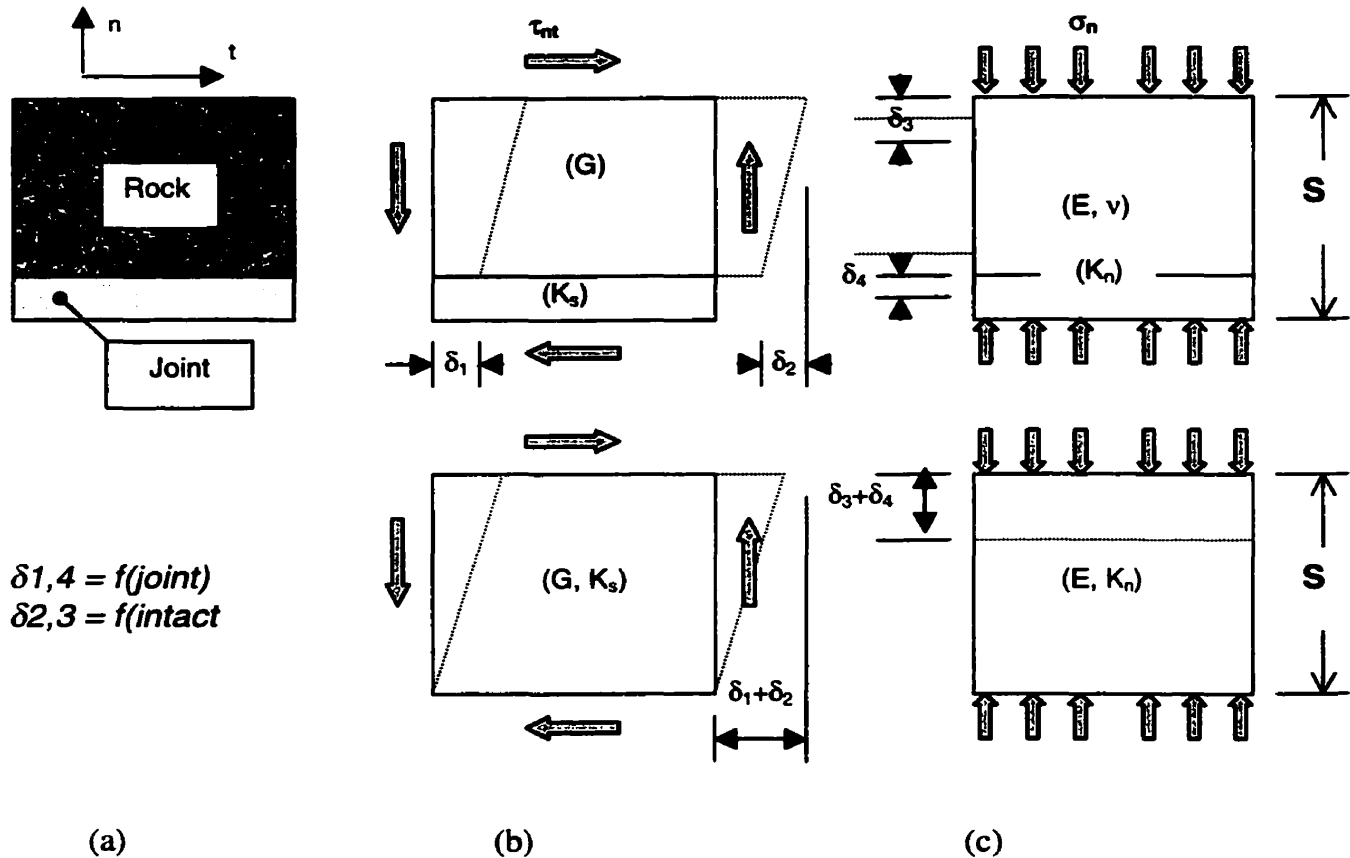
Figure 2.10 Concept of the equivalent anisotropic continuum: (a) basic unit, (b) behaviour in shear, (c) behaviour in normal compression

They adopt the axes n, t normal and parallel to the joint and therefore in the principal symmetry directions of the rock mass.

● The basic concept of the model is to replace the jointed body by an equivalent anisotropic continuum. As a result, shear and normal deformations of the equivalent continuum are equal to those of the jointed body. In the plane (n, t), the equivalent medium is described by two moduli: a shear modulus G_{nt} such that:

$$1 / G_{nt} = (1 / G) + [1 / (k_s \times S)] \qquad (2.15)$$

where $G = E / [2 \times (1 + v)]$ is the shear modulus of the intact rock and S the spacing between two joints − note that the joint thickness must be negligible compared with S − and a normal modulus E_n such that:

$$1 / E_n = (1 / E) + [1 / (k_n \times S)] \qquad (2.16)$$

As shown by the two latter equations, only four elastic constants are required to describe such a material: E, v, k_s, k_n.

The same concept is then introduced when the rock between the joints is itself anisotropic, for example, transversely anisotropic within a plane parallel to the joint set. In this case seven constants are needed to describe the material. This model can be applied to the deformability of layered, schistose rocks.

For the more general case of a body with three orthogonal joint sets, an equivalent orthotropic continuum, Amadei and Goodman (1981) proposed a solution assuming again that each joint set has a negligible thickness and does not create any Poisson's ratio effect, the constitutive relation of this equivalent orthotropic continuum is defined as follows:

$$\{\in\} = [A] \times \{\sigma\} \qquad (2.17)$$

where $[A] = [A]_{intact\ rock} + [A]_{joints}$, with the equivalent Young's modulus E_i^* defined by:

●

$$1 / E_i^* = (1 / E_i) + [1 / k_{ni} \times S_i)]$$ (2.18)

and the equivalent shear modulus G_{ij}^* defined by:

$$1 / G_{ij}^* = (1 / G_{ij}) + [1 / (k_{si} \times S_i)] + [1 / (k_{sj} \times S_j)]$$ (2.19)

where the index * refers to equivalent moduli, the index $_i$ and the index $_j$ refer to the intact rock and the joints respectively. If the orientation of the joint sets with respect to a fixed system of coordinates (x, y, z) is known, we can rewrite the relation (2.17):

$$\{ \epsilon \}_{x,y,z} = [D]_{x,y,z} \times \{ \sigma \}_{x,y,z}$$ (2.20)

Amadei and Goodman's work (1981) reports also the closed form solutions for uniaxial and triaxial loading which were derived to demonstrate the applicability of the proposed constitutive relation.

2.5.5 Equivalent elastic moduli of a rock mass consisting of orthorhombic layers – C. M. Gerrard (1982)

In his analysis of a system of orthorhombic layers here briefly presented, Gerrard closely followed the previous analysis of Salamon (1968) for a system of cross-anisotropic layers. Salamon expressed the elastic properties of the equivalent material in terms of the thickness and elastic properties of the constituent layers. His analysis was extended by Wardle and Gerrard who considered special cases of compressibility and shear moduli in the respective layers, as well as the case of alternating two layer systems.

In the present work, equivalent elastic properties are given for a system of parallel layers, each of which consists of a homogeneous orthorhombic elastic material. This means that the material properties of each layer have three mutually perpendicular planes of symmetry.

The layers are aligned so that each set of three planes is respectively perpendicular to a single set of Cartesian coordinates x_1, x_2, x_3. The x_3 direction is chosen to be normal to the layering planes and hence for each layer one of the planes of elastic symmetry of the material properties is parallel to the layering planes.
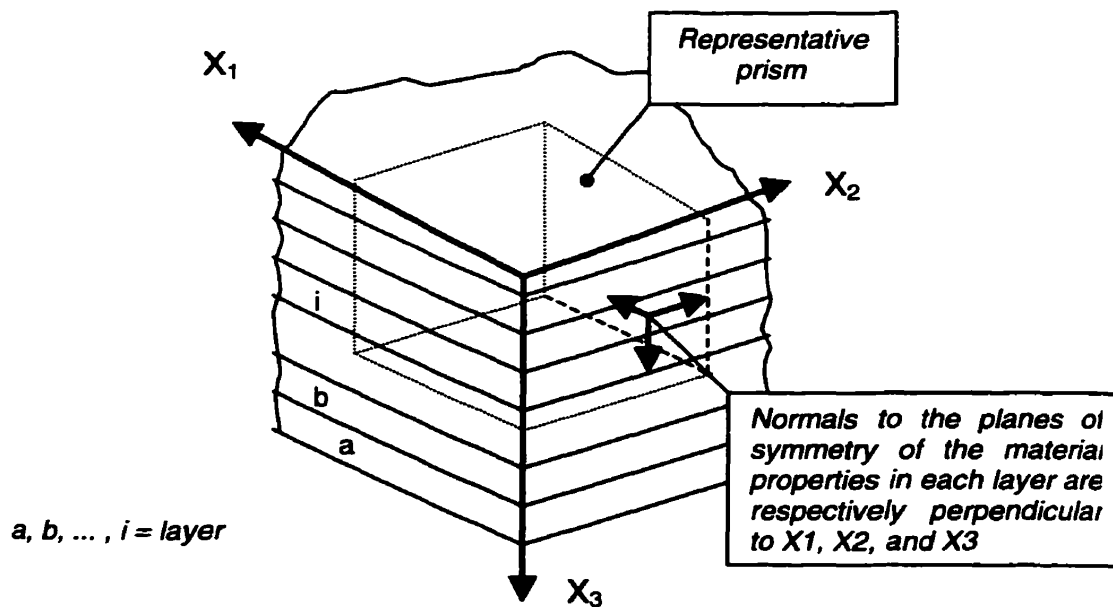
Figure 2.11 Orthorhombic body, definition of the geometry

This definition is the base of the major contributions to the previous work by Salamon, Wardle and Gerrard. Gerrard derived the equivalent elastic properties for the particular case of two alternating orthorhombic layers. They are expressed by the nine equivalent elastic parameters v_{12}, v_{13}, v_{23}, E_1, E_2, $1/E_3$, G_{12}, $1/G_{13}$, $1/G_{23}$, where the subscripts refer to the x-s axis directions.

2.5.6 Elastic models of rock masses having one, two and three sets of joints – C.M. Gerrard (1982)

Gerrard (1982) extended his previous analysis for the general case for one, two and three sets of perpendicular joints. Stephansson (1981), Duncan and Goodman (1968) and Amadei and Goodman (1981) had already discussed theories covering this topic. Stephansson's method (1981), based on consideration of the load-deformation behaviour while Gerrard used a strain-energy criterion, which gave similar results for most practical cases.

The works of Duncan and Goodman (1968) and Amadei and Goodman (1981) have the limitation of imposing a negligible joint thickness with regard to the joint spacing. Gerrard's analysis firstly covers the general case where the joint material can have any thickness and can have general properties. He did use of the orthorhombic layer theory discussed in the previous section. This theory is then applied in one coordinate direction for the case of a single set of joints, or repeatedly applied in two or three coordinate directions for the respective cases of two or three sets of orthogonal joints.

As a result, Gerrard (1982) established a table relating the material properties to the equivalent material properties for one, two and three sets of joints, where the general equation has the following form:

$$E_k = F_1(t_i, t_j, E_i, E_j) \qquad (2.21)$$

where F_1 is a functional defined by a relation involving the elastic parameters. The indices $_i$ and $_j$ refer to the moduli for intact rock and joints respectively.

Finally, Gerrard extended his work to a particular case simplifying the computations, especially when the joint thickness is negligible. Such case is represented by a jointed system having thin, soft joints.

2.5.7 Effective elastic properties for a randomly jointed rock mass – A.F. Fossum (1985)

In his technical note, Fossum (1985) derived a constitutive model for a randomly jointed rock mass behaving elastically based on the study conducted by Amadei and Goodman (1981).

Fossum (1985) has then used a geometric averaging process to determine isotropic effective properties. He has finished his analysis proposing the effective isotropic properties $E_{average}$ and $v_{average}$ which can be determined from the effective bulk and shear moduli, $K_{average}$, $G_{average}$. So:

$$E_{average} = (9 \times K_{average} \times G_{average}) / [3 \times (K_{average} + G_{average})] \qquad (2.22)$$

and

$$v_{average} = (3 \times K_{average} - 2 \times G_{average}) / 2 \times [3 \times (K_{average} + G_{average})] \qquad (2.23)$$

where $K_{average}$, $G_{average}$ = f (joint spacing, joint stiffness, E, v).

Here again, the joint thickness is considered negligible compared with the joints spacing. Note that in the limit as the joint spacing becomes large, $K_{average}$ and $G_{average}$ reduce to the familiar relations between isotropic properties of an intact body, i.e.:

$$K_{average} = E / [3 \times (1 - 2v)] \qquad (2.24)$$

and

$$G_{average} = E / [2 \times (1 + v)] \qquad (2.25)$$

2.5.8 Joint stiffness and the deformation behaviour of discontinuous rock – R. Yoshinaka and T. Yamabe (1986)

In their work, Yoshinaka and Yamabe (1986) have investigated in depth the behaviour of the single joint following the concept of joint stiffness proposed by Goodman (1981).

The analysis of compressibility k_n stiffness and shear stiffness k_s was carried out in great detail as well as a study of the relation between them. As a result they proposed a relation which is convenient from the practical point of view for estimating one stiffness from another.

Using the idea of the deformation of joints in a rock mass, Yoshinaka and Yamabe (1986) consider the deformation of a jointed rock mass as the summation of the deformations of joints and intact rock. An equivalent deformation modulus E_t and shear modulus G_t have been then proposed taking into account the dip and properties of two sets of joints and intact rock as shown below:
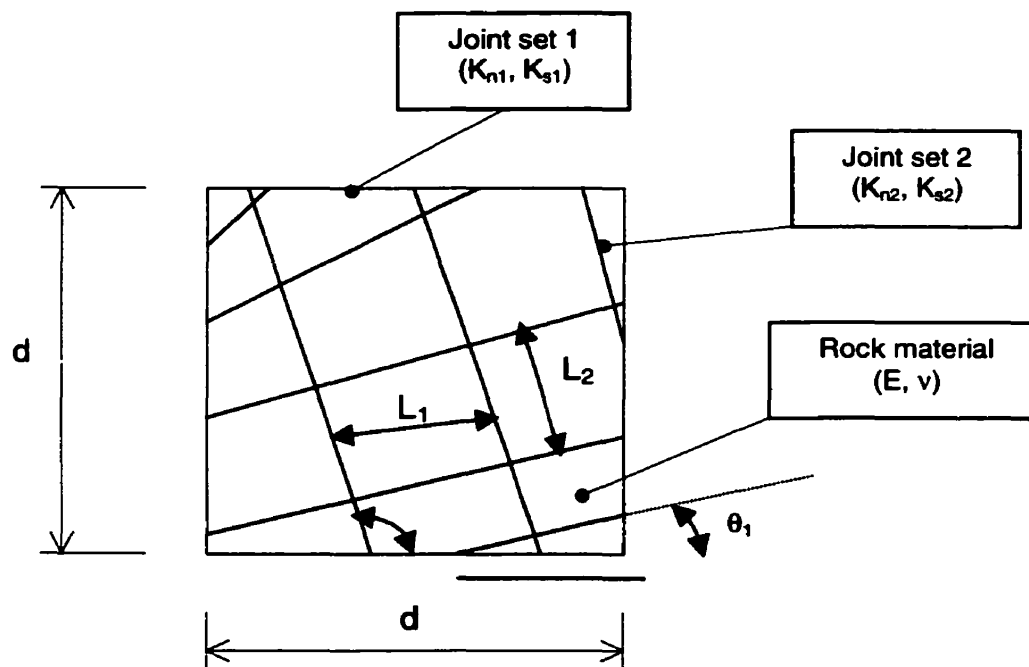
Figure 2.12 Mechanical model for jointed rock mass with two sets of joints

The limitation of two joint sets is accompanied by the condition that the dip of these joints is parallel to the axis of minimum principal stress σ_3.

2.5.9 Estimation of the elastic properties of fractured rock masses – K.X. Hu and Y. Huang (1993)

The approach used in this work for determining the effective elastic moduli of a fractured body consists of considering the joint as a non-persistent crack. Three kinds of in plane crack orientations are studied by the authors: randomly distributed cracks, parallel distributed cracks and two sets of perpendicular cracks.

The matrix material (uncracked rock) is considered isotropic while the rock mass shows an orthotropic behaviour. The resulting expressions of the effective elastic moduli E, G and v are related to the intact rock moduli and the crack planar density.

These expressions are here below reported for the case of randomly distributed cracks (Hu and Huang, 1983):

$$E_{average} / E = (1 - v) / (1 - v^2\epsilon) \tag{2.26}$$

$$V_{average} = v(1 - \epsilon) / (1 - v^2\epsilon) \tag{2.27}$$

$$G_{average} = 1 - (1/2 \times \epsilon) \tag{2.28}$$

where ϵ = planar crack density $[m/m^2]$ and E, v, G are the elastic parameters of the intact rock.

2-40
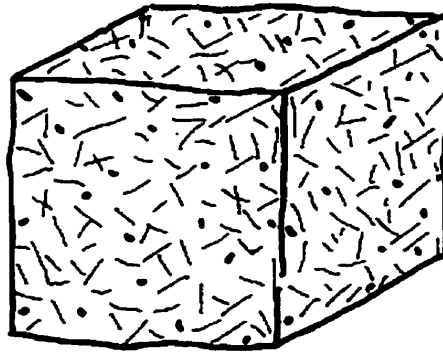
Figure 2.13 Schematic diagram of a distribution of random cracks

2.5.10 Elastic moduli for fractured rock mass – T.H. Huang, C.S. Chang and Z.Y. Yang (1995)

The work done by these authors aimed to derive close-form expressions of elastic moduli for rock masses with three sets of non-orthogonal intersecting joints. These expressions are derived explicitly in terms of properties of joints and intact rock. Related to such expressions is the proposed stress-strain model for an assemblage of intact rock blocks separated by joint planes. The model accounts for spacing and orientation of the joint sets.

Basically, Huang et al. (1995) assume that a rock mass consisting of M sets of joints subjected to a small increment of stress has a corresponding incremental strain which consists of two components: one include from the movements of the M sets of joints and the other from intact rock deformation. The joints behaviour is assumed to be the same in all directions on the joint plane concerning the deformation and neglecting the effect of shear displacement caused be the normal stress.

Based on these assumptions, the constitutive constants are derived by the authors for a rock mass with three intersecting sets of joints as shown in Figure 2.13:
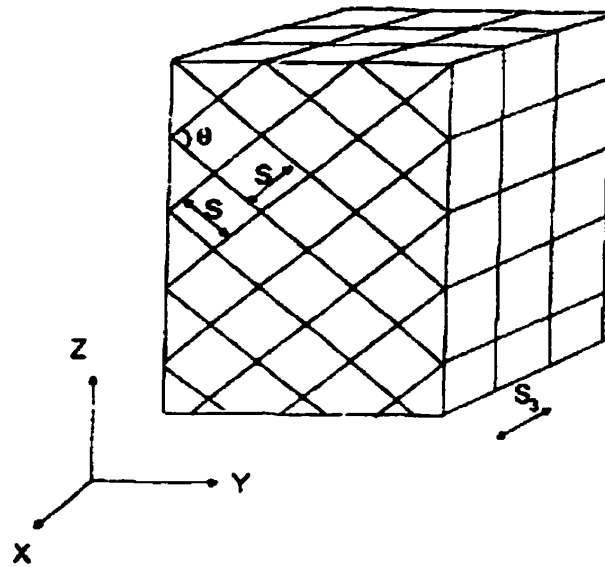
Figure 2.14 Geometry definition

However, the first two sets of joints are assumed to have the same joint stiffness k_n and k_n, which are different from the joint stiffness k_{n3} and k_{s3} of the third joint set. Similarly, the spacing is the same for the first two sets.

The resulting elasticity matrix takes into account the properties of intact rock namely Young's modulus E, shear modulus G and Poisson's ratio v, as well as the properties of the joints by joint Young's modulus E_x, E_y, E_z and joint shear modulus G_x, G_y, G_z.

The expressions of the joint modulus are functions of the stiffness, spacing and orientations of the joint sets given by the angle. When the angle $\theta = 90°$, the expressions of the elastic parameters reduce to the expressions proposed by Amadei and Goodman (1981) and discussed in a previous section.

Chapter 3

FINITE ELEMENT MODEL

3.1 Constitutive model

The discussion in the previous chapter has clearly shown how strongly the pattern of fabric of joints can influence the rock mass behaviour. Otherwise stated, the pattern of fabric of joints will govern the deformational and strength properties of rock masses.

During the last decade, many authors have based their analysis on these models in the attempt to generalise them proposing an equivalent media model including a random set of joints. However, no one has completely succeeded in this task because of the difficulty to gather simple input data with reliable simulation results. Currently, the most popular models reproducing a constitutive law for the rock mass which take into account the fabric of joints are those of Amadei and Goodman (1981) presented in section 2.5.4 of the previous chapter. Those models have been appreciated by the scientific community for their completeness, their practical aspects regarding the determination of the parameters and their relative simplicity.

Therefore, the author of this thesis has adopted the conceptual model proposed by Amadei and Goodman for a rock mass characterized by one family of discontinuities. The model is then formulated for the implementation into a two-dimensional finite element code.

3.2 Finite element equations

Finite element method has been increasingly applied in solving geotechnical problems. The finite element mesh employs in this case of two-dimensional analysis a 4-node isoparametric element shown in Figure 3.1 with its local system of coordinates (s, t).
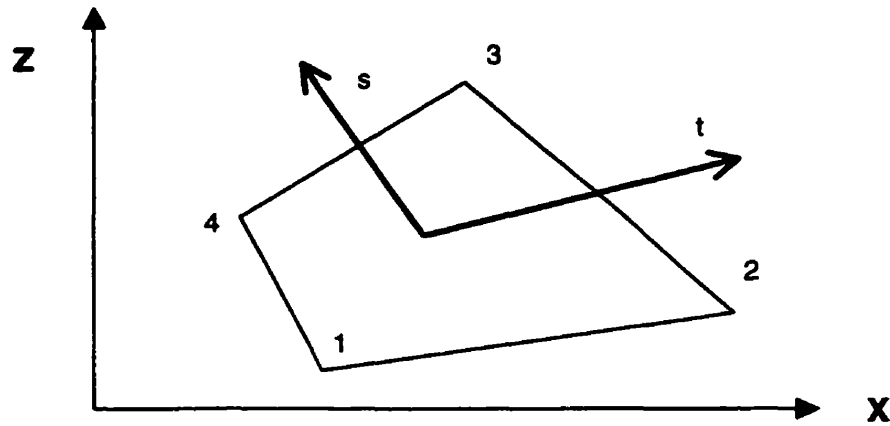
Figure 3.1 Isoparametric 4-node element in the global and local systems of coordinates

The global coordinates (x, z) of any point in the element are related to the local coordinates (s, t) through the following equations:

$$x = [N]\{X\}$$ (3.1)
$$z = [N]\{Z\}$$

where <N> is an array of interpolating shape functions and {X} as well as {Z} are the global x, z coordinates of the element nodes. The shape functions are expressed in terms of local coordinates and have the following form for the 4-node isoparametric element:

$$N_1 = \tfrac{1}{4}(1 - s)(1 - t)$$ (3.2)
$$N_2 = \tfrac{1}{4}(1 + s)(1 - t)$$
$$N_3 = \tfrac{1}{4}(1 + s)(1 + t)$$
$$N_4 = \tfrac{1}{4}(1 - s)(1 + t)$$

In order to formulate the finite element equations, it is necessary to adopt a model for the field variable within the element. In the deformation and stress analysis, the field variable is the total deformation (δ) and a model has to be adopted for its variation within the

element. The code hereby presented considers that the total deformation within the element follows the interpolating functions presented above, which means that the distribution of the deformations is bilinear. The distribution of the total deformation in the element is summarized by the following equation:

$$\{\delta\} = \{u,v\} = [N_{(s,\,t)}]\{\delta^e\} \tag{3.3}$$

where: δ = deformation at any point,

[N] = shape function matrix,

$\{\delta^e\}$ = vector of deformations at the nodes.

Problems in solid mechanics frequently involve description of the stress distribution in a body in static equilibrium under the combined action of surface and body forces. Determination of the stress distribution must take into account the requirement that the stress field maintains static equilibrium throughout the body. This condition requires satisfaction of the equations of static equilibrium for all differential elements of the body.
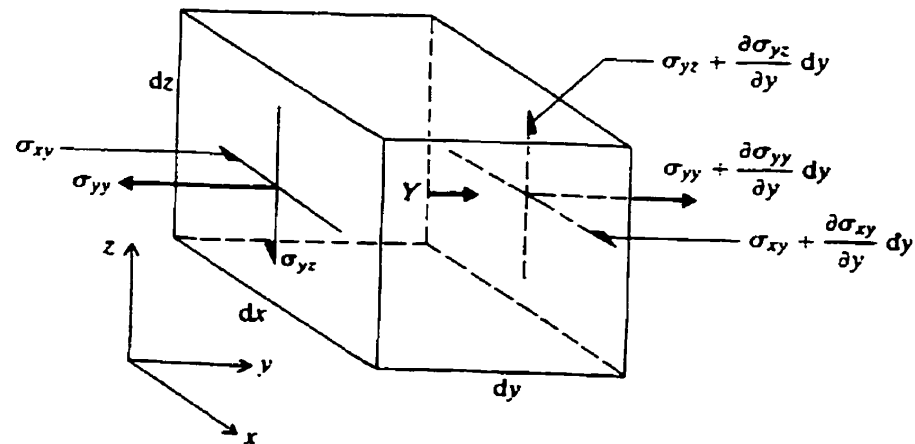
Figure 3.2 Free-body diagram for the development of the differential equations of equilibrium (Brady and Brown, 1992)

The stress distribution in the body is described in terms of a set of stress gradients and can be written in a tensor form as follows:

$$\frac{\partial \tau_{ij}}{\partial x_j} + F_i = 0 \qquad (3.4)$$

where τ_{ij} is the stress tensor and F_i represents the applied body forces.

The static equilibrium equations have been adapted to the needs of a two-dimensional finite element code giving the analytical formulation for the element static equilibrium. In displacement finite element method, equilibrium is expressed by the conventional equation:

$$\{P\} = [K]\{\delta\} \qquad (3.5)$$

where: $\{P\}$ = global load vector,

$\quad\quad$ [K] = global stiffness matrix,

$\quad\quad$ $\{\delta\}$ = displacements vector

In the finite element formulation, the element stiffness [k] is a key parameter. The procedure used to compute the stiffness is presented below.

The strains are defined by Lekhnitskii (1963) in his theory of elasticity for small displacements as:

$$\varepsilon_x = \frac{\partial u}{\partial x}$$

$$\varepsilon_z = \frac{\partial v}{\partial z} \qquad (3.6)$$

3-4

$$\gamma_{xz} = \left(\frac{\partial u}{\partial z} + \frac{\partial v}{\partial x} \right)$$

or, in term of product of a matrix and a vector, as:

$$\begin{Bmatrix} \varepsilon_x \\ \varepsilon_z \\ \gamma_{xz} \end{Bmatrix} = \begin{bmatrix} \dfrac{\partial}{\partial x} & 0 \\ 0 & \dfrac{\partial}{\partial z} \\ \dfrac{\partial}{\partial z} & \dfrac{\partial}{\partial x} \end{bmatrix} \begin{Bmatrix} u \\ v \end{Bmatrix} \tag{3.7}$$

where the matrix in the above equation is called [L] and is a differential operator.

The shape functions are given in terms of local coordinates s ant t, and must be computed in terms of the global coordinates. Toward this end and starting from the relationship between the strains and the displacements presented in (3.6), the strains within the element are expressed with the aid of (3.7) as function of the nodal point displacements. The following is obtained:

$$\{ \varepsilon \} = \begin{Bmatrix} \dfrac{\partial u}{\partial x} \\ \dfrac{\partial v}{\partial z} \\ \dfrac{\partial u}{\partial z} + \dfrac{\partial v}{\partial x} \end{Bmatrix} = \begin{Bmatrix} \displaystyle\sum_{i=1}^{m} \dfrac{\partial N_i}{\partial x} u_i \\ \displaystyle\sum_{i=1}^{m} \dfrac{\partial N_i}{\partial z} v_i \\ \displaystyle\sum_{i=1}^{m} \dfrac{\partial N_i}{\partial z} u_i + \dfrac{\partial N_i}{\partial x} v_i \end{Bmatrix} \tag{3.8}$$

To set up the right-hand side matrix of equation (3.8), the derivatives of the shape functions, which are available as functions of the local coordinates s, t, are required with respect to the global coordinates x, z. These unknown quantities may be advantageously combined using the chain rule of differentiation as follows:

3-5

$$\left\{\begin{array}{c} \dfrac{\partial N_i}{\partial s} \\[2mm] \dfrac{\partial N_i}{\partial t} \end{array}\right\} = \left\{\begin{array}{c} \dfrac{\partial N_i}{\partial x}\dfrac{\partial x}{\partial s} + \dfrac{\partial N_i}{\partial z}\dfrac{\partial z}{\partial s} \\[2mm] \dfrac{\partial N_i}{\partial x}\dfrac{\partial x}{\partial t} + \dfrac{\partial N_i}{\partial z}\dfrac{\partial z}{\partial t} \end{array}\right\} \tag{3.9}$$

The right-hand side of (3.9) may be presented as the product of a matrix and a vector. Thus:

$$\left\{\begin{array}{c} \dfrac{\partial N_i}{\partial s} \\[2mm] \dfrac{\partial N_i}{\partial t} \end{array}\right\} = \left[\begin{array}{cc} \dfrac{\partial x}{\partial s} & \dfrac{\partial z}{\partial s} \\[2mm] \dfrac{\partial x}{\partial t} & \dfrac{\partial z}{\partial t} \end{array}\right] \left\{\begin{array}{c} \dfrac{\partial N_i}{\partial x} \\[2mm] \dfrac{\partial N_i}{\partial z} \end{array}\right\} \tag{3.10}$$

where the matrix of (3.10) is the Jacobian matrix [J]. Performing matrix operations, the derivative of the interpolating function with respect to x and z can be determined, and the equation is rewritten as:

$$\left\{\begin{array}{c} \dfrac{\partial N_i}{\partial x} \\[2mm] \dfrac{\partial N_i}{\partial z} \end{array}\right\} = [J]^{-1} \left\{\begin{array}{c} \dfrac{\partial N_i}{\partial s} \\[2mm] \dfrac{\partial N_i}{\partial t} \end{array}\right\} \tag{3.11}$$

As a result of appropriate combination of all the above vectors, the strain equation can now be written in matrix form as:

$$[\epsilon] = [B]\{\delta^e\} \tag{3.12}$$

where: $[B] = [L][N] =$ strain-displacement matrix

$\{\epsilon\} =$ strain vector

$\{\delta^e\} =$ nodal displacements vector (u, v)

In the previous paragraphs, it is stated that the strain within the element can be expressed in terms of the nodal displacements. The computation of the strain-displacement matrix

[B], which contains the derivatives of the shape functions expressed in local coordinates $N_i(s, t)$ with respect to the global coordinates, has been also dealt with.

The determination of the equivalent elastic properties of the rock mass plays a crucial role in the finite element code since it is the material's variable within the stiffness matrix as also mathematically stated in (3.3).

Stresses and strains in a two-dimensional Cartesian coordinate system (x, z) are related in the familiar manner according to Hook's law by the constants of elasticity E and v:

$$\sigma_x = \frac{E}{1-v-2v^2}[(1-v)\varepsilon_x + v\varepsilon_z]$$

$$\sigma_z = \frac{E}{1-v-2v^2}[v\varepsilon_x + (1-v)\varepsilon_z] \qquad (3.13)$$

$$\tau_{zx} = \frac{E}{2(1+v)}\gamma_{zx}$$

The matrix form is stated in Chapter 2 by (2.4) and relates the stress vector to the elastic strains:

$$\{\sigma\} = [D]\{\varepsilon\} \qquad (3.14)$$

The following expression for the stress vector within the element in terms of nodal point displacements is obtained by combining (3.12) and (3.14):

$$\{\sigma\} = [D][B]\{\delta^e\} \qquad (3.15)$$

Now that a relationship between the stresses and the strains in the element stiffness matrix and load vector has been established, a displacement based formulation procedure using the Virtual Work Principle will be adopted to derive the element.

The Principle of Virtual Work is an independent formulation procedure for finite element equations based on assuming a displacement function, which despite the alternatives shown in the following Figure 3.3, still being a much more widely used method. The presentation to follow in this chapter will thus focus on the formulation of element stiffness matrix needed in the displacement method.

```
                        FE formulative procedures
  ┌──────────┬──────────────┬──────────────┬──────────────┬──────────────┐
  direct       ▓▓▓▓▓▓▓▓▓      stationary     weighted        variational
  formulation  ▓▓▓▓▓▓▓▓▓      potential      residual        method
                              energy
         ┌──────────┐              ┌──────────┬──────────┐
      ▓▓▓▓▓▓▓▓    virtual       Galerkin   collocationa    least
                  forces        method     l method        square
```
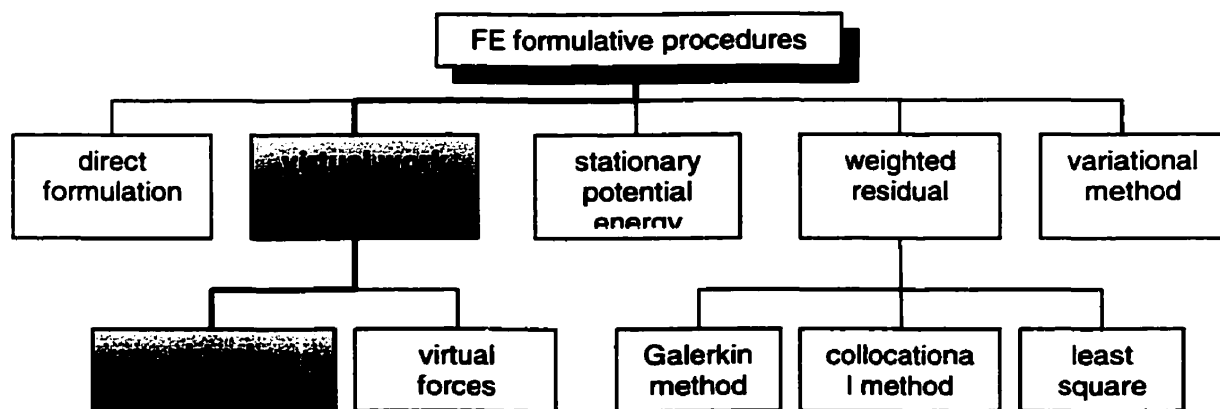
Figure 3.3 Formulation procedures for FE analysis

This formulation procedure leads to the conventional principles of stationary potential energy and complementary energy. Otherwise stated, if a body in equilibrium under the applied loads is subjected to a kinematically admissible virtual displacement state, then the change in the total potential energy of the body is zero and:

$$\delta\Pi = \delta U + \delta V = 0 \qquad (3.16)$$

where: $\delta\Pi$ = change in the potential energy,

δU = change in virtual strain energy,

δV = change in potential of applied load,

or, if a body in equilibrium under the applied loads is subjected to a kinematically admissible virtual displacement state, then the total virtual work is equal to the total external virtual work. Thus, for the two definitions to be equivalent:

$$\delta W_i = \delta W_e \qquad (3.17)$$

and

$$\delta W_i = \delta U \qquad (3.18)$$
$$\delta W_e = -\delta V$$

where: W_i = internal virtual work,

W_e = external virtual work.
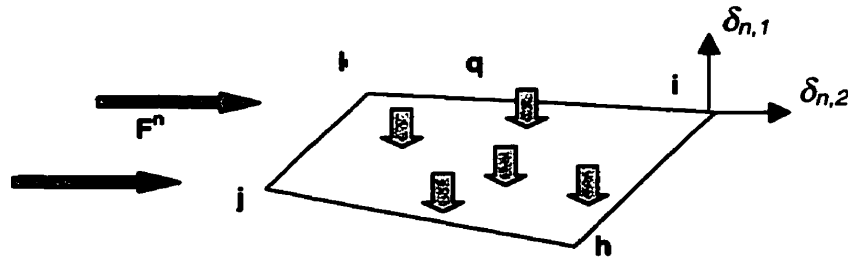
F^n = nodal forces,   q = distributed load inside the element, $\delta_{n,2}$ = nodal displacements

Figure 3.4 Definition of the problem

Assume now a displacement field as described in (3.3) and the strain-displacement relationship of (3.12). The virtual displacements $\delta\Delta$ and the resulting virtual strain components $\delta\epsilon$ can be expressed in a similar form. Hence:

3-9

$$\delta\Delta = [N]\{\delta\Delta_i\} \qquad\qquad (3.19)$$

$$\delta\epsilon = [B]\{\delta\Delta\} \qquad\qquad (3.20)$$

The total change in the potential of the applied loads (nodal forces and distributed loads) in consequence of the virtual displacements of (3.16) is:

$$\delta W_e = -\delta V = \delta W_n + \delta W_d \qquad\qquad (3.21)$$

where:

$$\delta W_n = \{F_n\}\{\delta\Delta\} \qquad\qquad (3.22)$$

$$\delta W_d = \int_v q\delta\Delta d_v = \int_v q[N]\{\delta\Delta_i\}d_v = \{F_d\}\{\delta\Delta\} \qquad\qquad (3.23)$$

with q representing the load intensity per unit volume and $F_{n,d}$ are the load vectors due to nodal and distributed forces respectively. This latter expression is also called the consistent load vector. Accordingly we have:

$$-\delta V = \{F_n\}\{\delta\Delta\} + \{F_d\}\{\delta\Delta\} = \{\delta\Delta\}^T [\{F_n\} + \{F_d\}] \qquad\qquad (3.24)$$

The total internal virtual work (virtual strain energy) done by the action of stresses through the virtual strains is:

$$\delta U = \int_v \{\delta\epsilon\}^T \{\sigma\}d_v \qquad\qquad (3.25)$$

where:

$$\{\sigma\} = [D]\{\epsilon\} - [D]\{\epsilon_0\} + \{\sigma_0\} \qquad (3.26)$$

and σ_0 is the initial stress and ϵ_0 is the initial strain. [D] is the elasticity matrix. Substitution of (3.19) and (3.20) into (3.26) leads to:

$$\delta U = \int_v \{\delta\Delta\}^T [B]^T [D][B]\{\Delta\}d_v - \int_v \{\delta\Delta\}^T [B]^T [D]\{\epsilon_0\}d_v + \int_v \{\delta\Delta\}^T [B]^T \{\sigma_0\}d_v =$$
$$\delta U = \{\delta\Delta\}^T [\int_v [B]^T [D][B]\{\Delta\}d_v - \{F\epsilon_0\} + \{F\sigma_0\}] \qquad (3.27)$$

According to the principle of virtual displacements expressed in (3.16), from (3.20) and (3.24), it appears that:

$$\int_v [B]^T [D][B]d_v\{\Delta\} = \{F_n\} + \{F_d\} + \{F\epsilon_0\} + \{F\sigma_0\} \qquad (3.28)$$

where:

$\{F_n\}$ = load vector due to nodal forces

$\{F_d\}$ = load vector due to distributed body forces

$\{F_{\epsilon 0}\}$ = load vector due to initial strains (boundary tractions) = $\int_v [B]^T [D][B]\{\epsilon_0\}d_v$

$\{F_{\sigma 0}\}$ = load vector due to initial stress = $\int_v [B]^T \{\sigma_0\}d_v$

and can be rewritten as:

$$[K]\{\Delta\} = \{P\} \qquad (3.29)$$

which is identical to equation (3.5).

For the two-dimensional analysis, the thickness of the element is considered to be constant over the entire domain. The finite element equation can be written as:

$$t\int_A [B]^T [D][B] d_A\{\Delta\} = \{P\}$$ (3.30)

where t is the thickness of the element.

As already stated, special attention is given to the elasticity matrix [D] following the model of an equivalent elastic medium for the rock mass, i.e. taking into account the properties of the bedding planes, as proposed by Amadei and Goodman and largely discussed in chapter 2 of this thesis. The matrix [D] in the two-dimensional form is:

$$[D] = \begin{bmatrix} \dfrac{1}{E} & \dfrac{-v}{E} & \dfrac{-v}{E} & 0 \\ \dfrac{-v}{E} & m & \dfrac{-v}{E} & 0 \\ \dfrac{-v}{E} & \dfrac{-v}{E} & \dfrac{1}{E} & 0 \\ 0 & 0 & 0 & n \end{bmatrix}$$ (3.31)

where:

$$m = \frac{1}{E} + \frac{1}{k_n S}$$ (3.32)

$$n = \frac{1}{2G} + \frac{1}{2k_s S}$$ (3.33)

The matrix contains <u>four elastic independent parameters</u>: E, v describing the intact rock properties and $k_n S$, $k_s S$ describing the joint properties stiffness as well as the spacing S between bedding planes.

3-12

3.3 Model features and limitations

The bedded rock mass model features anisotropy simulation of the rock mass depending on the discontinuities mechanical behaviour, see Figure 3.5, as well as their orientation and frequency in the domain analysed. The model has been implemented in a existing, 2-dimensional code called e-z tools (Mitri, 1993). The code is developed by the numerical modelling group at McGill University. e-z tools has the following features:

- Up to 5'000 nodes and 5'000 elements can be generated
- Up to 9 geological materials can be modelled
- Up to 3 mining sequences are simulated
- Modelling of rock bolts and cable bolts.

On the other hand, e-z tools has the following limitations:

- Linear elastic behaviour of the material; no elastoplasticity or viscoplasticity is accounted for
- Static analysis only; no dynamic loading is permitted in the code
- Only 2-dimensional, plane stress or plain strain analysis can be carried out.

Furthermore, the limitations of the model for bedded rock are presently the following:

1. Only one set of parallel discontinuities
2. Simulation of post-peak behaviour (dilatancy) of the discontinuities not permitted
3. Negligible joint thickness; handling of the joint thickness not possible
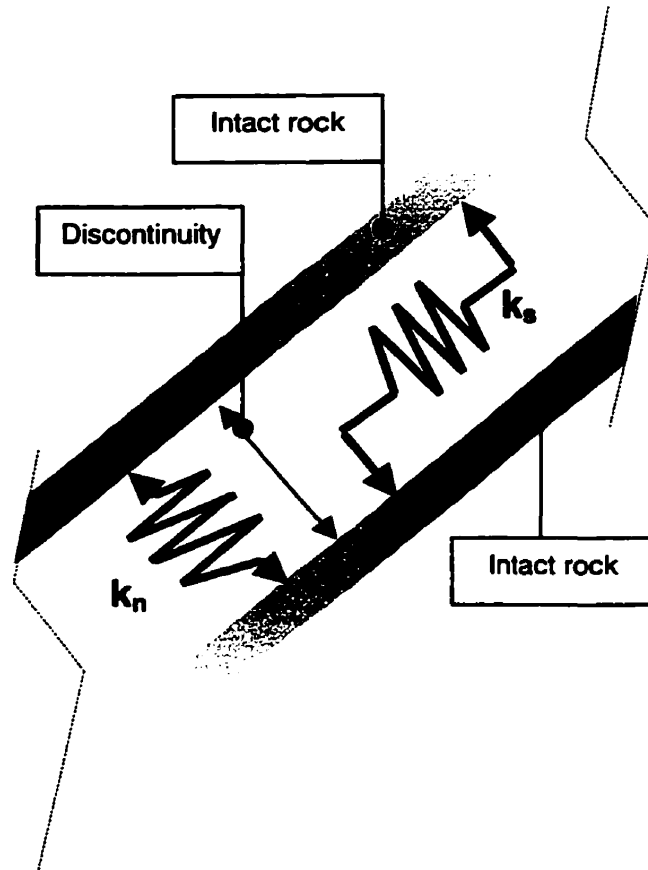4. Imposed upper limit for the B/S ratio (span / joint spacing).

Figure 3.5 Simulation of the discontinuity in a bedded rock mass

3.4 Model input parameters

As stated in the introductory section, this report's aim is the determination of equivalent elastic properties for a bedded rock mass. The Hooke's law for isotropic elasticity which describes the stress-strain relationship is presented in Chapter 2. In the previous section 3.3, the two-dimensional matrix form of the equivalent elastic medium has been presented, where particular attention is given to the four elastic parameters needed to model the bedded rock mass.

Otherwise stated, the jointed rock mass is replaced by an equivalent anisotropic continuum with equivalent elastic properties which are a function of the intact rock (E,v) and the joint fabric.

The joint fabric is described by k_n = f (normal stress, joint opening, ϕ gauge material) and k_s = f(tangential stress, joint opening, and gauge material)).

In the identification of the input parameters it becomes clear that difficulties arise in the determination of the joint parameters. First, the definition of intact rock parameters can be interpreted as suggested in Figure 3.6:
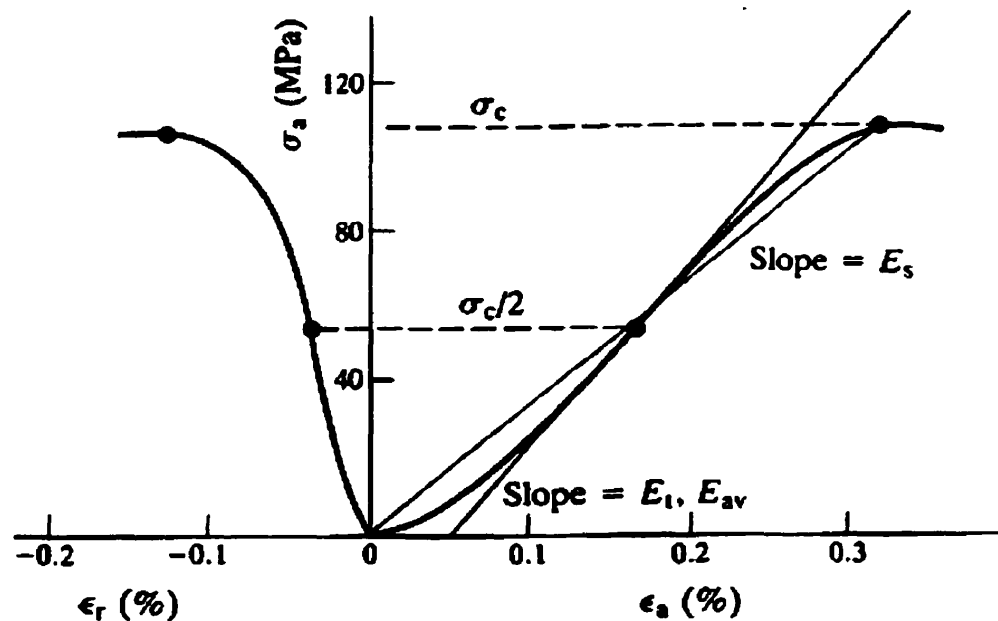

Figure 3.6 Definition of the Young's modulus (Brady and Brown, 1992)

Corresponding to any value of the tangent Young's modulus E_t, average Young's modulus E_{av} or secant Young's modulus E_s, a value of Poisson's ratio may be calculated:

$$\nu = -(\Delta\sigma_a/\ \Delta\varepsilon_a)\ /\ (\Delta\sigma_a/\ \Delta\varepsilon_r) \qquad (3.34)$$

The compressibility of the joint can be obtained from the difference in deformation between intact and jointed rock specimens in uniaxial compression or by triaxial cell test in case of joints filled with material. The next figure shows typical deformation behaviour of three kinds of joint surfaces used in the experiments by Yoshinaka and Yamabe (1986).
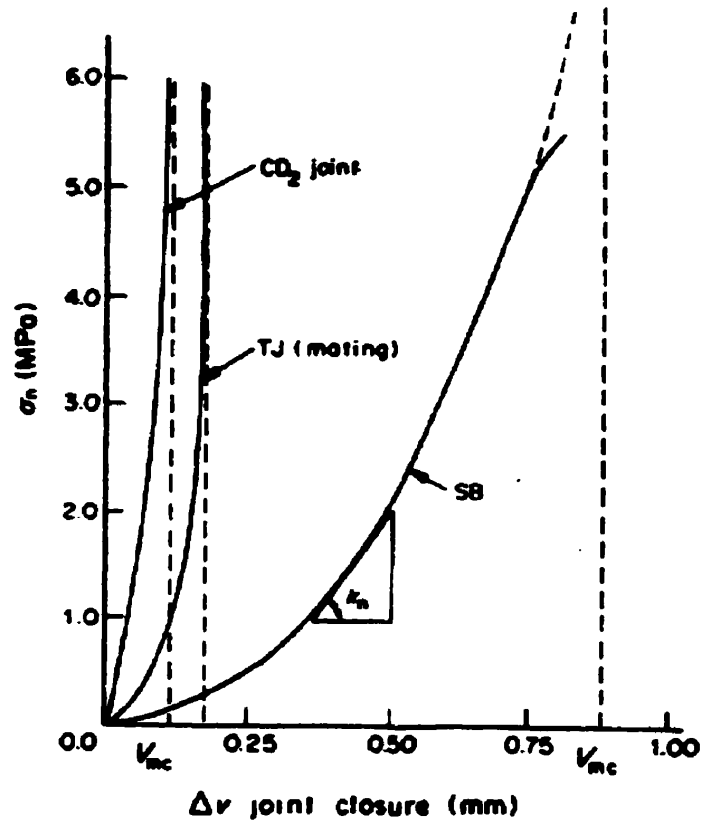

Figure 3.7 Joint closure compressive stress curve (Yoshinaka et al., 1986)

The curve is defined by the following equation:

$$k_n = d\sigma / d(\Delta V) \tag{3.35}$$

Yoshinaka and Yamabe (1986) proposed the following relation expressing k_n as a function of the maximum joint closure V_{mc} and material constants ℓ and m:

$$k_n = m \, (\ell \times \Delta V / V_{mc}) \tag{3.36}$$

while Amadei and Goodman (1981) proposed a better defined secant joint normal stiffness based on the idealized figure presented by Figure 2.7 in Chapter 2.

The joint shear deformation versus shear stress curve for a test conducted on a joint under constant normal stress can be characterized by the idealized Figure 2.8 shown in the previous Chapter. The slope characterising the elastic region is termed the unit shear stiffness k_s after Goodman (1968). Yoshinaka and Yamabe (1986) have established a relation between stiffness of the two joints:

$$k_{si}(k_s) = C' \times (k_n)\beta \tag{3.38}$$

where C' = f (gauge material constants α, β; atmospheric pressure p_a; joint maximum disclosure V_{mc}).

The advantage of this complex approach resides in the fact that the value of k_{si} and k_n can be measured from the same shear and compression tests under the same normal stress. Furthermore, this approach is convenient from the practical point of view because one can estimate one stiffness from another.

3.5 Model sensitivity analysis

The present section focuses on the parametric study of the behaviour of an underground opening in bedded rock. In fact, the performance of the model can be shown by the means of a sensitivity analysis of given parameters, i.e. the joint spacing S, on the overall behaviour of the bedded rock mass around the opening.

A stratified host rock is not uncommon in tunnelling practice. As already stated in Chapter 1, an excavation in a sedimentary setting or in presence of planes of weakness in a metamorphic formation is frequently encountered in tunnelling. In order to evaluate the influence of bedding planes, the span-to-joint spacing ratio (B/S) is defined; see Figure 3.8.
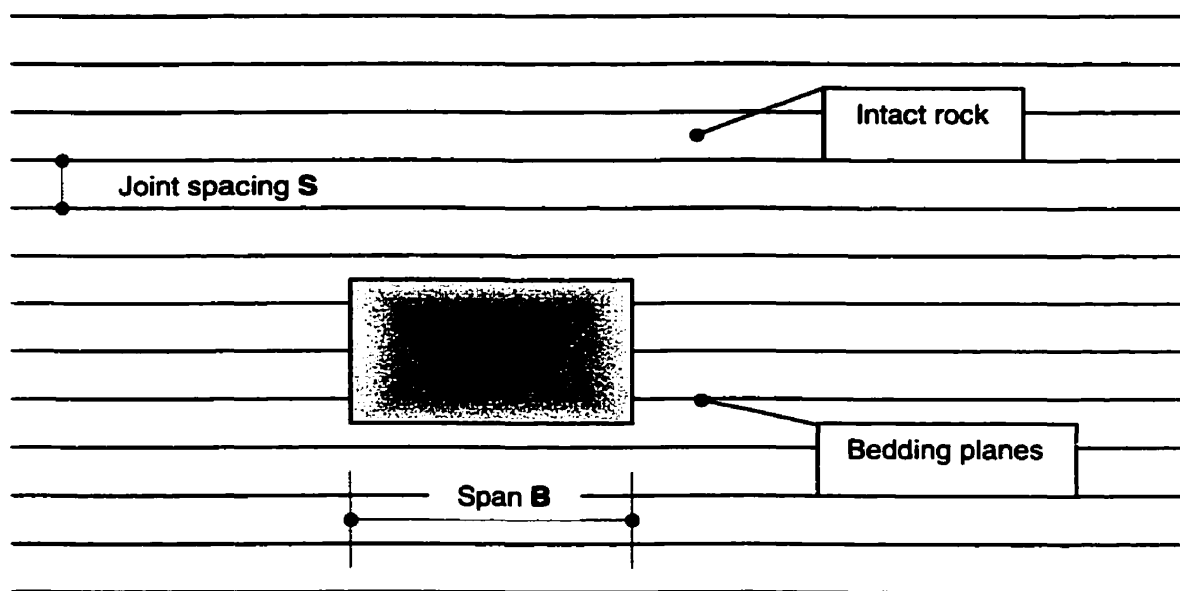

Figure 3.8 Definition of span-to-joint ratio B/S

Figure 3.8 also shows the model for the parametric study carried out to investigate the influence of the joint spacing, dip angle and joint stiffness on the roof deformations at the centreline of the opening. The results of this analysis should be of some value since cases

in which the optimisation of the opening shape in a bedded rock mass largely depend on the B/S ratio. This is particularly true as the dimensions of the excavation increase like in the case of utility caverns. In addition, the sensitivity of the elastic parameters of the intact rock, i.e. Young's modulus and Poisson's ratio are also examined. The finite element mesh of the problem for the parametric study is presented in Figure 3.9; it consists of 3'000 isoparametric elements.

◇ fixed   free   * x fixed   □ y fixed
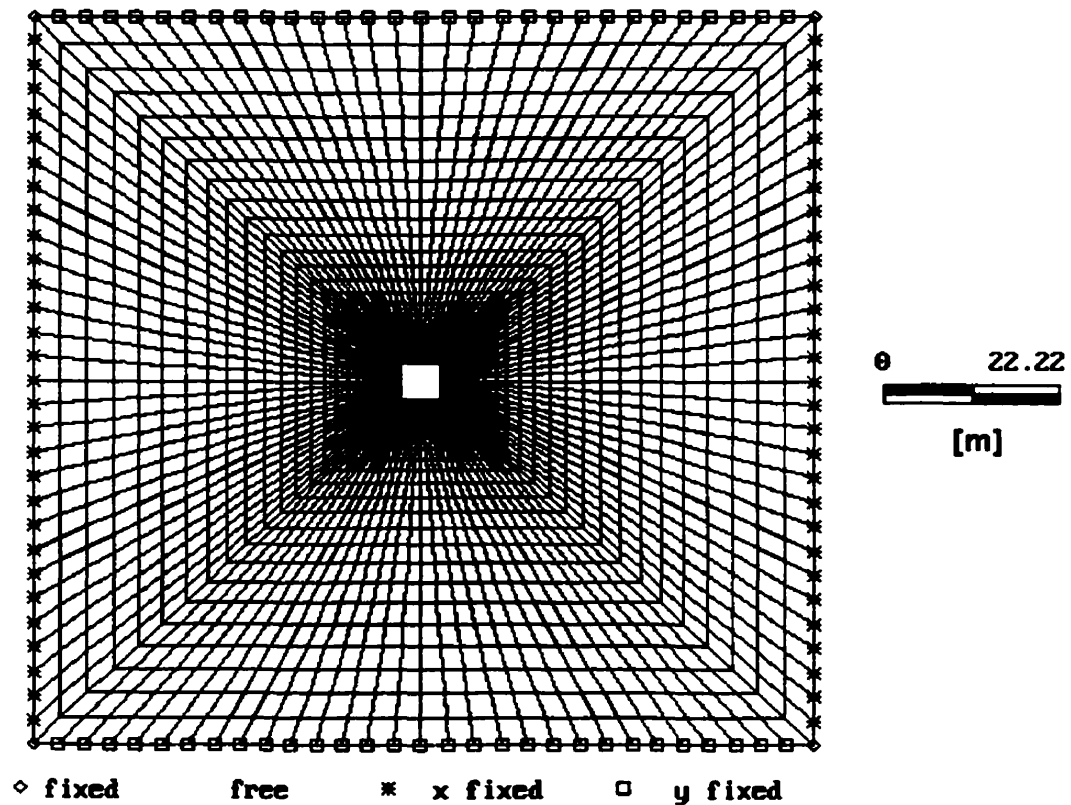
Boundary conditions: - overburden H = 800 m (at point 0;0)

In situ stresses: $-\sigma_x^0 = K\gamma H$ and $\sigma_z^0 = K\gamma$

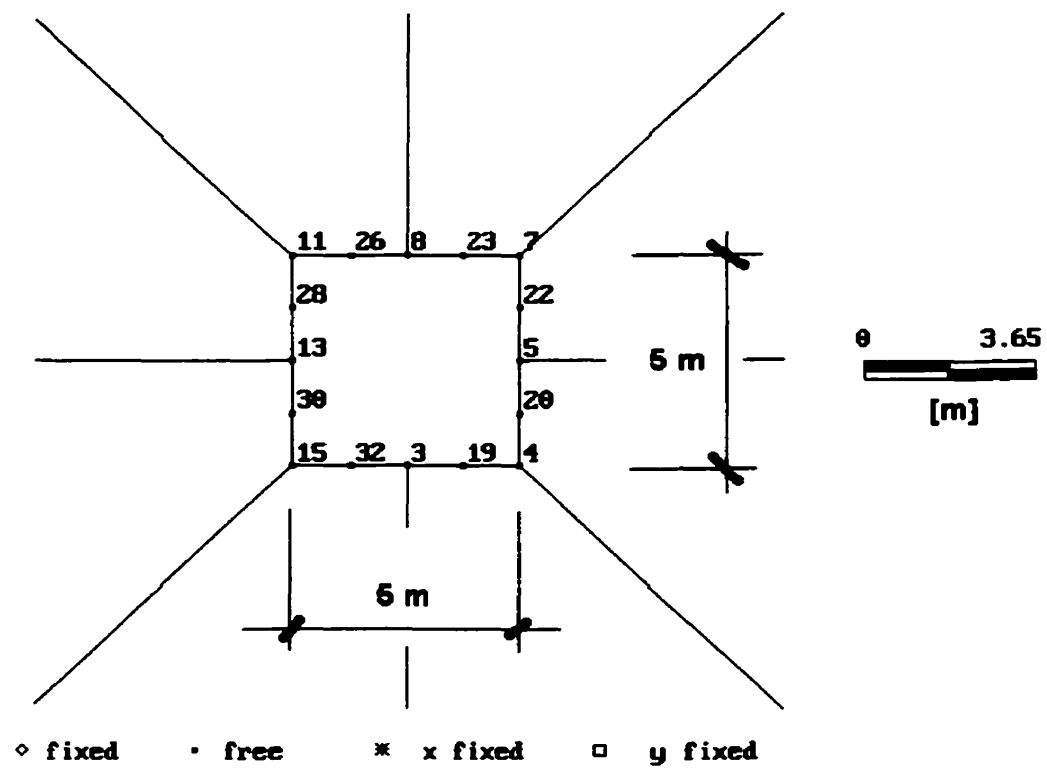Figure 3.9 Finite element mesh of the parametric study model

Figure 3.10 Opening dimensions of the parametric study model

3.5.1 Numerical results

Table 3.1 reports the simulations carried out for the sensitivity analysis. Next to the denomination are listed the values of input data of each simulation computed where the variable is put in evidence by shadowed boxes.

15.000,0	0,2	10.000,0	15.000,0	0,50	10,0	0
30.000,0	0,2	10.000,0	15.000,0	0,50	10,0	0
60.000,0	0,2	10.000,0	15.000,0	0,50	10,0	0
40.000,0	0,1	10.000,0	15.000,0	0,50	10,0	0
40.000,0	0,2	10.000,0	15.000,0	0,50	10,0	0
40.000,0	0,4	10.000,0	15.000,0	0,50	10,0	0
40.000,0	0,2	1.000,0	15.000,0	0,50	10,0	0
40.000,0	0,2	5.000,0	15.000,0	0,50	10,0	0
40.000,0	0,2	15.000,0	15.000,0	0,50	10,0	0
40.000,0	0,2	10.000,0	10.000,0	0,50	10,0	0
40.000,0	0,2	10.000,0	20.000,0	0,50	10,0	0
40.000,0	0,2	10.000,0	40.000,0	0,50	10,0	0
40.000,0	0,2	10.000,0	15.000,0	0,05	100,0	0
40.000,0	0,2	10.000,0	15.000,0	0,05	100,0	30
40.000,0	0,2	10.000,0	15.000,0	0,05	100,0	45
40.000,0	0,2	10.000,0	15.000,0	0,05	100,0	60
40.000,0	0,2	10.000,0	15.000,0	0,05	100,0	90
40.000,0	0,2	10.000,0	15.000,0	0,10	50,0	0
40.000,0	0,2	10.000,0	15.000,0	0,10	50,0	30
40.000,0	0,2	10.000,0	15.000,0	0,10	50,0	45
40.000,0	0,2	10.000,0	15.000,0	0,10	50,0	60
40.000,0	0,2	10.000,0	15.000,0	0,10	50,0	90
40.000,0	0,2	10.000,0	15.000,0	0,25	20,0	0
40.000,0	0,2	10.000,0	15.000,0	0,25	20,0	30
40.000,0	0,2	10.000,0	15.000,0	0,25	20,0	45
40.000,0	0,2	10.000,0	15.000,0	0,25	20,0	60
40.000,0	0,2	10.000,0	15.000,0	0,25	20,0	90
40.000,0	0,2	10.000,0	15.000,0	1,00	5,0	0
40.000,0	0,2	10.000,0	15.000,0	1,00	5,0	30
40.000,0	0,2	10.000,0	15.000,0	1,00	5,0	45
40.000,0	0,2	10.000,0	15.000,0	1,00	5,0	60
40.000,0	0,2	10.000,0	15.000,0	1,00	5,0	90

40.000,0	0,2	10.000,0	15.000,0	5,00	1,0	0
40.000,0	0,2	10.000,0	15.000,0	5,00	1,0	30
40.000,0	0,2	10.000,0	15.000,0	5,00	1,0	45
40.000,0	0,2	10.000,0	15.000,0	5,00	1,0	60
40.000,0	0,2	10.000,0	15.000,0	5,00	1,0	90
40.000,0	0,2	10.000,0	15.000,0	50,00	0,1	0
40.000,0	0,2	10.000,0	15.000,0	50,00	0,1	30
40.000,0	0,2	10.000,0	15.000,0	50,00	0,1	45
40.000,0	0,2	10.000,0	15.000,0	50,00	0,1	60
40.000,0	0,2	10.000,0	15.000,0	50,00	0,1	90
40.000,0	0,2	-	-	-	-	-

Table 3.1 Summary of model sensitivity analysis

The deformation of the tunnel roof is presented in Figure 3.11a for different E and in Figure 3.11b for different υ. Here the other parameters of the rock mass have been held constants, i.e. normal and shear stiffness k_n respectively k_s, the dip angle as well as the B/S ratio. The result of the investigation indicates that the deformation of the roof is practically not affected by the variation of the Poisson's ratio. The deformation of the roof is, however, only slightly dependent on the magnitude of the Young's modulus E. Figure 3.12 shows the sensitivity of k_n and k_s with constant Young's modulus and Poisson's ratio of E = 40 GPa, and υ = 0.2. As can be seen, the shear stiffness of the bedding planes plays a more significant role than the normal stiffness in controlling the large deformations.
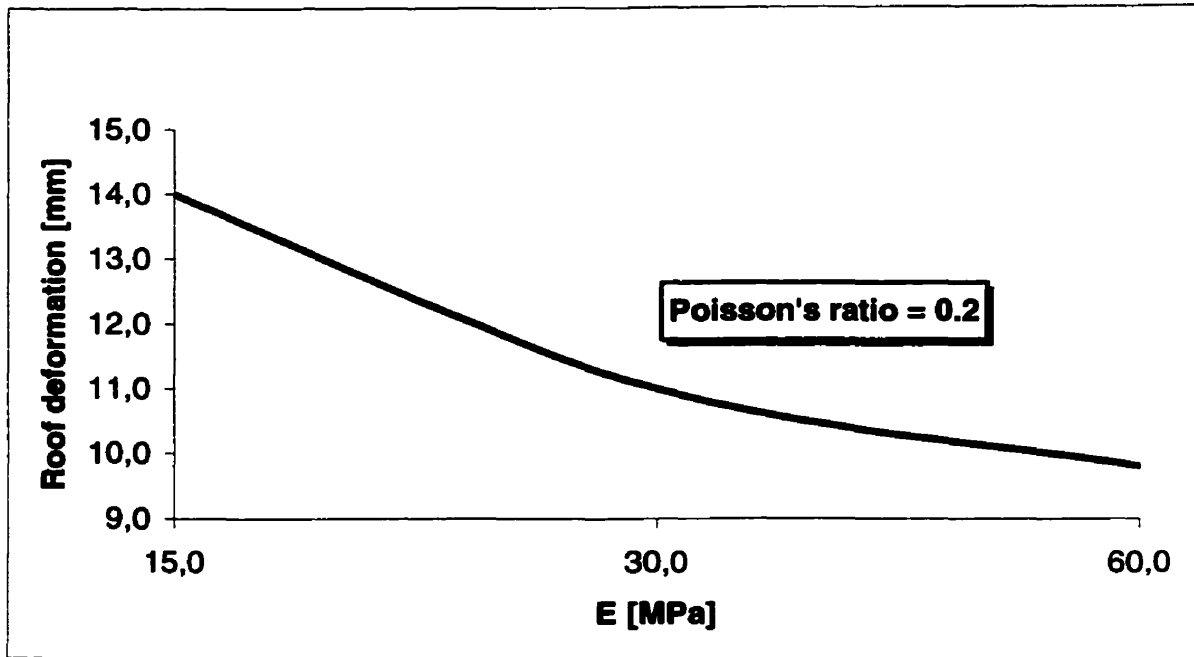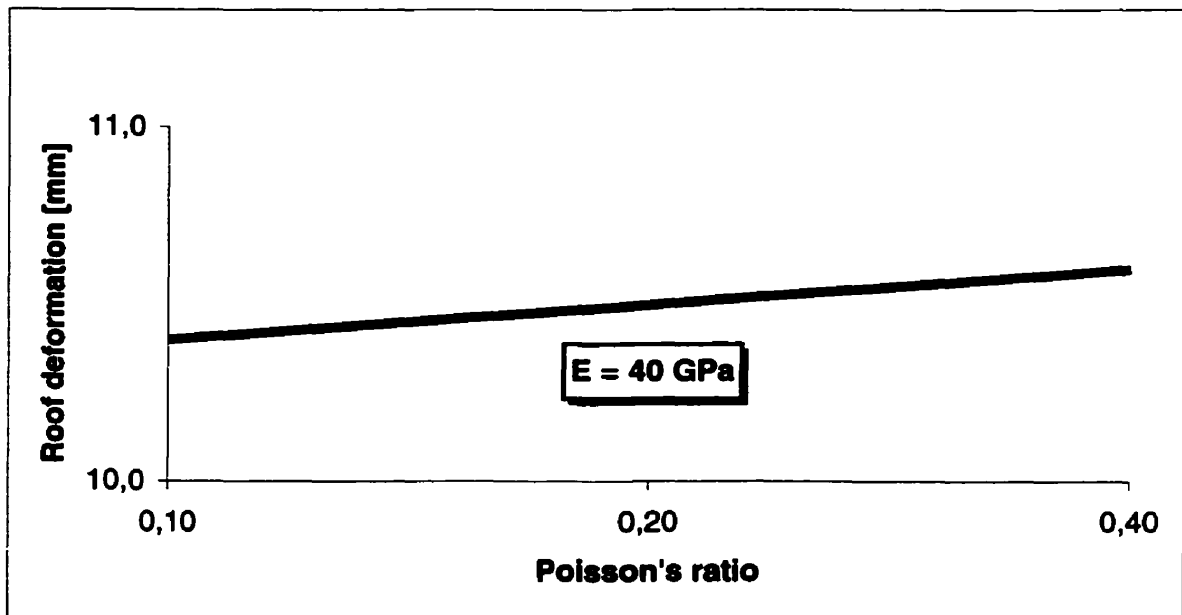
Figure 3.11a Roof settlements as a function of E

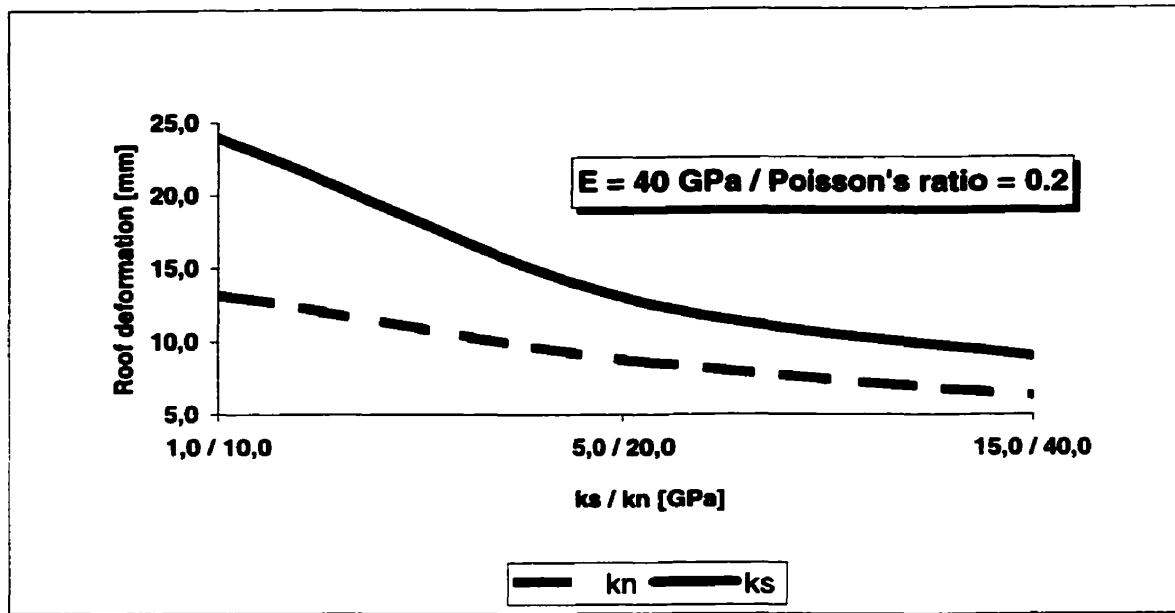Figure 3.11b Roof settlements as a function of υ

25,0

E = 40 GPa / Poisson's ratio = 0.2

Roof deformation [mm]

20,0

15,0

10,0

5,0

1,0 / 10,0   5,0 / 20,0   15,0 / 40,0

ks / kn [GPa]

kn   ks

Figure 3.12 Roof settlements as a function of k_n and k_s

Figure 3.13 presents the roof deformation as a function of the B/S ratio and the dip angle for a constant Passion's ratio of $\upsilon = 0.2$ and a Young's modulus of E = 40 GPa. It is primarily to notice from the surface resulting by changing simultaneously the two parameters that the roof deformations are not linearly dependent on both the dip angle and the B/S ratio. Furthermore, it may be recognised that they cause only a small influence on the elastic deformations of the roof in the range of low and very low value of B/S.

Otherwise stated, for the case depicted in Figure 3.13, which regards an opening with a span B = 5.0 m, one can say that for a spacing between discontinuities greater than 0.5 m (or B/S $\leq$ 10) the roof settlement is geotechnically insignificant - i.e. δ_{roof}/B less than 1/500 - and regardless of the strata inclination and spacing. This confirms the "isotropy" of the media for small B/S ratios tending to zero. This is simply explained by the scale effect; in fact, for very large spacing S between the joints, their effect at the work scale vanishes and only the properties of the surrounding intact rock control the behaviour of the opening.
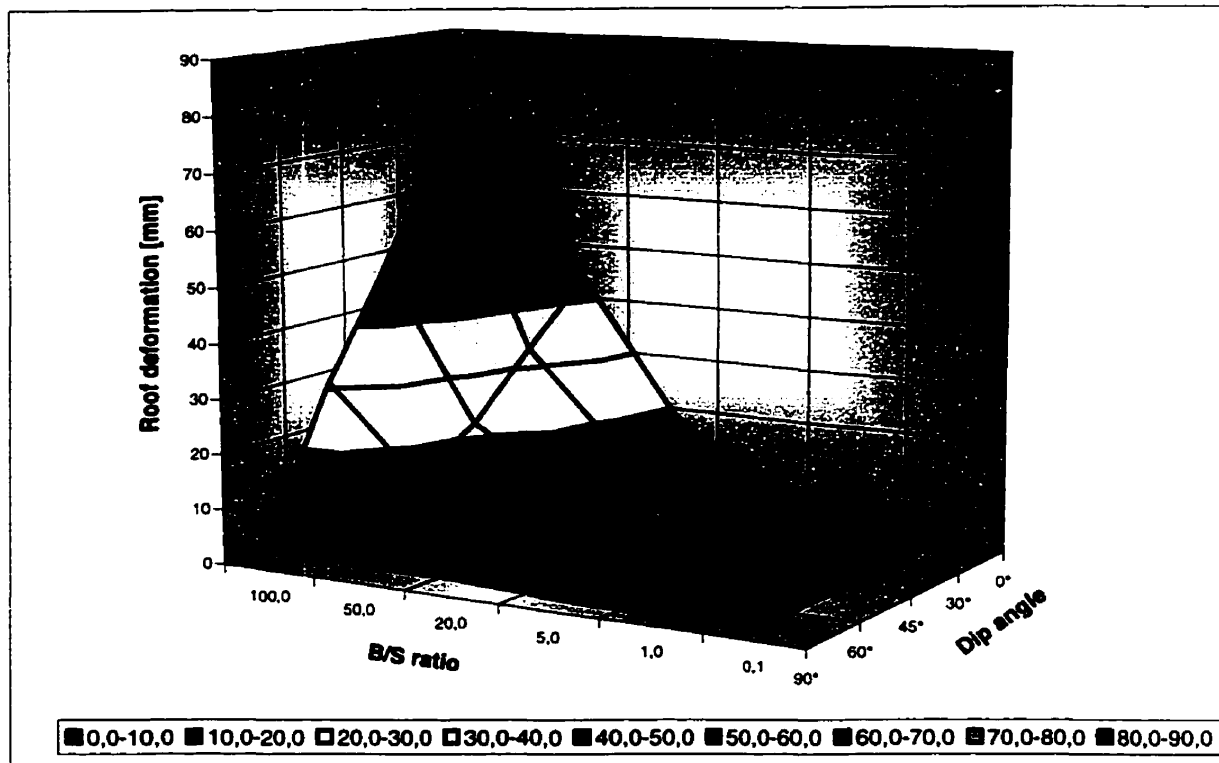
Figure 3.13 Roof deformation as a function of B/S and strata dip angle

Since a relatively large area of rock mass above the roof is unloaded as a result of excavation, deformations extend upwards for quite some distance. To illustrate this behaviour, the vertical displacement along the plane of symmetry is plotted as a function of the distance from the roof (at the tunnel centre) in Figure 3.14. The analysis of the scale of the unloaded zone becomes interesting for the bedded rock mass with horizontal strata, which represents the worst-case according to Figure 3.13.
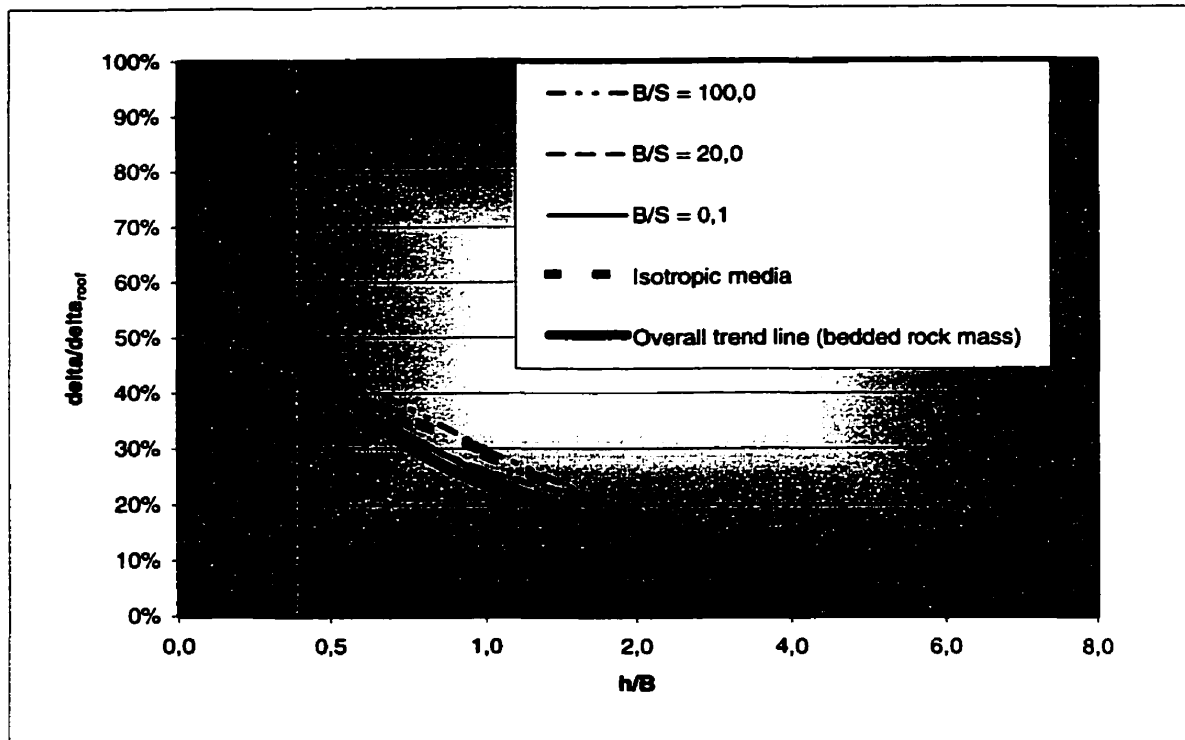
Figure 3.14 Reduction of vertical displacement with increasing distance from the roof

In addition, increases in stresses arise in the sidewalls of the opening. In the case where the bedding planes are horizontal, the increase of the vertical stress extends along the X-axis over a length, which is approximately 4 times the opening span S as depicted in Figure 3.15:
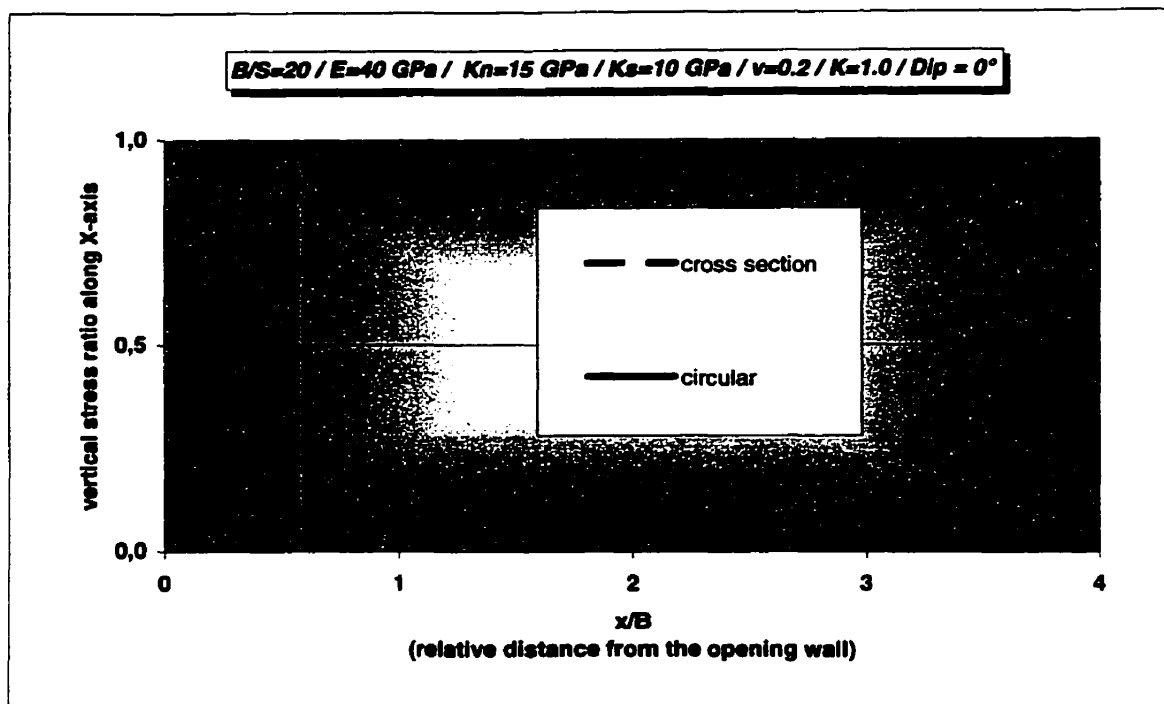
Figure 3.15 Extent of vertical stress in the sidewall

It is of interest to notice how the shape of the opening influences the flow of the stress at the same point. In the case of circular cross section the stress reaches its maximal value at the centreline of the sidewall (for an ideal isotropic hydrostatic case this is equal to twice the in situ stress, hence 1.0 on the Y-axis of Figure 3.1) while the highest vertical stress for a cross section is reached at the corner; thus, the increase of stress at the sidewall is much less abrupt as demonstrated by the above graphic.

The influence of the discontinuities may also be recognized from the deformation of the opening wall illustrated in Figure 3.16 for stratas dipping with 45°.
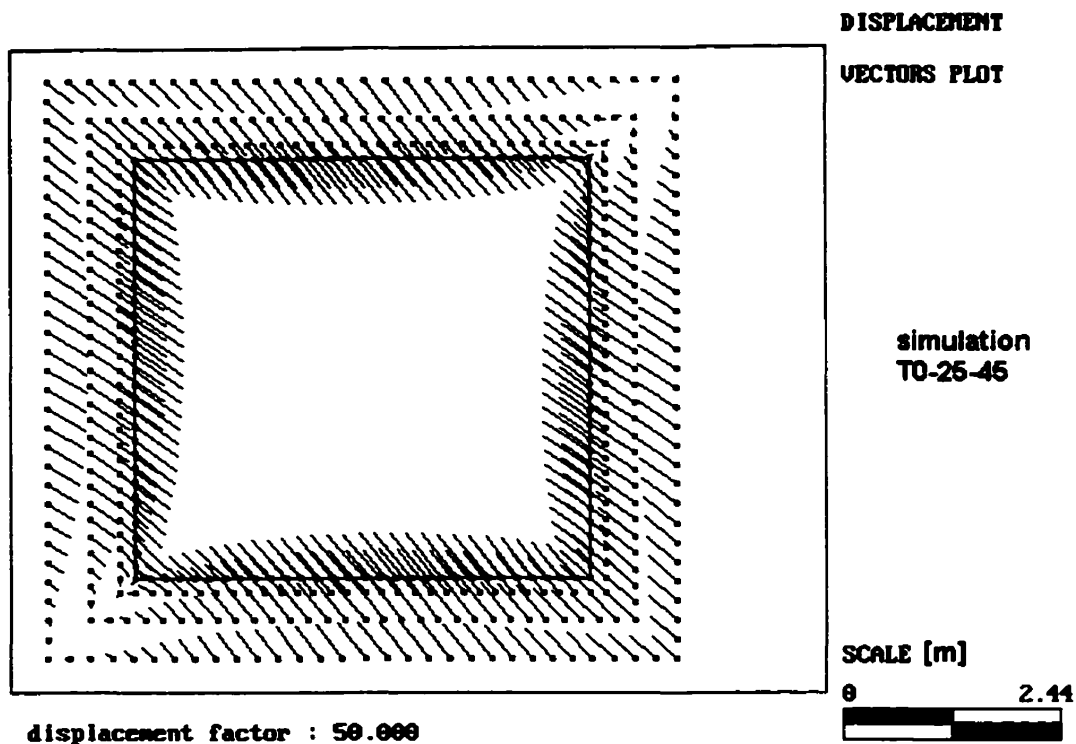
Figure 3.16 Unsymmetrical tunnel deformations for a dip angle of 45°

It should be mentioned that Figures 3.13 and 3.14 might, if applied to a specific case, be used when making a first approach of design for an opening. In fact, it is possible to optimise the excavation shape as a function of the discontinuity spacing or to give a rough interpretation of measured deformations caused by driving. On this subject, it is worth mentioning that even when plastic deformations arise, the elastic deformations are also present and must be taken into account during the design and the interpretation of the deformation measurements. In addition, elastic sensitivity analysis like the one presented here should always form the basis, if requested, for further elasto-plastic investigations.

Furthermore, the significance of discontinuity properties to the rock mass behaviour around an opening should be clear from the example presented by this sensitivity analysis. It shows that the spacing and dipping of the bedding planes of a rock mass exhibit a considerable influence over the form of deformation - and thus on stresses -

around the opening and the subsequent formation of palstic zones. Additionally, the influence of elastic constants has been found to be considerable as absolute value but the contribution to the range in which each constant separately modifies the displacement pattern around the opening is smaller than the contribution due to variation of joint spacing and dipping.

All these factors therefore influence stability. It is thus of great importance that the elastic constants and the geometry of the joints be determined as reliably as possible and that the influence of scatter be investigated in parametric studies as demonstrated here.

MODEL APPLICATION TO A CASE STUDY

4.1 Problem definition

The Swiss Alps are currently crossed in the North-South axe by the railway line of the St. Gotthard. This important railway was built at the end of the 19th century just at the beginning of the railway era in Europe. The railway line starts on the Swiss plateau at 400 m above sea level, reaches elevation 1.200 m by the old St. Gotthard tunnel then goes downhill in direction of the Italian borders, which lie at an elevation of 250 m. In order to overcome this abrupt change in elevation within about 100 km, the pioneer engineers proposed unusual solutions which led to the execution of a challenging project. In fact, the main features are the main 17 km long tunnel derived through the St. Gotthard Mountains and a sequence of helicoidal tunnels, which allow the train to gain elevation on a gentle slope.

Although this section still represents a valid technical solution a century after its construction, the amount of energy required to take the merchandise and passengers from one part to the other of the Alps cannot in today's world be met. Furthermore, the average rail haulage speed of 70 km/h between Milan and Zurich cannot compete economically with the opportunities given by highway transportation.

Therefore, the Swiss government has decided to start the development of a huge project in the beginning of the 90´s transforming the railway's concept of this primary line.

Among the major tunnel works planned within this section is the Piora tunnel, which is the subject of the case study presented here. It was mined out as a primary part of the geotechnical investigations of the Gotthard base tunnel. Subsequently, the 5,5 km long, 5,0 diameter TBM Piora exploratory tunnel was excavated near the town of Faido, in

Southern-Switzerland, with a maximum overburden depth of 1.750 m to provide information for the design of the main tunnel. In fact, in this area the Swiss Alp peaks exceed elevation 3.000 m and the valleys bottom are situated at 700 m above sea level. Figure 4.1 presents the location of the Piora exploratory tunnel in relation to the Gotthard base tunnel, which will have at the completion of the project a total length of 57 km; a 3-D view of the Piora exploratory tunnel is given also in Figure 1.4, Chapter 1.
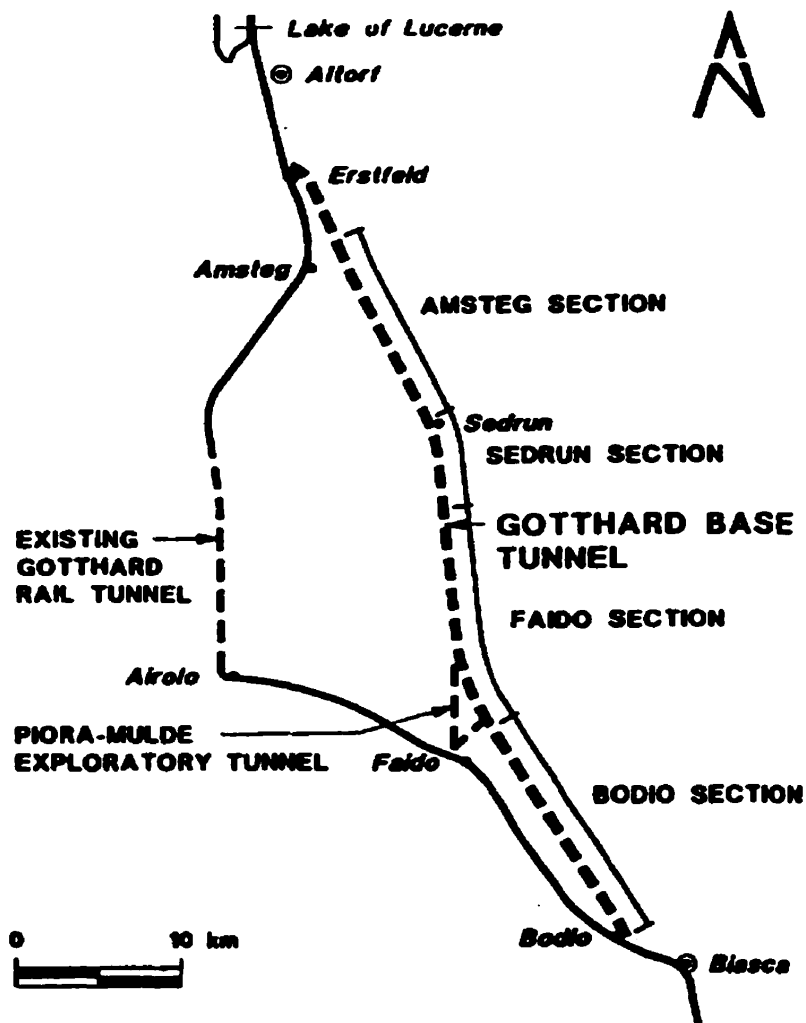

Figure 4.1 Location of the Piora exploratory tunnel

Along with the main purpose of the exploratory tunnel which was to investigate the possible presence of a potentially very unfavourable geological formation referred to as the Piora-Mulde and consisting of sugar-dolomite – also named the "miner's pest"- the Piora exploratory tunnel has also provided an invaluable gathering of information regarding previously unknown rock mass behaviour of the stratified gneissic rock formations under high overburden. In addition, an unusual wide range of geotechnical investigations were carried out within the exploratory tunnel and included, among others, instrumentation monitoring as well as lab tests for the competent evaluation of any parameter needed in the design stage. Thus, the Piora exploratory tunnel represents a good example on how the design has been influenced by a rock mass transacted by a major family of discontinuities.

Therefore, the validation of the numerical model for bedded rock is performed on the design of the Piora exploratory tunnel. The test of the numerical code is undertaken for the simulation of the behaviour of the rock mass around the opening at the chainage km 1.619 where a detailed back analysis had been carried out by the engineers in order to explain overstressing / breakouts phenomena. Finite element simulations were conducted to comprehend such phenomena particularly at chainage km 1,619. The results of such analyses are compared with those obtained from the numerical code developed in this thesis, to serve as a basis for model validation.

4.2 Geomechanical data

The tunnel passes throughout hard rock formations, which are typical of the Swiss Alps. The encountered rocks belong to the Leventina and Lucomagno gneiss families. Within those rock families the mechanical properties of the different gneiss type are quite smooth. Figure 4.2 presents a longitudinal profile of the geology along the Piora exploratory tunnel alignment.
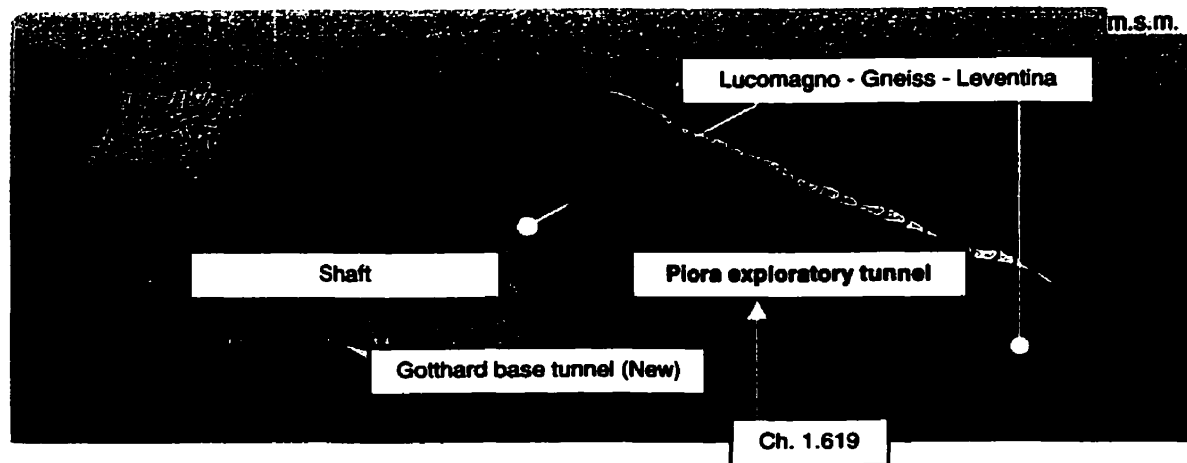
Figure 4.2 Geological profile of the Piora exploratory tunnel

Essentially, this metamorphic rock is considered to be a favourable medium for tunnelling because of its elevated self-bearing features. On the other hand, schistose has influenced its behaviour considerably. Furthermore, due to the small mutual spacing of the joint planes, the hazard of collapses of the vault is connected with the scale effect. All along this tunnel, the arrangement of those planes is particularly adverse for a bore with the dimension of the mined section.

Overstressing / breakouts phenomena occurred around chainage km 1,619. Despite the good mechanical qualities of the encountered rocks, the high primary pressures coped with an inconvenient disposition and filling of the joint planes have reduced the stability of the tunnel, so that in this area the above-mentioned phenomena were observed just after the passage of the head of the tunnel-boring machine (TBM).

Deformations of the cross section were also observed in presence of sub-vertical schistose planes and important overburden, where the resistance of the thin-layered rock sections is surpassed and a plastic behaviour of the rock has caused quite large deformations of the fault.

As stated, the two-dimensional simulation with e-z tools modelling software for bedded rock is carried out for the section at chainage km 1,619. At this location, the Leventina gneiss is described as a porphiritic biotite rich gneiss with prominent sub-horizontal porphiritic banding. The discontinuities in this case are due to the tormented geology induced by the tectonics of the Alps and mostly run on sub-horizontal planes striking the tunnel alignment almost perpendicularly. The thickness of the strata is about 0,5 m. The average elastic moduli of intact rock was determined by a series of uniaxial compressive tests which also showed an unusual scatter and its value is finally assumed to be 40 GPa. For the mechanical properties of the joints, it was possible to assume the mean value for the normal stiffness modulus on the basis of the same lab tests whereas the determination of the joint friction angles for the Leventina gneiss –the result of which is finally the value of the shear stiffness modulus - was based on direct shear tests. A summary of the geotechnical data used in the simulation with e-z tools for bedded rock mass is given in Table 4.1.

Table 4.1 Summary of the geotechnical parameters assumed

In situ stresses (at point 0;0 of the domain)	Vertical stress, $\sigma_y = \gamma H$ Horizontal stress, $\sigma_x = K_x \gamma H$ where: H = depth below surface γ = average unit weight for the rock mass K = horizontal to vertical stress ratio	$\sigma_y = 20.8$ MPa $\sigma_x = 20.8$ MPa H = 800 m $\gamma = 0.026$ MN/m^3 $K_x = 1.0$ $K_z = 1.0$
Intact rock	Young's modulus E, uniaxial compressive tests Poisson's ratio υ, uniaxial compressive tests	E = 40 GPa $\upsilon = 0.2$
Discontinuities	Normal stiffness k_n, uniaxial compressive tests Shear stiffness k_s, direct shear tests	$k_n = 15$ GPa $k_s = 10$ GPa
	Joint spacing S, geological mapping	S = 0.5 m
	Dip angle, geological mapping	$\beta = 10°$
	Strike, geological mapping	$\alpha = 270°$

4.3 Finite element model

The typical circular cross section at chainage km 1,619 was chosen for the 2-D analysis; see Figure 4.3. The diameter of the opening is 5,0 m and lining or rock support is considered at this stage of the simulation. The rock mass is considered to consist of one type of material due to the persistence of the same formation all over the domain. As a result of the method employed for tunnelling the Piora exploratory tunnel, which is TBM, just one stage of excavation is considered in the computation.
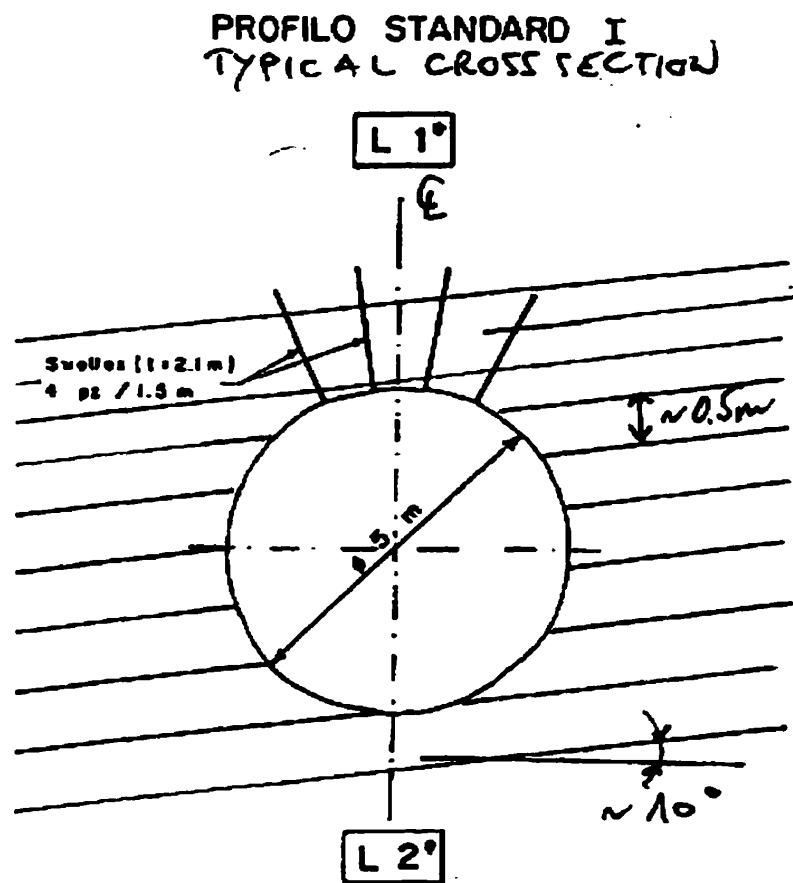
Figure 4.3 Typical cross section at chainage km 1,619

The generated mesh for the simulation has 3.120 nodal points and 3.000 isoparametric elements. The mesh is graded around the opening in order to decrease the size of the elements in the more crucial area of high stress gradients. The dimensions of the domain are 100 m by 100 m so that the boundaries are far enough, and will not influence stresses around the tunnel. Figure 4.4 shows the mesh designed for this analysis. In order to test the sensitivity of the stress flow around the opening to the more uncertain input parameters, i.e. the mechanical joint properties which are the normal and the shear stiffness k_n respectively k_s as well as the K ratio between horizontal and vertical stress magnitudes, two models have been designed:

- Model I: input parameters as in Table 4.1 with K_x taking values of **0.5 / 1.0 / 1.5**
- Model II: input parameters as in Table 4.1 with $\kappa = E/k_n$ ranging from **0.1** to **1.0** and $k_n/k_s = 1.5$

The modification of the k_n/k_s ratio influences only slightly the behaviour of the rock mass. Figure 4.5 presents graphically this statement. As a result, any further investigation has been carried out regarding the changing of the ratio between joint stifnesses. Following cases have been then simulated with e-z tools for bedded rock mass:

Table 4.2 Model input parameters for different scenarios analysed

	10.000,0	15.000,0	0,50	10	10,0	0,5
	10.000,0	15.000,0	0,50	10	10,0	1,0
	10.000,0	15.000,0	0,50	10	10,0	1,5
	3.333,3	5.000,0	0,50	10	10,0	0,5
	3.333,3	5.000,0	0,50	10	10,0	1,0
	3.333,3	5.000,0	0,50	10	10,0	1,5
	26.666,7	40.000,0	0,50	10	10,0	0,5
	26.666,7	40.000,0	0,50	10	10,0	1,0
	26.666,7	40.000,0	0,50	10	10,0	1,5
	isotropic rock					0,5
	isotropic rock					1,0
	isotropic rock					1,5

generated mesh for the Piora expl. tunnel

SCALE :

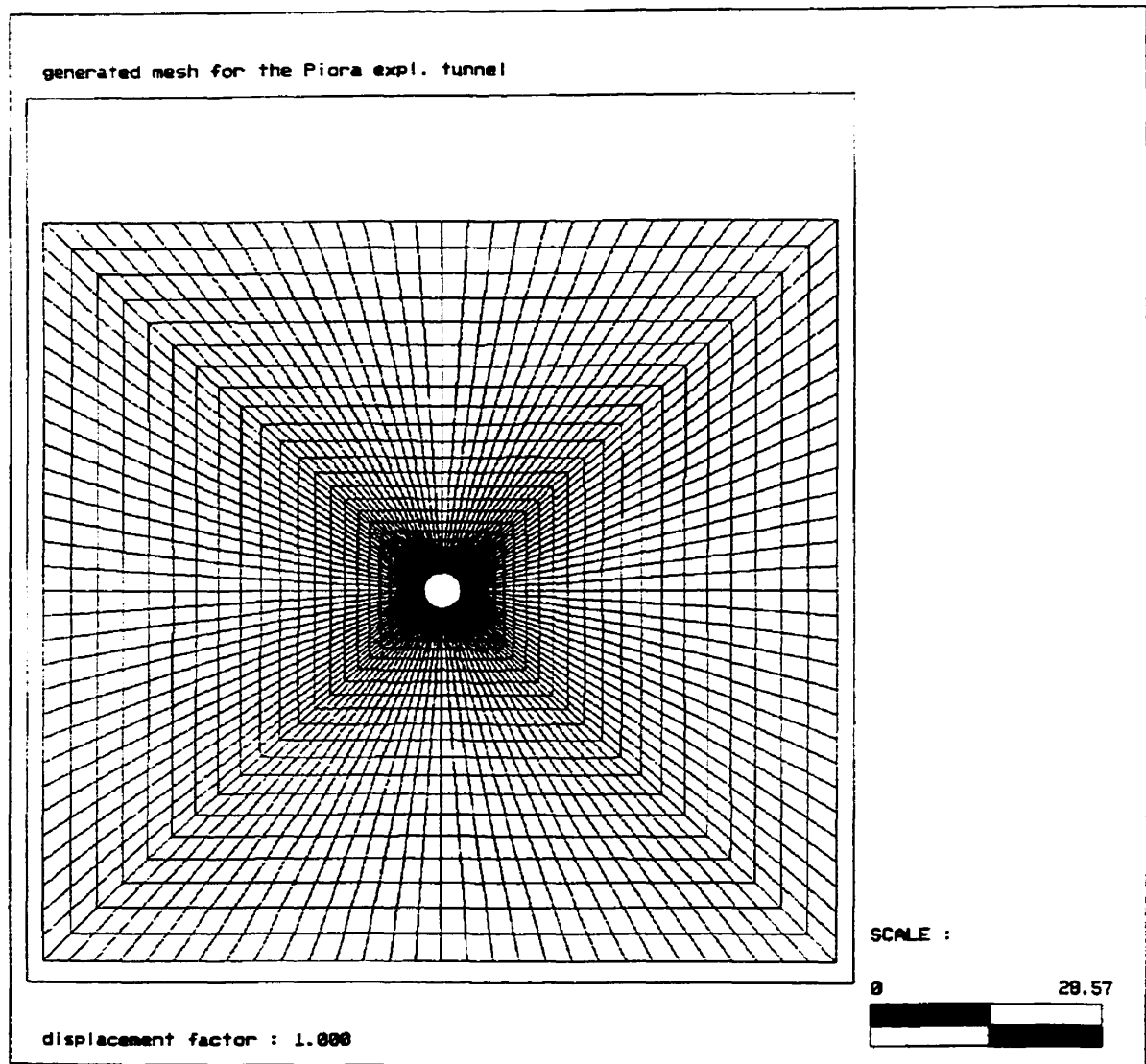0   20.57

displacement factor : 1.000

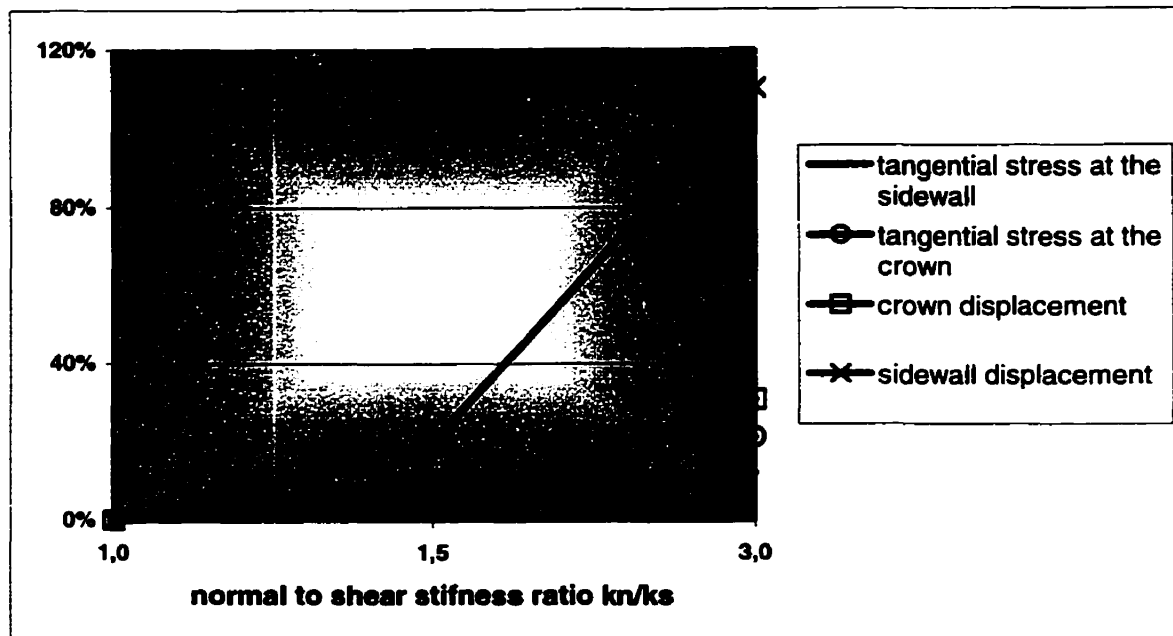Figure 4.4 Generated mesh for the FE analysis

Figure 4.5 Joint stiffness ratio mutual influence

4.4 Results

The results of the simulations are presented in terms of plots of stress levels and displacements around the opening of the Piora exploratory tunnel at chainage km 1,619; those plots are presented in Figures 4.6 to 4.10.
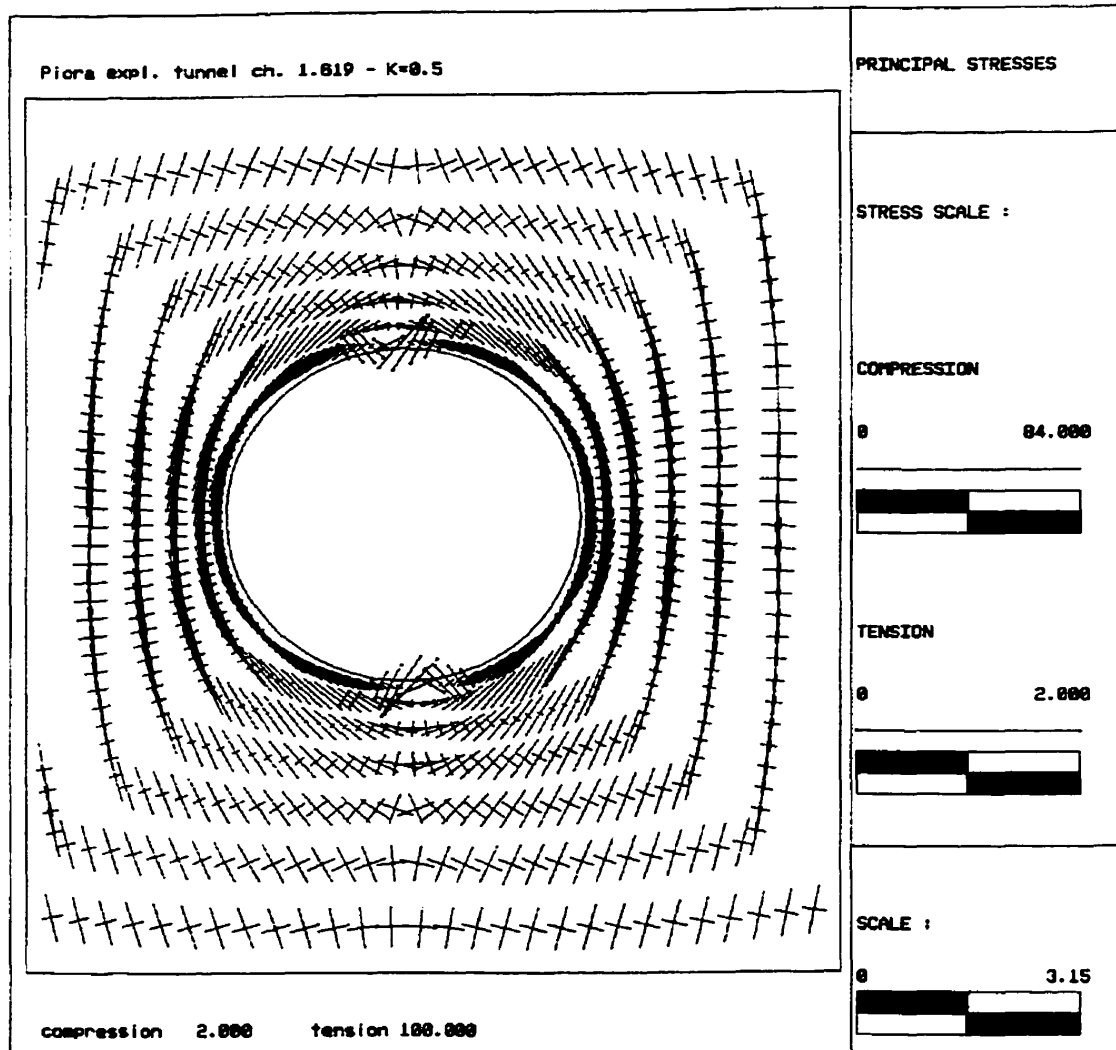
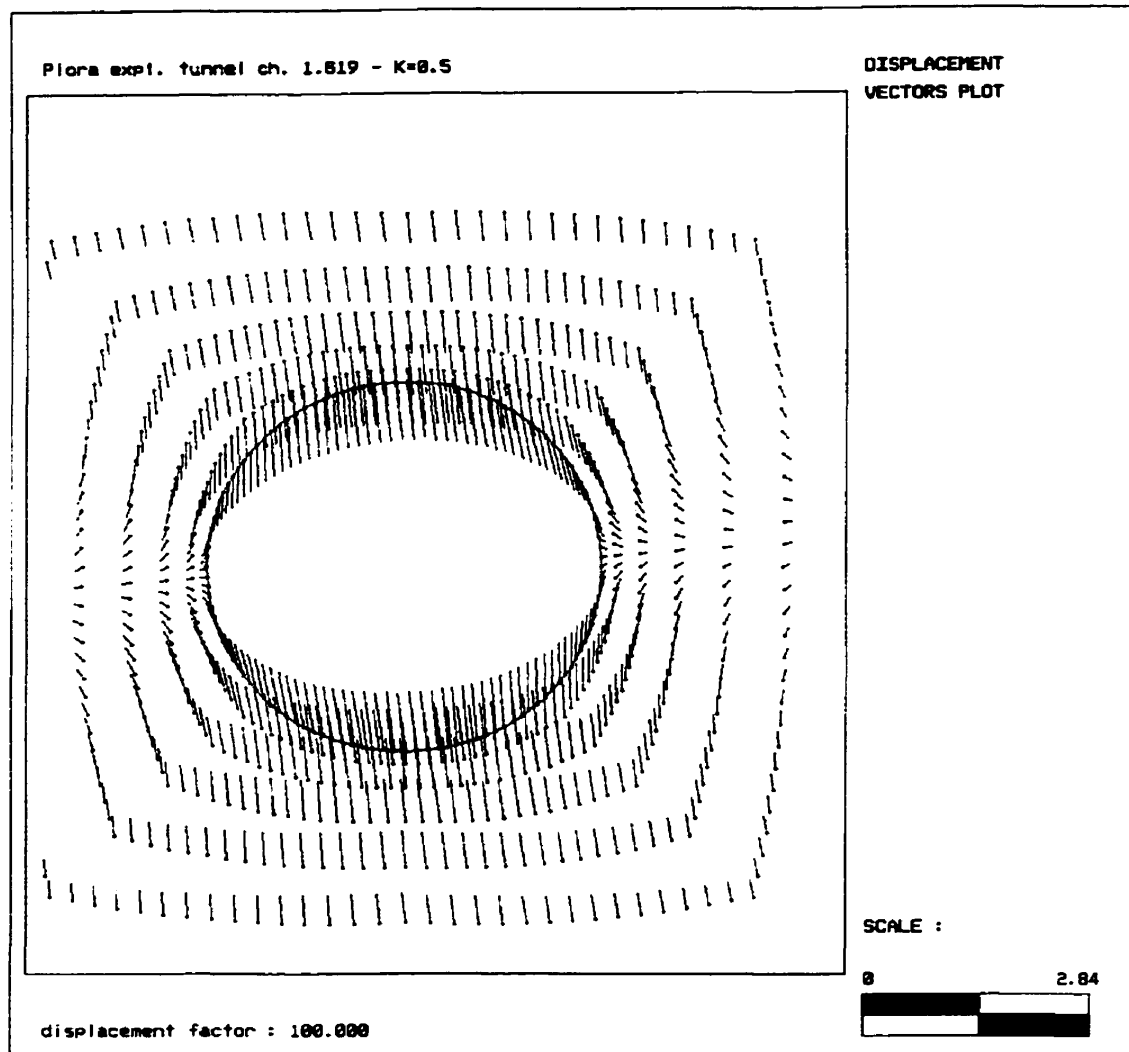Figure 4.6 Zoom-in view of principal stresses around the tunnel for the model MI-K0-5

Figure 4.7 Zoom-in view of displacement vectors around the tunnel, model MI-K0-5
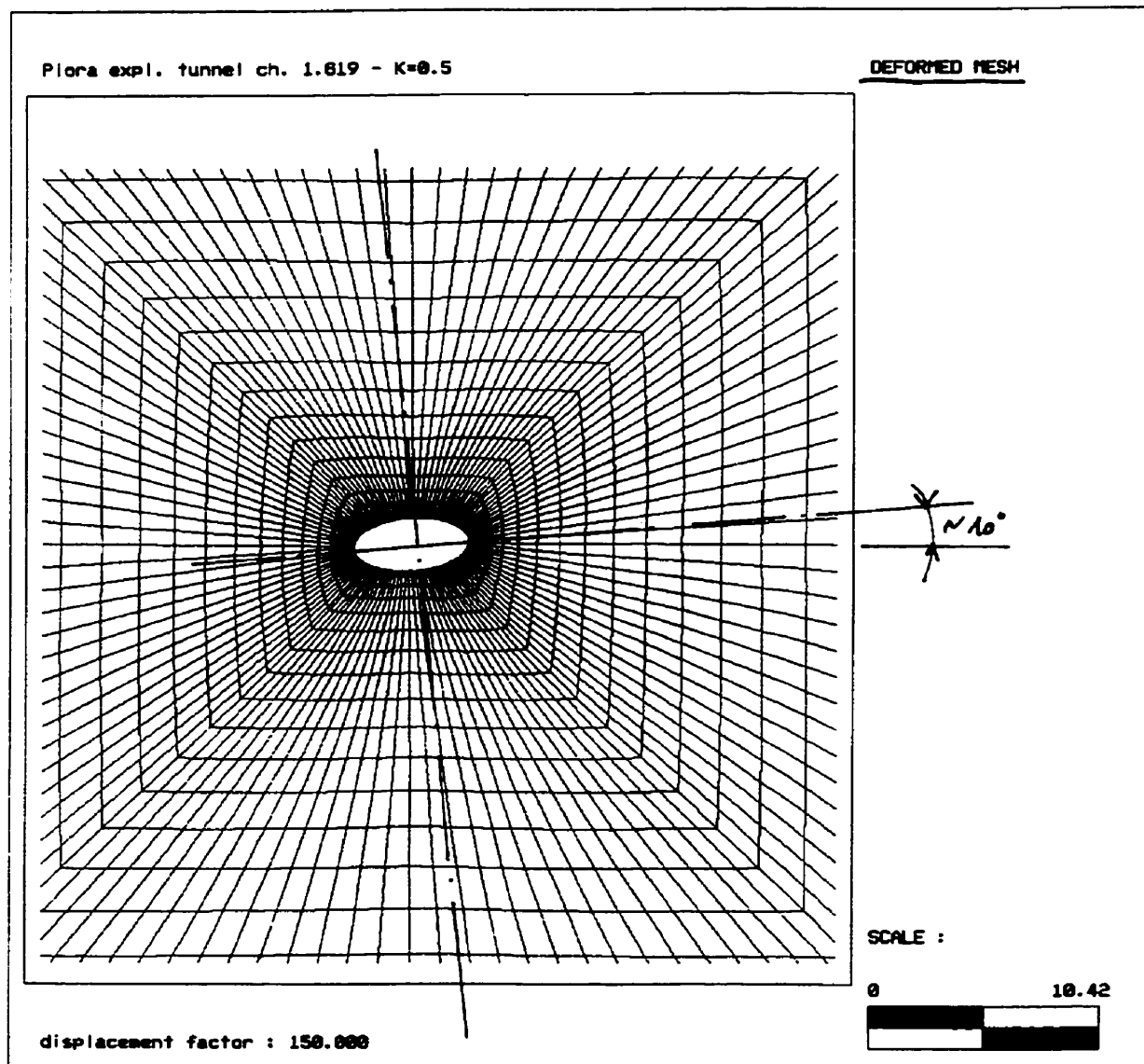
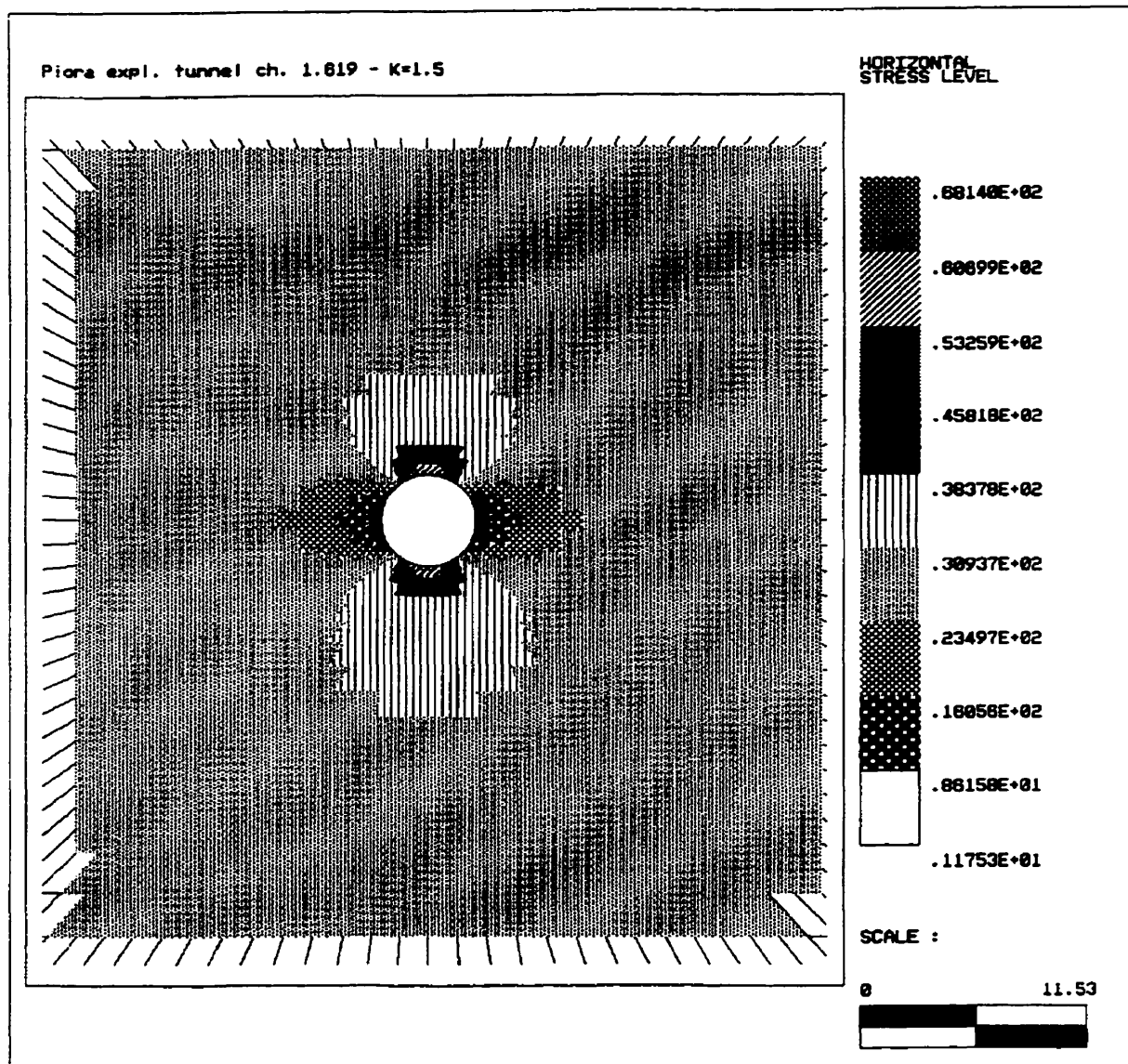Figure 4.8 Displacements presented as deformed mesh for the model MI-K0-5

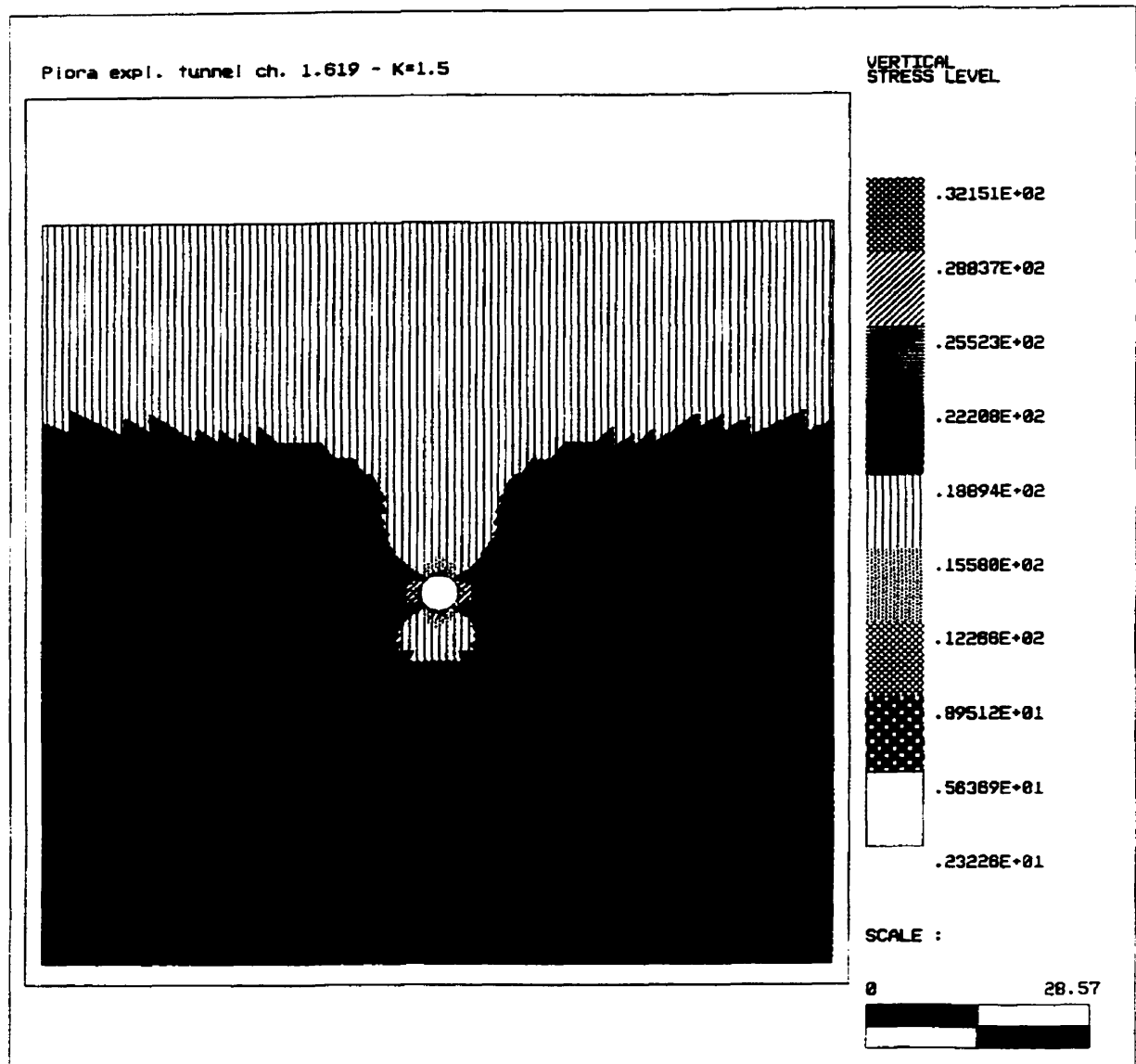Figure 4.9 Horizontal stress levels for the model MI-K1-5

Figure 4.10 Vertical stress levels for the model MI-K1-5

For a better understanding of the stress distribution for Model I – cases MI-K0-5 / MI-K1 / MI-K1-5 referred to Table 4.2 - the simulations regarding vertical and horizontal stresses above the crown as well as at the sidewall are shown in Figure 4.11 to 4.13 for different K ratios where h_x and h_y represent the distance from the opening boundary related to the span B along the X and Y-axes, respectively.
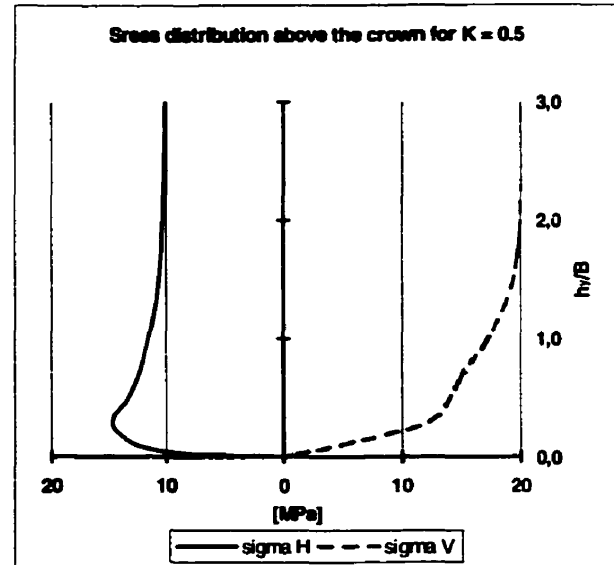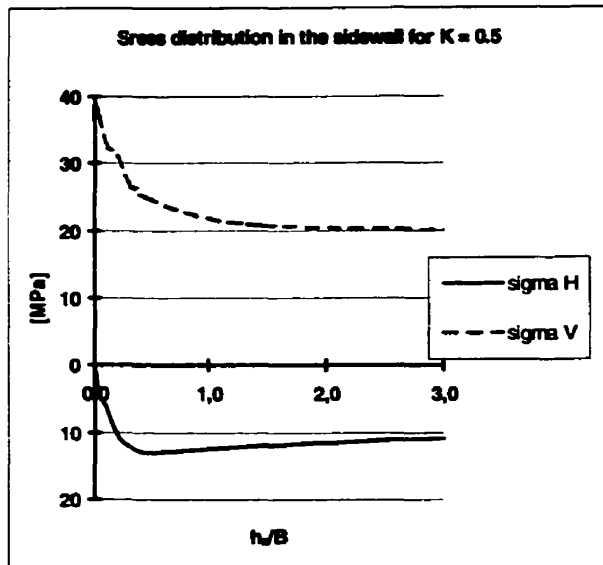
Figure 4.11 Crown and sidewall stress distributions for K=0.5
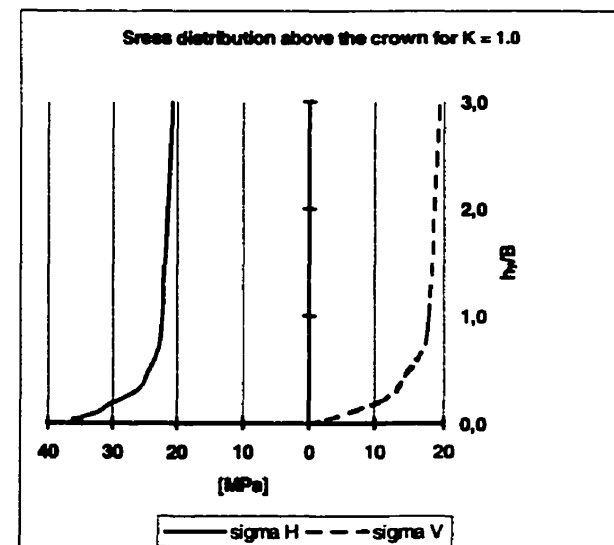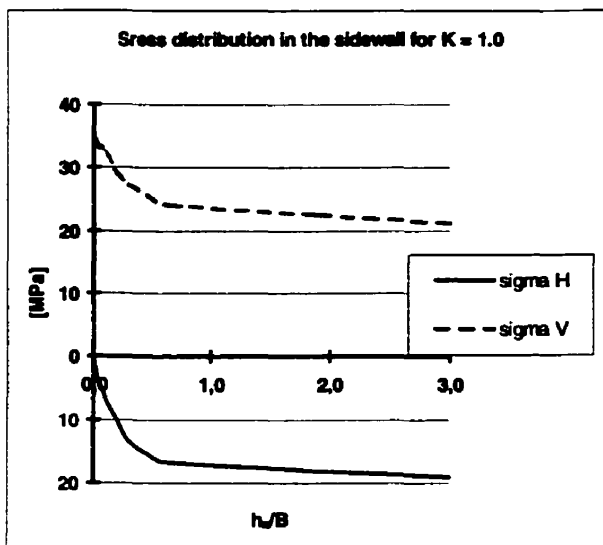
Figure 4.12 Crown and sidewall stress distributions for K=1.0

4-15
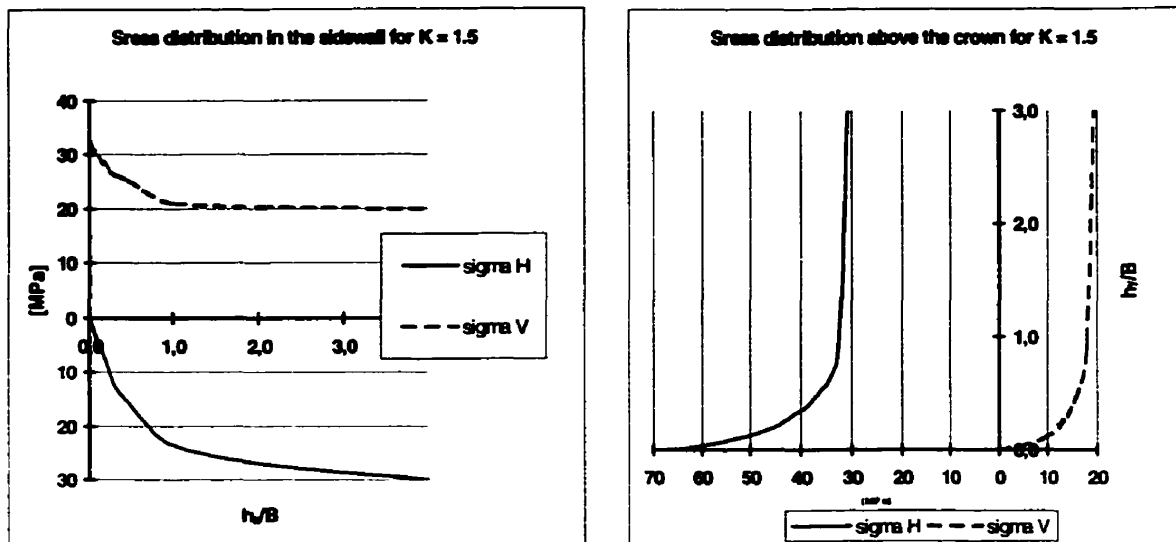
Figure 4.13 Crown and sidewall stress flows for K=1.5

Running the program for Model II has given the results depicted in Figure 4.14, which show the distribution of horizontal stresses above the opening crown for different magnitudes of the mechanical properties of the joints as function of the K ratio whereas the next Figure 4.15 is a detail of the same plot for the lower K ratio, where the stresses approach the zero value; thus, the limit between compression and traction in the rock mass.

Figure 4.14 Crown tangential stress as a function of K for different joint mechanical properties
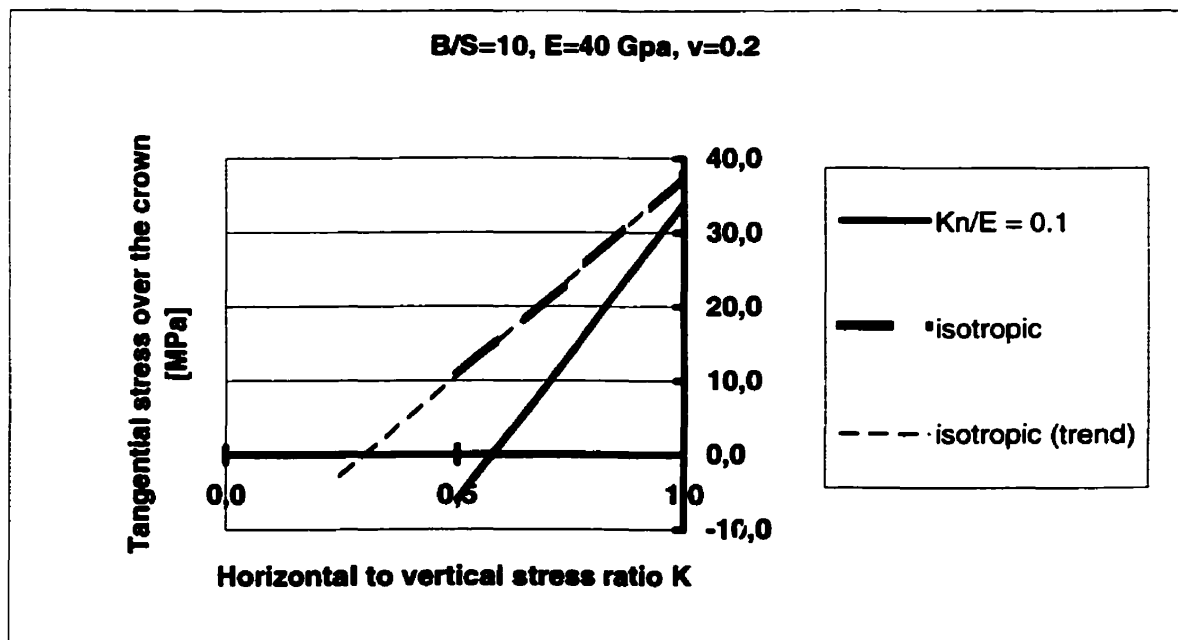
Figure 4.15 Detail of Figure 4.14
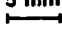
In the latter two figures is also introduced the simulation for an isotropic, homogenous and linear elastic rock mass carried out with e-z tools code. The purpose is to compare the behaviour of an ideal isotropic domain giving the lowest K ratio needed to have traction on the crown with the same value resulting from the analysis for a bed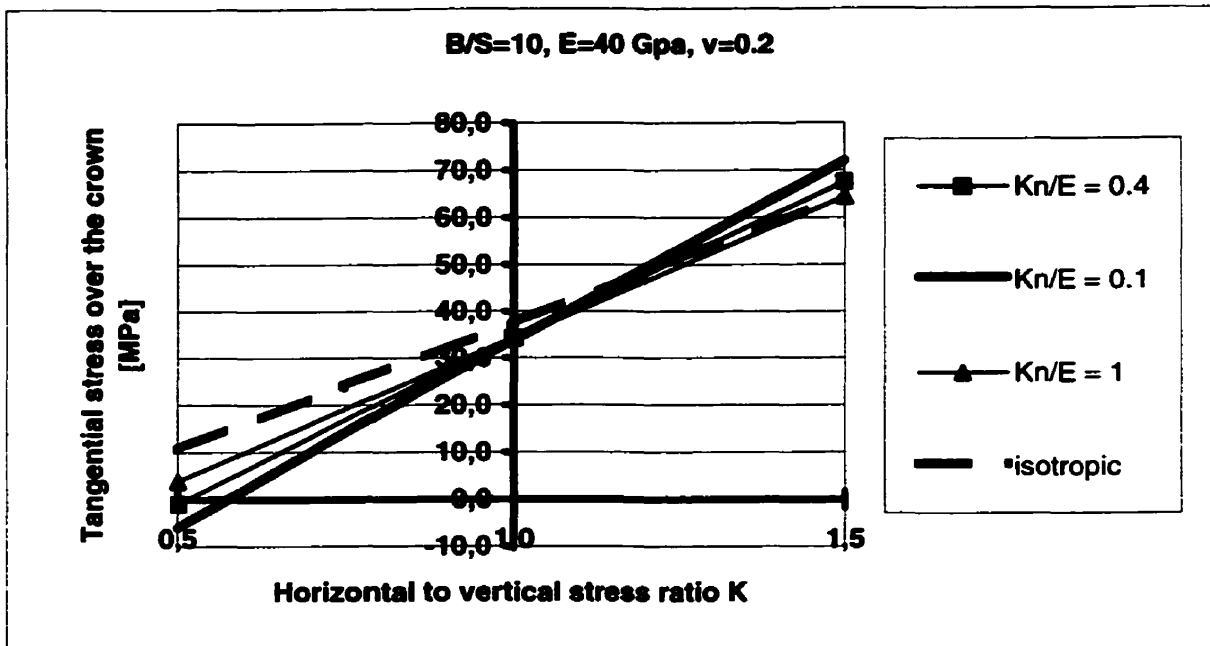ded rock mass. According to the statements of chapter two, where decrease of the mechanical properties of a rock mass containing discontinuities is described, the magnitude of the K ratio with tangential stresses approaching a traction state should be in case of bedded rock mass also higher then the one for isotropic rock as confirmed in Figure 4.15. Consequently, the gap between those two values could be seen as an index giving the extent of the overall degrading of the rock mass.

4.5 Discussion

The results of the field monitoring carried out by the surveyors for the displacements of the Piora exploratory tunnel at chainage km 1,619 is plotted in Figure 4.16.

Visto nel senso dell'avanzamento
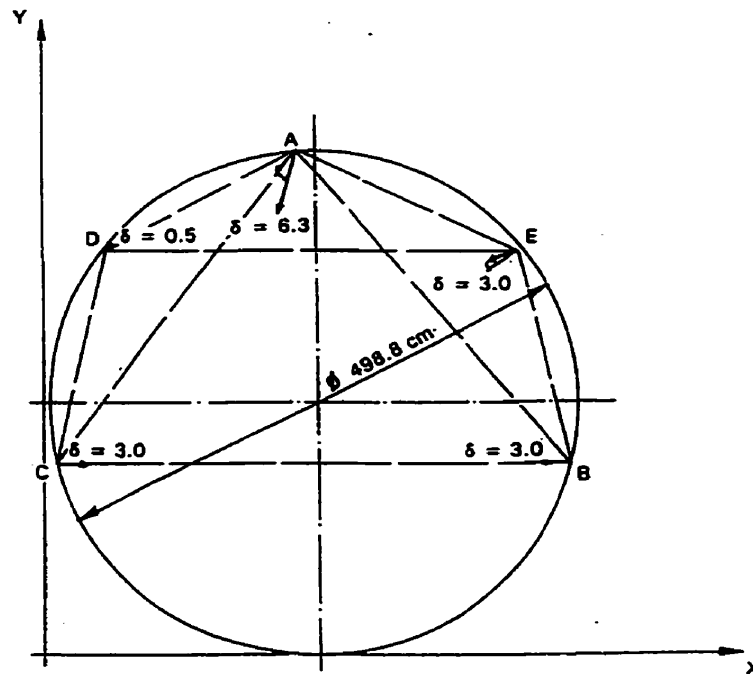
Deformazione radiale media : 3.5 mm

Figure 4.16 Field displacement monitoring at chainage. km 1,619 (Lombardi, 1994)

Figures 4.17, 4.18 and 4.19 present the outcomes from the two-dimensional finite element back-analysis conducted by Lombardi (1994), which is based on the computation for a quarter of the cross section made for the chainage km 1,619 of the Piora exploratory tunnel, for the cases with K = 0.5, 1.0 respectively 1.5, i.e. λ in the above mentioned figures. The code used, which is named P0759 (Lombardi, 1992), was developed in order to simulate a jointed rock mass. The joint properties are introduced in the code as a

function of the joint closure v as depicted in Figure 2.8 and the average mutual distance of the bridging points between the upper and lower neighbouring host rock. The joint closure $v = e = 0.4$ mm is equivalent to about a joint shear stiffness of $k_n = 15$ MPa, which is the stifness introduced in the simulation with e-z tools code for bedded rock mass, see also Table 4.1.
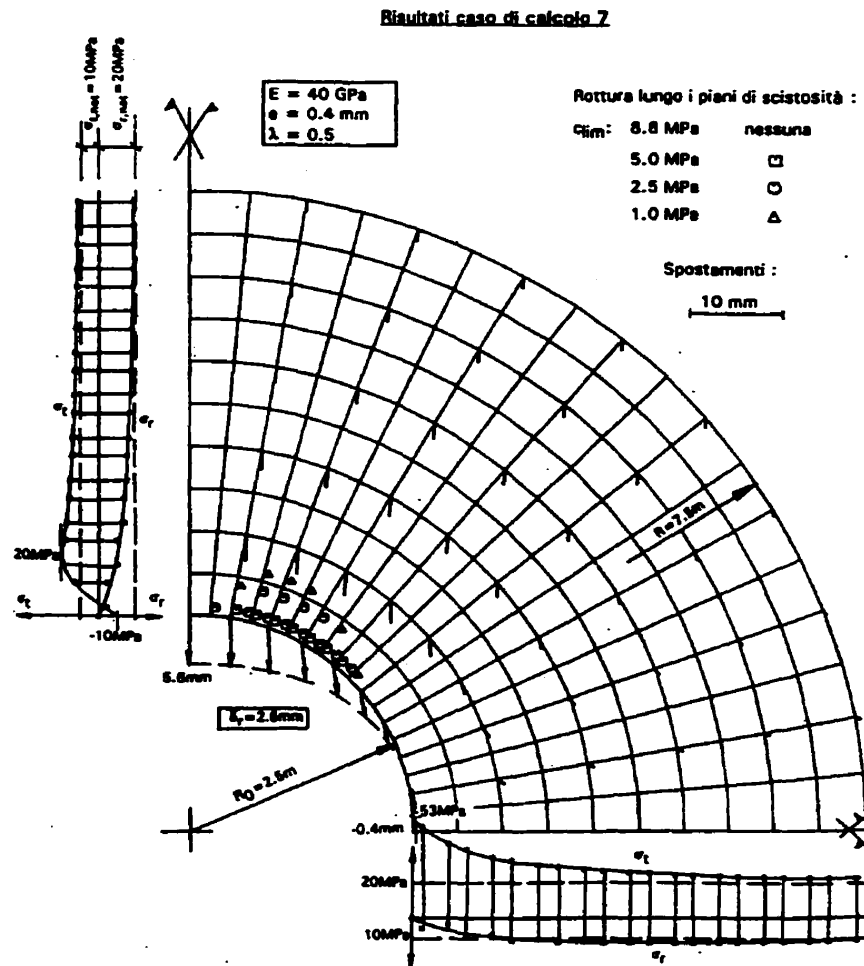
Figure 4.17 FE simulation of the Piora tunnel for K=0.5 (Lombardi, 1994)
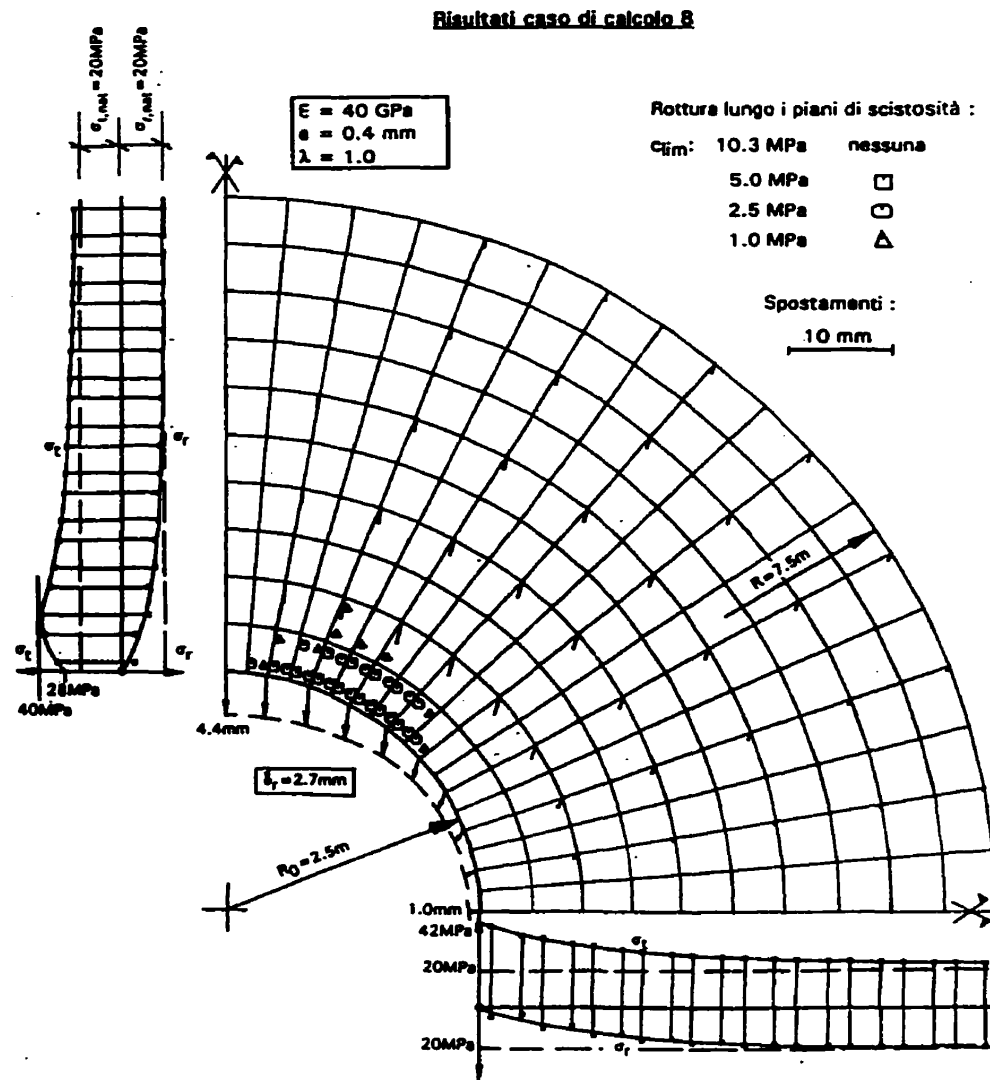
Figure 4.18 FE simulation of the Piora tunnel for K = 1.0 (Lombardi, 1994)
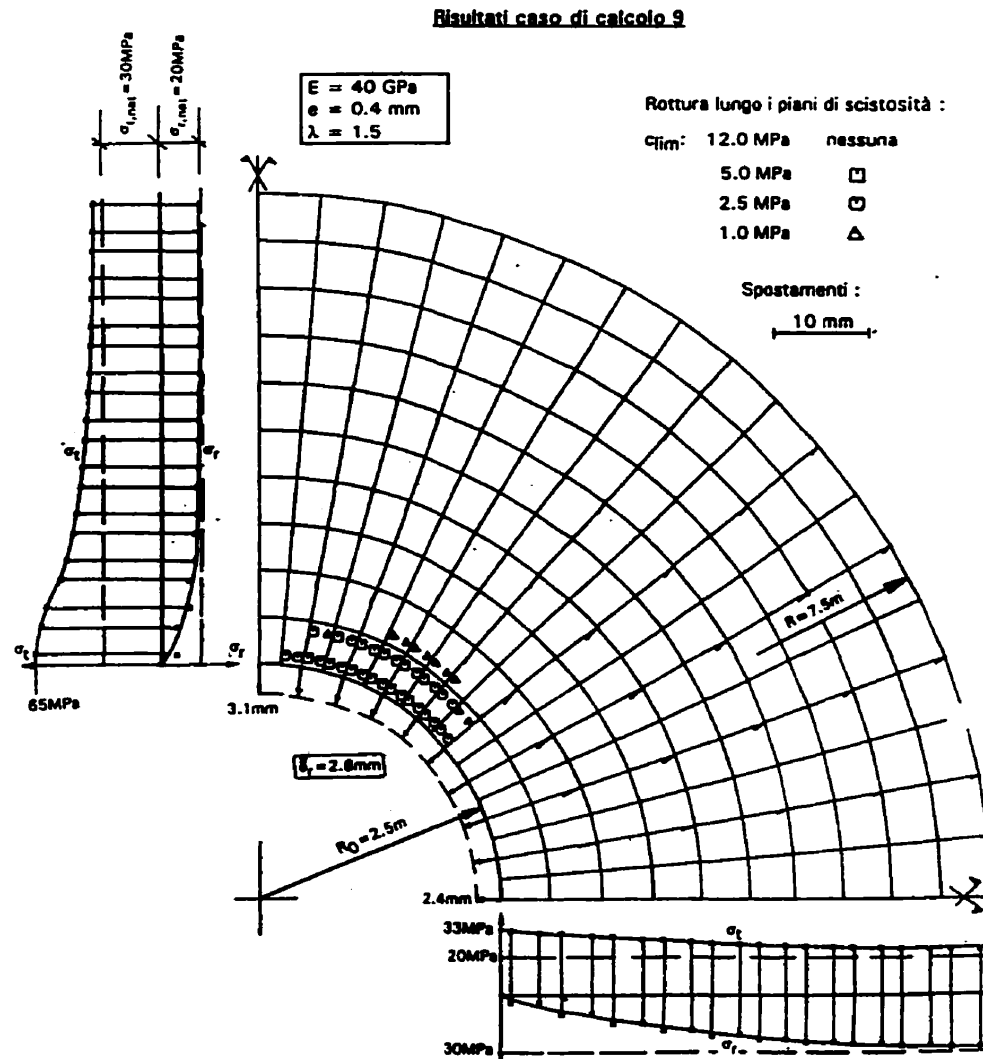
Figure 4.19 FE simulation of the Piora tunnel for K = 1.5 (Lombardi, 1994)

The results displayed in Figure 4.17 to 4.19 can then be directly compared with Figures 4.11 to 4.13.

In the following Figure 4.20 is presented the magnitude of the tangential stress at the crown of the opening described in Figure 4.17 to 4.19 as a function of the K (λ) ratio and different joint closure values v (e).

$$E = 40 \text{ GPa}$$

Ipotesi :

- copertura rocciosa   h = 800 m
- peso unitario roccia γ = 26 kN/m^3
- coefficiente spinta laterale $\lambda = \sigma_H / \sigma_V$
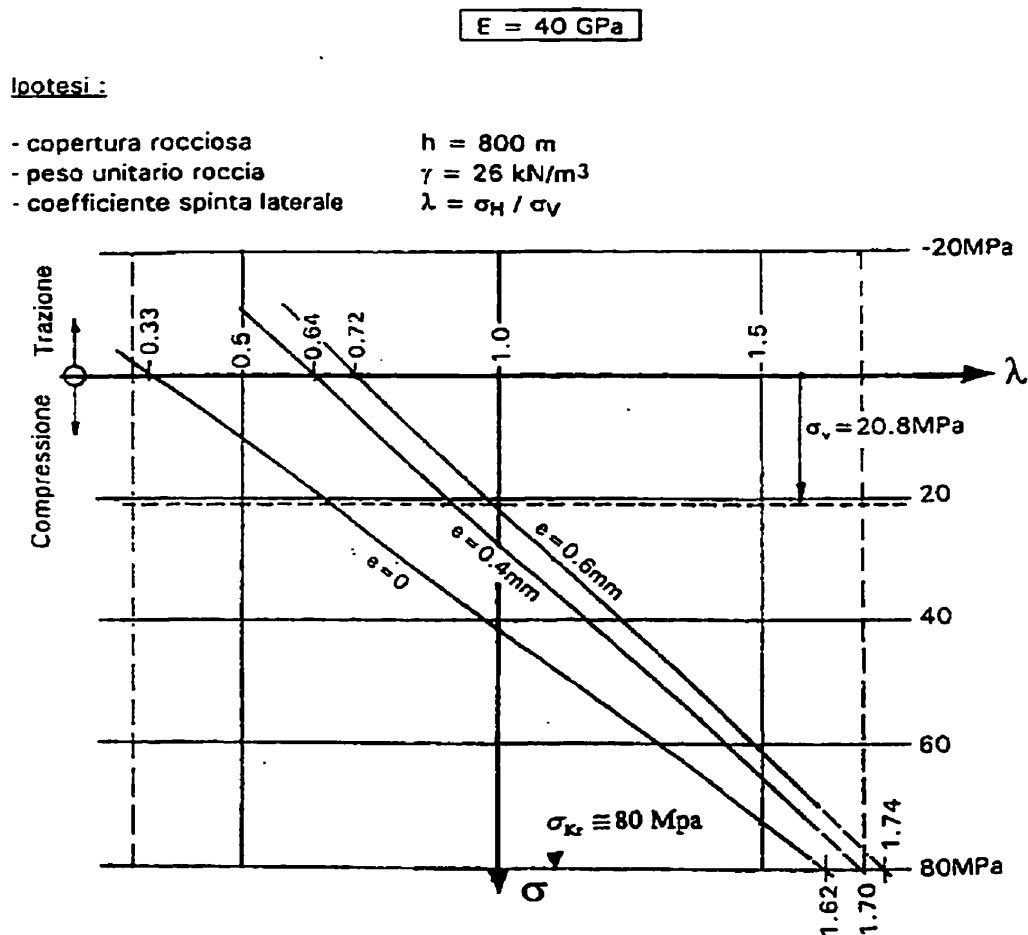
Figure 4.20 Tangential stress as a function of K for different stiffnesses of the joints

(Lombardi, 1994)

In addition to the monitored and the computed displacements, a third method to determine the radial deformation of the cross section at chainage km 1,619 has been used by Lombardi (1994) in the attempt to asses the ideal elastic behaviour of the rock mass at this location by means of the computation of the characteristic curve. Although this analytical method is suitable only for a homogeneous rock mass and can be carried out for circular shapes only – since it is based on close-form solutions – it is useful in giving a first rough approach tool for the understanding of more complex behaviour of the media around the opening.

The first half of Table 4.3 compares the results concerning the displacements determined form the various approaches. Similarly, in the second half, the stress magnitudes in the crown and sidewall are compared.

Table 4.3 Comparison of the results

e-z tools for bedded rock mass	7,7	-0,7	6,7	1,2	5,2	3,1
Lombardi (1994)	5,6	-0,4	4,4	1,0	3,1	2,4
Characteristic curves			5,8	5,8		
Field survey (reported by Lombardi, 1994)			6,3	3,0		

e-z tools for bedded rock mass	-1 / 15	39	34 / 37	36	68	32
Lombardi (1994)	-10 / 18	53	28 / 39	42	65	33

Based on the review of the results of all the simulations that were carried out with the different methods it is fully appreciated that it is difficult to accurately reproduce the in situ observations of displacements. The results of the simulation with e-z tools for bedded rock are however quite similar to the field monitoring results regarding the deformations. According to the stress computation outputs mentioned in Table 4.3, it can certainly be stated that the results of both the finite element methods are very similar in magnitude and tendency. The slight differences could be explained by the different designing of the mesh and by the different approaches to obtain the mechanical properties of the joints, in particular regarding the approach to simulate the shear stiffness used by the code of Lombardi.

Furthermore, the value of K for which the compression-traction limit is reached has a magnitude of 0.64 according to Lombardi, see Figure 4.20 and 0.59 according to the computation with e-z tools for bedded rock mass, see Figure 4.15. It is interesting to note that the same K ratio takes a value of 0.33 and 0.31 respectively, for the case of ideal elastic computation of the rock mass, i.e. e = 0 respectively $K_n/E \rightarrow \infty$ (isotropic material).

Finally, all those differences are to be seen as unimportant at the scale of the problem confirming thus the validity of both the FEM codes.

Chapter 5

CONCLUSIONS AND RECOMMANDATIONS

5.1 Summary and conclusions

Tunnelling has become of more and more interest in geotechnical engineering because of the steadily increasing demand for underground space. The design and construction of tunnels requires among other things, knowledge of the characteristics and behaviour of the rock mass, to enable the assessment of tunnel stability and support requirements. It has been demonstrated from the review in Chapter 2 that, in view of the rock mass complex characteristics, it is extremely difficult to develop a model that describes the behaviour of naturally occurring rock types to a stage adequate for design purposes and which is simple enough for stability analysis carried out at a reasonable cost. In addition, it is not possible to obtain closed mathematical solutions using analytical approaches. The only way to solve such complex problems lies in the application of numerical procedures of computation. In this context, the finite element method has come very much to the forefront in recent years.

This thesis deals with the stability analysis of tunnel openings, which are driven in bedded rock mass, a situation which is not uncommon in real life. A mechanical model of bedded rock, based on the structural model presented in Chapter 3, and developed on the basis of Amadei and Goodman work (Amadei and Goodman, 1981) was adopted and implemented in a FE code, called e-z tools. The code was previously developed at McGill University (Mitri, 1993).

The bedded rock model is described as an equivalent anisotropic continuum. This approach allows to study the influence of joints and intact rock properties and state of stress on the deformability of a bedded rock mass. It is based on the assumption of linear elastic stress-strain behaviour of the rock fabric and takes into account anisotropic

5-1

strength and deformability of the discontinuities thus enabling consideration to be given to a single family of joints in rock mass without difficulty. e-z tools for bedded rock mass performs 2-D, static analysis and calculates stresses and displacements in the domain analyzed.

A detailed model parametric study was conducted where the sensitivity of the input parameters has been tested. In particular, the study has shown the influence of the bedding planes orientation coupled with the scale effect by introducing the span-to-joint spacing ratio (B/S) and the dip angle. A number of interesting conclusions were drawn from this sensitivity analysis. It is found that the joint properties, which appear in the model in terms of sets of products involving joint stiffness and spacing, affect negatively the displacement and stress distribution only in case of very low normal and shear stiffnesses. On the other hand, the elastic modulus of the intact rock dominates, as expected, the overall behaviour of the rock mass as the joint spacing increases. This statement also concurs with the suggestion for more investigation on this subject by Amadei and Goodman (1981).

A case study was conducted on a real tunnelling project in the Swiss Alps, the Piora exploratory tunnel, where another FE model accounting for the fractured rock mass had been applied to the analysis (Lombardi, 1994). The results obtained validate the present model for bedded rock mass, showing consistency with displacements and stress distributions. Also, comparison with monitoring results and an analytical method used by the tunnel project engineer showed good agreement.

5.2 Suggestions for further research

In the present model, it was assumed that the joint normal and shear stiffnesses are constant. However, it is well known (Goodman, 1976) that those quantities can be normal stress dependent. A numerical procedure can be constructed to incorporate this dependency as well as an eventual dilatancy component.

e-z tools for bedded rock mass can be finally improved by adding the capability to handle the general 3-dimensional states of stress and strain. While the 2-dimensional model developed in this thesis is considered adequate for the study of the tunnel wall and crown stability, a 3-dimensional model will enable the study for tunnel face stability, e.g. during the driving of the tunnel.

It may also be desirable to increase the number of joint families in the rock mass simulation. Accurate characterisation of the rock joints will become quite important, and it may be more suitable at this point, when more than one joint family are dominant, to resort to a discontinum numerical method of analysis like the discrete element method.

REFERENCES

- AlpTransit AG, 1996, "Galleria di base del S. Gottardo: le rocce, la galleria, le macchine", booklet of the Swiss Federal Railway Society, Bern.

- AlpTransit AG, 1997, "La nuova galleria di base del S. Gottardo", booklet of the Swiss Federal Railway Society, Bern.

- AlpTransit AG, 1997, "Gotthard-basistunnel, Sondiersystem Piora-Mulde / Schlussbericht Sondierstollen Piora-Mulde, Phase 1: Geologie, Geotechnik, Hydrogeologie, Geothermie", Swiss Federal Railway Society, Report no. 144.1-30 / 425cs, Bern.

- AlpTransit AG, 1997, "Cunicolo di sondaggio della Piora – Considerazioni sui distacchi in calotta verificatisi durante lo scavo del cunicolo di sondaggio della Piora tra le progressive 1500 – 2200 circa", Swiss Federal Railway Society, Report no. 144.1-30 / 1327.4-R-1A, Bern.

- Amadei, B. et al., 1981, "A 3-D constitutive relation for fractured rock masses", Proceeding of the international symposium of mechanical behaviour of structural media, pg. 249-268, Ottawa.

- Amadei, B. et al., 1981, "Formulation of complete plane strain problems for regularly jointed rocks", Proceedings 22nd US symposium on rock mechanics, pg. 245-251, Cambridge, Massachusset

- Amadei, B., 1983, "Rock anisotropy and the theory of stress measurements", Springer Verlag, Berlin and New York.

- Amadei, B., 1988, "Strength of regularly jointed rock mass under biaxial and axisymmetric loading conditions", International journal of rock mechanics in mining sciences and geomechanics, vol. 25, pg. 3-13.

- Association Francaise des Travaux Souterrains, 1993, "Description des massifs rocheux utile à l'étude de la stabilité", Supplément au n° 117, mai-juin de Tunnel et Ouvrages Souterrains.

- Ayyub, B.L. et al., 1996, "Numerical methods for engineers", Prentice Hall, New Jersey.

- Barton, N.R., 1974, "Estimating the shear strength of rock joints", Proceedings of the 3rd ISRM congress, vol. 2A, pg. 219-245, Denver.

- Barton, N.R. et al., 1974, "Engineering classification of rock masses for the design of tunnel support", Rock mechanics, vol. 6, pg. 189-239.

- Barton, N.R. et al., 1983, "Application of Q-system and index tests to estimate shear strength and deformability of rock masses", Proceedings of the international symposium on engineering geology and underground construction, vol. 2, pg. 51-70, Lisbon.

- Beniawski, Z.T., 1973, "Engineering classification of jointed rock masses", South African institution of civil engineers.

- Beniawski, Z.T., 1976, "Rock mass classifications in rock engineering", Balkema, Cape Town.

- Beniawski, Z.T., 1978, "Determining rock mass deformability – experience from case histories", International journal of rock mechanics in mining sciences, vol. 15, no. 5, pg. 237-248.

- Beniawski, Z.T., 1984, "Rock mechanics design in mining and tunnelling", Balkema, Rotterdam.

- Beniawski, Z.T., 1989, "Engineering rock mass classifications", Wiley and Sons, New York.

- Beniawski, Z.T., 1992, , "Design, methodology in rock engineering", Balkema, Rotterdam.

- Brady, B.H.G. et al., 1995, "Rock mechanics for underground mining – second edition", Chapman & Hall, London.

- Brauch, W. et el., 1995, "Mathematik fuer Ingenieure" , B.G. Teubner, Stuttgart.

- Buchanan, R.G., 1995, "Finite element analysis – 2nd edition", Schaum´s outlines series, McGraw-Hill, New York.

- Burnett, D.S., "Finite element analysis from concepts to applications", Addison-Wisley Publishing Company, Reading, Mass.

- Cook, R.D. et al., 1989, "Concepts and applications of finite element analysis", Wiley and Sons, New York.

- Cundall, P.A. et al., 1971, "A computer model for simulating progressive, large scale movements in blocky rock system", Symposium of International Society of Rock Mechanics, paper II-8, Nancy.

- Cundall, P.A., 1980, "UDEC – A generalized distinct element program for modelling jointed rock masses", Final technical report to European Research Office, US Army, Contract DAJA37-79-C-0548, NTIS order no. AD-A087 610/2.

- Deere, D.U., 1968, "Geological considerations", Rock mechanics in engineering practice, pg. 1-20.

- Desai, C.S. et al., 1984, "Thin-layer elements for interfaces and joints", International journal of numerical and analytical methods in geomechanics, vol. 8, no. 1, pp. 19-43.

- Descoeudres, F., 1989, "Mecanique des roches", Ecole Polytechnique Federale de Lausanne, Institut des sols, roches et fondations, Lausanne.

- Duncan, J.M. et al., 1968, "Finite element analysis of slopes in jointed rock", US Army Engineer, Waterways Experiment Station, Corps of Engineers, Report CE-S-68-3, Vicksburg, Mississippi.

- Eissa, E.S.A., 1979, "Stress analysis of underground excavation in isotropic and stratified rock using the boundary element method", Ph.D. Thesis, University of London, Imperial College, London.

- Gerrard, C.M., 1982, "Equivalent elastic modulus for a rock mass consisting of orthorhombic layers", International journal of rock mechanics in mining sciences and geomechanics, vol. 19, pg. 9-14.

- Gerrard, C.M., 1982, "Elastic models of rock masses having one, two and three sets of joints", International journal of rock mechanics in mining sciences and geomechanics, vol. 19, pg. 15-23.

- Ghaboussi, J. et al., 1973, "Finite elements for rock joints and interfaces", Journal of soil mechanics, ASCE, vol. 99, no. SM10, pp. 727-744.

- Goodman, R.E. et al., 1968, "A model for the mechanics of jointed rock", Journal of soil mechanics, ASCE, vol. 94, no. SM3, pg. 637-659.

- Goodman, R.E., 1976, "Methods of geological engineering", Wiley and Sons, New York.

- Goodman, R.E, 1977, "Analysis in jointed rocks", Finite element in geomechanics, Wiley and Sons, New York.

- Goodman, R.E., 1979, "Introduction to rock mechanics", Wiley and Sons, New York.

- Goodman, R.E. et al., 1985, "Block theory and its application to rock engineering", Prentice-Hall, New Jersey.

- Goodman, R.E. et al., 1995, "Advances in computation of jointed rock", Computer methods and advances in geomechanics, vol. 4, pg. 2469-2663.

- Hoek, E. et al., 1980, "Empirical strength criterion for rock masses", Journal of the geotechnical engineering division, ASCE, vol. 106, no. GT9, pg. 1013-1035.

- Hu, K.X. et al., 1993, "Estimation of the elastic properties of fractured rock masses", International journal of rock mechanics in mining sciences and geomechanics, vol. 30, no. 4, pg. 381-394.

- Huang, T.H. et al., 1995, "Elastic modulus for fractured rock mass", Rock mechanics and rock engineering, vol. 28, no. 3, pg. 133-144.

- International Society for Rock Mechanics, 1978, "Suggested methods for the quantitative description of discontinuities in rock masses", International journal of rock mechanics in mining sciences and geomechanics, vol. 15, pg. 319-368.

- Jäger, J.C. et al., 1979, "Fundamentals of rock mechanics - 3rd edition", Chapman & Hall, London.

- Laubscher, D.H. et al., 1976, "The importance of geomechanics classification of jointed rock masses – mining applications", Institution of mining metallurgy.

- Lekhnitskii, S.G., 1963, "Theory of elasticity of an anisotropic elastic body", Holden Day Inc.

- Lombardi, G., 1992, "The FE rock mass model, Part I", Dam Engineering, vol. III, pg. 49-72.

- Luetgendorf, H.O., 1971, "Quantitative Gebirgsmechanic der Untertagebauten im geklueften Gebirge", Verlag Glueckhauf, Essen.

- Maidl, B., 1988, "Handbuch des Tunnel- und Stollenbaus – Band I und II", Verlag Glueckhauf, Essen.

- Mitri, H.S., 1993, "Numerical modelling applications in mining and geomechanics", Proceedings of the first Canadian symposium on numerical modelling in mining and geomechanics, Montreal.

- Mitri, H.S. et al., 1994, "FEM modelling of cable-bolted stopes in hard rock underground mines", SME annual meeting, New Mexico.

- Mitri, H.S., 1993, "e-z tools, 2-dimensional finite element software", Numerical Modelling Laboratory, Dept. of mining, McGill University, Montreal.

- Morland, L.W., 1976, "Elastic anisotropy of regularly jointed media" Rock mechanics, vol. 8, pg. 35-48.

- Pande, G.N. et al., 1990, "Numerical methods in rock mechanics", John Wiley and Sons, New York.

- Peitrequin, P., 1978, "Construction de tunnels", Ecole Polytechnique Federale de Lausanne, Chaire de route et tunnels, Lausanne.

- Raphael, J.M. et al., 1979, "Strength and deformability of highly fractured rock", Journal of the geotechnical division, ASCE, vol. 105, no. GT11, pg. 1285-1300.

- Salamon, M.D.G., 1968, "Elastic modulus of stratified rock mass", International journal of rock mechanics in mining sciences, vol. 5, no. 6, pp. 519-527.

- Serafim, J.L. et al., 1983, "Consideration of the geomechanical classification of Beniawski", Proceedings of international symposium on engineering geology and underground constructions, Lisbon.

- Singh, B., 1972, "Continuum characterization of jointed rock masses - part I and II", Rock mechanics and rock engineering.

- Smoltczyk, U., 1992, , "Grundbau- Taschenbuch – Dritte Auflage" , Ernst & Sohn, Berlin.

- Steiner, W. et al., 1980, "Improved design of tunnel supports: vol. 5 – empirical methods in rock tunnelling – review and recommendations", Report N. UTMA-MA-06-0100-80-8, U.S. Department of Transportation, Washington.

- Stephansson, O., 1981, "The Nasliden project – rock mass investigations", Applications of rock mechanics to cut and fill mining, pg. 145-161, London.

- Thiel, K., 1989, "Rock mechanics in hydroengineering", Geotechnical engineering, vol. 51.

- Thieme, D., 1990, , "Einführung in die Finite Elemente Methode fuer Bauingenieure" , Verlag fuer Bauwesen, Berlin.

- Wardle, L.G. et al., 1972, "The equivalent properties of layered rock and soil masses", Rock mechanics, vol. 4, pg. 155-175.

- Wittke, W., 1977, "Static analysis for underground openings in jointed rock", Numerical methods in geotechnical engineering, pg. 589-638, McGraw-Hill, New York.

- Wittke, W., 1990, "Rock mechanics", Springer Verlag, Berlin Heidelberg New York.

- Yoshinaka, R. et al., 1986, "Joint stiffness and the deformation behaviour of discontinuous rock", International journal of rock mechanics in mining sciences and geotechnique, vol. 23, no. 1, pg. 19-28.

- Zienkiewicz, O.C. et al., 1968, "Stress analysis of rock as a non-tensional material", Geotechnique, vol. 18, pg. 56-66.

- Zienkiewicz, O.C. et al., 1970, "Analysis of non-linear problems in rock mechanics with particular reference to jointed rock systems", Proceedings of the 2nd international congress on rock mechanics, Belgrade.

- Zienkiewicz, O.C. et al., 1977, "Time dependent multilaminate model of rocks – a numerical study of deformation and failure of rock masses", International journal of numerical and analytical methods in geomechanics, vol. 1, pg. 219-247.

- Zienkiewicz, O.C. et al., 1977, "The finite element method - 3rd edition", McGraw Hill, London.